SYNTHESIS OF NANOSIZED PT AND PT-SN CATALYSTS FOR CINNAMALDEHYDE HYDROGENATION REACTION

By
Chalisa Kruprasert

A Thesis Submitted in Partial Fulfillment of the Requirements for the Degree
MASTER OF ENGINEERING
Department of Chemical Engineering
Graduate School
SILPAKORN UNIVERSITY
2010

SYNTHESIS OF NANOSIZED PT AND PT-SN CATALYSTS FOR CINNAMALDEHYDE HYDROGENATION REACTION

By
Chalisa Kruprasert

A Thesis Submitted in Partial Fulfillment of the Requirements for the Degree
MASTER OF ENGINEERING
Department of Chemical Engineering
Graduate School
SILPAKORN UNIVERSITY
2010

การสังเคราะห์ตัวเร่งปฏิกิริยาแพลทินัมและแพลทินัม-ดีบุกขนาดนาโนเมตรสำหรับปฏิกิริยาไฮโดรจิเนชันของซินนามอลดีไฮด์

โดย

นางสาวชาลิสา ครูประเสริฐ

วิทยานิพนธ์นี้เป็นส่วนหนึ่งของการศึกษาตามหลักสูตรปริญญาวิศวกรรมศาสตรมหาบัณฑิต

สาขาวิชาวิศวกรรมเคมี

ภาควิชาวิศวกรรมเคมี

บัณฑิตวิทยาลัย มหาวิทยาลัยศิลปากร

ปีการศึกษา 2553

ลิขสิทธิ์ของบัณฑิตวิทยาลัย มหาวิทยาลัยศิลปากร

The Graduate School, Silpakorn University has approved and accredited the Thesis title of "Synthesis of nanosized Pt and Pt-Sn catalysts for cinnamaldehyde hydrogenation reaction" submitted by Chalisa Kruprasert as a partial fulfillment of the requirements for the degree of Master of Engineering in Chemical Engineering

.....
(Associate Professor Sirichai Chinatangkul, Ph.D.)

Dean of Graduate School

……../……/……..

The Thesis Advisor

Asst.Prof.Dr. Okorn Mekasuwandumrong

The Thesis Examination Committee

..... Chairman
(Asst.Prof.Dr. Choowong Chaisuk)
...../...../.....

..... Member
(Asst.Prof.Dr. Joongjai Panpranot)
...../...../.....

..... Member
(Dr. Supakij Suttiruengwong)
...../...../.....

..... Member
(Asst.Prof.Dr. Okorn Mekasuwandumrong)
...../...../.....

52404209 : MAJOR : CHEMICAL ENGINEERING
KEY WORDS : PT-SN/ HYDROGENATION/ EFFECT OF PREPARATION/ EFFECT OF SUPPORT
CHALISA KRUPRASERT : SYNTHESIS OF NANOSIZED PT-SN CATALYSTS FOR CINNAMALDEHYDE HYDROGENATION REACTION. THESIS ADVISOR : ASST. PROF. OKORN MEKASUWANDUMRONG, D.Eng. 100 pp.

In this thesis, the synthesis of nanosized platinum and platinum-tin catalysts supported on titania (TiO_2) and zirconia (ZrO_2) for cinnamaldehyde hydrogenation to cinnamyl alcohol has been studied. Two methods were employed for catalyst preparation. In the first method, the catalyst was prepared by impregnation of platinum and tin on the support which prepared by glycothermal method (Gly-Imp). In the second method, the catalysts were prepared by one-step flame spray pyrolysis (FSP). These catalysts were characterized by using N_2-physisorption, X-ray diffraction (XRD), transmission electron microscopy (TEM), CO chemisorption and temperature programmed reduction (H_2-TPR). From the experimental results, it was found that catalyst prepared by impregnation method (Gly-Imp) exhibited anatase phase of TiO_2 and tetragonal phase of ZrO_2, respectively. Impregnation-made Pt and Pt-Sn supported catalysts had larger the BET surface area than FSP-made supported catalysts. Impregnation-made Pt and Pt-Sn catalysts supported on TiO_2 had the narrow pore size distribution with mean pore size around 16.1-22.6 nm with the total pore volume around 0.44-0.57 cm^3(STP)/g and the mean particle size (from TEM) about 11.1-13.0 nm while ZrO_2 supported catalysts gave the mean pore size about 4.6-4.9 nm with the total pore volume about 0.17-0.18 cm^3(STP)/g and the mean particle size (from TEM) about 13.0-15.6 nm. For FSP-made TiO_2 supported catalysts gave the mean pore size about 24.9-30.9 nm with the total pore volume about 0.43-0.55 cm^3(STP)/g and the mean particle size (from TEM) about 16.6-22.7 nm while FSP-made ZrO_2 supported catalysts gave the mean pore size about 24.1-41.4 nm with the total pore volume about 0.32-0.54 cm^3(STP)/g and the mean particle size (from TEM) about 19.9-21.1 nm. FSP-made catalysts had higher platinum active sites and platinum dispersion than Impregnation-made catalysts (except 0.5%Pt-1.0%Sn/ZrO_2). For catalytic activity, it cannot conclude clearly because it had not trend obviously but it can run reaction.

Department of Chemical Engineering Graduate School, Silpakorn University Academic Year 2010
Student's signature .....
Thesis Advisor's signature .....

52404209 : สาขาวิชาวิศวกรรมเคมี
คำสำคัญ : แพลทินัม-ดีบุก/ ปฏิกิริยาไฮโดรจิเนชัน/ผลของการเตรียม/ผลของตัวรองรับ

ชาลิสา ครูประเสริฐ : การสังเคราะห์ตัวเร่งปฏิกิริยาแพลทินัมและแพลทินัม-ดีบุกขนาดนาโนเมตรสำหรับปฏิกิริยาไฮโดรจิเนชันของซินนามอลดีไฮด์. อาจารย์ที่ปรึกษาวิทยานิพนธ์ : ผศ.ดร.โอกร เมฆาสุวรรณดำรง. 100 หน้า.

ในงานวิจัยนี้ได้ศึกษาการสังเคราะห์ตัวเร่งปฏิกิริยาแพลทินัม และแพลทินัม- ดีบุกขนาดนาโนเมตรสำหรับปฏิกิริยาไฮโดรจิเนชันของ ซินนามอลดีไฮด์ให้เป็ นซินนามิลแอลกอฮอล์ การเตรียมตัวเร่งปฏิกิริยาจะใช้ 2 วิธี วิธีแรกจะถูกเตรียมโดยการเคลือบฝังแพลทินัมและดีบุกบนตัวรองรับที่ได้จากวิธีไกลโคเทอร์มอล วิธีที่สองเตรียมด้วยวิธีเฟลมสเปรย์ไพโรไลซิส ตัวเร่งปฏิกิริยาเหล่านี้จะถูกทดสอบคุณลักษณะโดยการดูดซับทางกายภาพของไ นโตรเจน การเลี้ยวเบนของรังสีเอ็กซ์ การส่องจากกล้องจุลทรรศน์อิเล็กตรอนแบบส่องผ่าน การดูดซับทางเคมีของคาร์บอนมอนอกไซด์ และการรีดักชันตามอุณหภูมิของไฮโดรเจน จากการทดลองพบว่าการเตรียมด้วยวิธีเคลือบฝังจะให้เฟสอนาเทสของไททาเนียและเฟสเตตระโกนอลของเซอร์โคเนีย ตามลำ ดับ ในขณะที่การเตรียมด้วยวิธีเฟลมสเปรย์ไพโรไลซิสจะให้ทั้งเฟสอนาเทสและเฟสรูไทล์ของไททาเนีย และให้ทั้งเฟสเตตระโกนอลและเฟสโมโนคลินิคของเซอร์โคเนีย ตามลำดับ การเตรียมด้วยวิธีเคลือบฝังจะมีพื้นที่ผิวมากกว่าวิธีเฟลมสเปรย์ไพโรไลซิส การเตรียมด้วยวิธีเคลือบฝังบนไทท าเนียมีการกระจายตัวของขนาดรูพรุนที่แคบ ขนาดรูพรุนเฉลี่ย 16.1-22.6 nm ปริมาตรทั้งหมดในรูพรุน 0.44-0.57 cm^3(STP)/g และขนาดอนุภาคเฉลี่ย 11.1-13.0 nm ในขณะที่เคลือบฝังบนเซอร์โคเนีย จะให้ขนาดรูพรุนเฉลี่ย 4.6-4.9 nm ปริมาตรทั้งหมดในรูพรุน 0.17-0.18 cm^3(STP)/g และขนาดอนุภาคเฉลี่ย 13.0-15.6 nm สำหรับการเตรียมด้วยวิธีเฟลมสเปรย์ไพโรไลซิสบนไททาเนียจะให้ขนาดรูพรุนเฉลี่ย 24.9-30.9 nm ปริมาตรทั้งหมดในรูพรุน 0.43-0.55 cm^3(STP)/g และขนาดอนุภาคเฉลี่ย 16.6-22.7 nm ในขณะที่ ตัวเร่งปฏิกิริยาบนเซอร์โคเนียจะให้ขนาดรูพรุนเฉลี่ย 24.1-41.1 nm ปริมาตรทั้งหมดในรูพรุน 0.32-0.54 cm^3(STP)/g และขนาดอนุภาคเฉลี่ย 19.9-21.1 nm ตัวเร่งปฏิกิริยาที่เตรียมด้วยวิธีเฟลมสเปรย์ไพโรไลซิสจะมีแอคทีฟไซท์และการกระจายตัวของแพลทินัมที่มากกว่าการเตรียมด้วยวิธีเคลือบฝัง (ยกเว้น 0.5%Pt-1.0%Sn/ZrO_2) สำหรับแอคทิวิตี้ของตัวเร่งปฏิกิริยา นั้นยังไม่สามารถสรุปได้อย่างชัดเจน เนื่องจากมันไม่มีแนวโน้มอย่างเห็นได้ชัด แต่ปฏิกิริยายังสามารถเกิดได้

ภาควิชาวิศวกรรมเคมี บัณฑิตวิทยาลัย มหาวิทยาลัยศิลปากร ปีการศึกษา 2553
ลายมือชื่อนักศึกษา.....
ลายมือชื่ออาจารย์ที่ปรึกษาวิทยานิพนธ์ .....

Acknowledgements

I would like to express my sincere gratitude and appreciation to my advisor, Assistant Professor Okorn Mekasuwandumrong D.Eng for valuable suggestions, encouragement during my study, and useful discussions throughout this research. In addition, the author would also be grateful to Assistant Professor Choowong Chaisuk, as the chairman, Assistant Professor Joongjai Panpranot, and Dr. Supakij Suttiruengwong as the members of the thesis committee. The financial supports from Graduate school of Silpakorn University are gratefully acknowledged. I would like to thank the Center of Excellence on Catalysis and Catalytic Reaction Engineering, Department of Chemical Engineering, Faculty of Engineering, Chulalongkorn University for good support of equipments and instruments.

Most of all, I would like to express my highest gratitude to my parents who always pay attention to my all the times for suggestions and have provided support and encouragements. The most success of graduation is devoted to my parents.

Finally, I thank the members of the Center of Excellence on Catalysis and Catalytic Reaction Engineering, Department of Chemical Engineering, Faculty of Engineering, Chulalongkorn University and the members of Department of Chemical Engineering, Faculty of Engineering and industrial technology, Silpakorn University for many helpful suggestions and assistances.

Contents

List of Figures

List of Tables

CHAPTER 1

INTRODUCTION

Nowadays nanometer-sized particles (1–100 nm) are of interest for a wide variety of applications, such as using in the electronic, chemical or mechanical industries including superconductors, catalyst, drug carriers, sensors, magnetic materials, pigment, and in structural and electronic materials, due to their unique or improved properties that are primarily determined by size, composition and structure (Okuyama and Lenggoro 2003: 537). The control and design of the nanostructure is essential for catalytic materials with good performance. This includes chemical and physical properties not only of the active site, where the reaction takes place, but also of the surrounding material, i.e. of the support for dispersed metal nanoparticles (Strobel, Baiker and Pratsinis 2006: 457).

There are several techniques for synthesis of nanoparticles such as flame synthesis and solvothermal method. The flame spray pyrolysis is a process for one-step synthesis of the supported metal catalysts. This method has many advantages over the other methods as it is low-cost, easy to control particle size, simple processing, high production yield, and ease of conversion to mass manufacturing (Karthikeyan et al 1997: 61-74). The hydrothermal or solvothermal method is a preparation method which is carried out at relatively low temperature and did not require organometallic or toxic precursors. A solvothermal method was developed as a mild route to synthesize materials. In contrast to conventional synthetic methods, the solvothermal technique offers many advantages, including the enhancement of solubility, diffusion, and crystallization as well as the control of morphologies, sizes and phase transformation, etc. The choice of appropriate organic solvents played a key role in the solvothermal synthesis, because the solvent properties such as redox, polarity, complexation and viscosity, vapor tension, etc. strongly influence the solubility and transport behavior of the precursors involved in such heterogeneous

liquid-solid reactions (Zhang et al 2003: 7528).

Because of bimetallic Pt-Sn catalysts were widely used in industry such as reforming and dehydrogenation of hydrocarbons in the petroleum industry and selective hydrogenation reactions in fine chemistry. In addition, they had better performance in terms of activity and stability than monometallic platinum catalyst. Bimetalic platinum-tin catalysts were used in the research. As an example, the addition of tin to platinum modifies the selectivity in naphtha reforming, resulting in a higher resistance against deactivation by coke deposition (Paál 1995: 19).

One important hydrogenation reaction used in the fine chemical industry is cinnamaldehyde hydrogenation as reaction in this study. This reaction is also frequently used as a model reaction to study catalyst properties (Gallezot and Richard 1998: 81). The hydrogenation of cinnamaldehyde can proceed via two pathways, i.e. via the formation of cinnamyl alcohol or via the formation of hydrocinnamaldehyde. In both cases the final product is hydrocinnamyl alcohol (or 3-Phynyl-1-propanol). The reaction via hydrocinnamaldehyde is thermodynamically more favorable however the most desired product is the partially hydrogenated product cinnamyl alcohol. Because of cinnamyl alcohol is a fragrance ingredient used in many fragrance compounds. It may be found in fragrances used in decorative cosmetics, fine fragrances, shampoos, toilet soaps and other toiletries as well as in non-cosmetic products such as household cleaners and detergents (Letizia et al. 2005: 839). In addition, cinnamyl alcohol is also an important additive in food industry and an intermediate in the production of certain pharmaceutics.

In this study, supported Pt and Pt-Sn catalysts were prepared by two methods. First, they were prepared by flame spray pyrolysis (FSP). Second, supports were prepared by solvothermal method and then added platinum and tin into these supports with impregnation method (Gly-Imp). These catalysts were characterized by using N_2 physisorption, X-ray diffraction (XRD), CO-chemisorptions, transmission electron spectroscopy (TEM) and temperature program reduction (H_2-TPR). The catalytic activity was tested for catalytic activities in cinnamaldehyde hydrogenation reaction.

Objectives of the Research

To investigate the physiochemical and catalytic properties of nanosized Pt and Pt-Sn catalysts synthesized by various methods for cinnamaldehyde hydrogenation reaction

Scopes of the Research

1) Prepare nanosized platinum catalysts (0.5%wt Pt) by varying the preparation conditions:
   i. Supports were varied two metal oxide such as TiO_2 and ZrO_2.
   ii. Sn Concentration was varied from 0-1.5%wt.
   iii. Preparation methods were varied by flame spray pyrolysis (FSP) and glycothermal-impregnation method (Gly-Imp).

2) Characterize the prepared catalysts.
   i. BET surface area
   ii. X-ray Diffraction (XRD)
   iii. Transmission Electron Microscopy (TEM)
   iv. CO-chemisorptions
   v. Temperature program reduction (H_2-TPR)

3) Evaluate the catalytic activity and selectivity of the prepared catalysts on cinnamaldehyde hydrogenation reaction in a well stirred high temperature high-pressure stainless steel autoclave reactor.

4) Analyze reaction products by gas chromatography.

CHAPTER 2

LITERATURE REVIEWS

2.1 The bimetallic platinum-tin catalyst

Bimetallic catalysts are widely used in industrial processing. Particularly, supported Pt-Sn catalysts are widely used for reforming and dehydrogenation of hydrocarbons in the petroleum industry and for selective hydrogenation reactions in fine chemistry because of their better performance, in terms of activity and stability, than monometallic platinum catalyst.

2.1.1 Pt-Sn catalysts in reforming

In reforming processes, addition of tin to monometallic Pt/Al_2O_3 catalysts provides better stability, mitigates the sintering effect, improves selectivity by inhibition of the hydrogenolytic effect of platinum, and decreases isomerisation and coke deposition, while aromatisation is increased (Antos, Moser and Lapinski 2004: 335; Audo et al. 2001: 157; Zavala et al. 1998: 62; Beltramini and Trimm 1987: 113; Bednarova et al. 2002: 335; Rangel et al. 2000: 174).

Two different effects caused by tin addition are suggested in the literature: one geometrical, in which a physical dilution of platinum by tin takes place, and one electronic, where the formation of alloys causes a change in bond strength between the chemisorbed hydrocarbon and the active metal (Fujikawa, Ribeiro and Somorjai 1998: 58; Palazov et al. 1987: 249; Burch and Garla 1981: 360; Che and Bennett 1989: 55; Bariås, Holmen and Blekkan 1996: 1).

2.1.2 Pt-Sn catalysts in dehydrogenation

Catalytic dehydrogenation processes are of increasing importance because of growing demand for light olefins such as propylene and isobutene. Supported platinum is a good catalyst for reforming and dehydrogenation reactions. Addition of Sn to Pt/Al_2O_3 naphtha-reforming catalysts is well known to promote desired dehydrogenation reactions and inhibit coking reactions (Kogan and Herskowitz 2001: 179; Praserthdam, Grisdanurak and Yuangsawatdikul 2000: 215)

In these processes, supported Pt-Sn catalysts have shown advantages because of their lower deactivation rate and high selectivity for dehydrogenation reactions. The role of Sn in Pt-Sn catalysts has been extensively investigated in many studies. The effect of tin has been explained in terms of geometric effect and/or electronic effect (Llorca et al. 1999: 77). Geometric effect: tin decreases the size of platinum ensembles, reducing hydrogenolysis and coking reactions that require large platinum ensembles. Electronic effect: tin modifies the electronic density of Pt, either due to a positive charge transfer from Sn^{n+} species or to the different electronic structures in PtSn alloys (Kappenstein et al 1998: 2463). The dehydrogenation performance of PtSn catalysts depends on the Sn/Pt atomic ratio, the preparation method and, especially, the interactions between platinum and tin species.

2.1.3 Pt-Sn catalysts in hydrogenation

Addition of tin into supported platinum catalyst in hydrogenation reaction improved activity and selectivity. Example of the selective hydrogenation of α-β unsaturated aldehydes to the unsaturated alcohol, addition of tin has been explained as a result of the cooperation of two phenomena. On one hand, the carbonyl group is activated by ionic tin species, which interact with the oxygen atom of the carbonyl bond and thus facilitate its hydrogenation. On the other hand, the dilution of platinum atoms by metallic tin hinders the hydrogenation of C=C bond and suppresses the readsorption of the unsaturated alcohol formed, thus inhibiting its isomerization to the saturated aldehyde and even its further hydrogenation to the saturated alcohol (Colama et al. 1996: 63; Margìtfalvi et al. 2000: 474; Homs et al. 2001: 1782-1788).

2.2 Cinnamaldehyde hydrogenation reaction

Selective hydrogenation of α,β-unsaturated aldehydes yields unsaturated alcohols. They are industrially valuable products and intermediates for the synthesis of fine chemicals. The desired product in hydrogenation of cinnamaldehyde is cinnamyl alcohol, an important additive in food industry, perfumery and an intermediate in the production of certain pharmaceutics. However, it is a challenging task to accomplish selective hydrogenation of the C=O double bond since the hydrogenation of the C=C double bond is thermodynamically more favorable than the C=O hydrogenation. Many important factors can influence the activity and selectivity, such as the active metal, the catalyst support properties, the catalyst preparation method, the metal particle size, the solution properties and the presence of second and third metal.

Yu et al. (1999) studied the modification of some metal cations to polymer-stabilized platinum colloid. They found that some metal cations (Fe^{3+}, Co^{2+} and Ni^{2+}) can markedly increase both the activity and selectivity of PVP-stabilized platinum colloid in homogeneous liquid-phase selective hydrogenation of cinnamaldehyde to cinnamyl alcohol. The modification was due to the interaction of metal cations with the C=O groups in the reactants. The adsorbed metal cations activated the C=O double bonds and accelerated the reaction rate thus increased the selectivity to α,β-unsaturated alcohols. The steric hindrance also played an important role in the reaction. The metal cation can promote the hydrogenation of C=O double bonds and suppress the hydrogenation of C=C double bonds in the same time.

Lashdaf et al. (2004) studied the effects of the quality and quantity of the acidic on acetal formation and the effect of the acidity of beta zeolites on the formation of ether, on the platinum activity and on the selectivity to cinnamyl alcohol in cinnamaldehyde hydrogenation. They found that the acetal formation related to the amount of acid sites on the external surface of the zeolite and the acidity of the beta zeolite influenced the platinum dispersion, and the activity of the catalysts increased with total acidity of the beta zeolite.

Xi et al. (2008) studied using a new and cheap active carbon material of RHCs produced from the rice husk as an active catalyst support in the cinnamaldehyde hydrogenation in $scCO_2$. The chemical functional groups on the surface and the unique micro- and mesoporous textural properties of RHCs play an important role in controlling the product selectivity. The phase behavior presents a significant influence on the product selectivity, the selectivity to cinnamyl alcohol is high in the three-phase system, but it is very low with a detected level in the two-phase system in which all the cinnamaldehyde dissolved into the $scCO_2$ phase. This is attributed to the interactions between CO_2 and cinnamaldehyde molecules as well as the substrate concentration effects.

Chatterjee et al. (2004) studied the effects of different methods of synthesis on the activity and selectivity of the hydrogenation of cinnamaldehyde in scCO2 using Pt-supported MCM-48 catalysts. They found that high selectivity to the cinnamyl alcohol by the hydrogenation of C=O was achieved using in situ catalyst with well-dispersed smaller Pt^0 particles, at the edge of the single-phase region. Pt catalysts prepared by impregnation of hydrogenate C=C under the same reaction conditions consists of Pt^{2+} and Pt^0 with larger particles.

Plomp et al. (2008) studied the effects of particle size and the amount oxygen group on carbon nanofiber surface of platinum and ruthenium catalyst. The platinum catalysts with oxygen groups on the CNF surface showed the highest selectivity towards cinnamyl alcohol for the largest metal particles. After removal of the oxygen surface groups via a heat-treatment, the smallest metal particles resulted in the highest selectivity towards cinnamyl alcohol, resulting in a reversed particle size effect compared to the catalytic results obtained with polar supports. The observed particle size effects are explained by a change in the adsorption mode of the reactant as a function of the polarity of the support. After removal of oxygen surface groups, the non-polar support favors the adsorption of the phenyl ring, which enables the metal periphery to participate in the hydrogenation. This may result in the direction of the C=O bond to the metal periphery. For smaller metal particles, a higher metal periphery area is present and this will result in a higher increase in activity and selectivity compared to larger metal particles.

Koo-amornpattana and Winterbottom (2001) studied the effects of the use of biphasic solvents and the presence of basis salts on activity and selectivity. It was found that promotion of platinum catalysts with bases enhanced selectivity to cinnamyl alcohol. Moreover, the selectivity to cinnamyl alcohol is strongly influenced by the OH^-group as shown in the order of KOH > NaOH > LiOH > NH_4OH > KNO_3 > CH_3COOK > KCl, but the metal cation is also influential and both M^+ and OH^- appear to be vital to high activity and selectivity.

Li, Zhu and Zhou (2008) studied the use of Pt-Co catalysts supported on carbon nanotubes (CNTs) by wet impregnation. The results show that Pt particles are dispersed more homogeneously on the outer surface of the nanotubes, while the strong interaction between Pt and Co would improve the increasing of activated hydrogen number because of the hydrogen spillover from reduced Pt^0 onto CNTs and increase the catalytic activity and selectivity of cinnamaldehyde to cinnamyl alcohol.

Mahata et al. (2008) studied the effect of Fe and Zn promotion on the performance of Pt-based catalysts using a synthetic carbon xerogel as catalyst support. They found that the addition of Zn or Fe to the Pt catalyst was found to improve the activity as well as the selectivity to cinnamyl alcohol. The important promoting effects observed were explained by the creation of new sites for the activation of the carbonyl group in the cinnamaldehyde molecule and by the development of electronic and stereo-hindrances.

CHAPTER 3

THEORY

This chapter provided some background information necessary for this study such as the synthesis of catalyst by solvothermal technique, the synthesis of catalyst by flame processes and the hydrogenation of cinnamaldehyde reaction. The details were detailed as follows.

3.1 The synthesis of catalyst by solvothermal technique (Jackson and Hargreaves 2008: 633)

Hydrothermal processes involve using water at elevated temperatures and pressures in a closed system, often in the vicinity of its critical point. A more general term, "solvothermal," refers to a similar reaction in which a non-aqueous solvent (organic or inorganic) is used. Under solvo(hydro)thermal conditions, certain properties of the solvent, such as density, viscosity and diffusion coefficient, change dramatically and the solvent behaves much differently from what is expected under ambient conditions. Consequently, the solubility, the diffusion process and the chemical reactivity of the reactants (usually solids) are greatly increased or enhanced, enabling the reaction to take place at a much lower temperature than normal. The method has been widely applied and adopted for crystal growth of many inorganic materials, such as zeolites, quartz, metal carbonates, phosphates and other oxides and halides.

Solvothermal techniques have been extensively developed for the synthesis of metal oxides. Unlike many other synthetic techniques, solvothermal synthesis concerns a much milder and softer chemistry conducted at low temperatures. The mild and soft conditions make it possible to leave polychalcogen building-blocks

intact while they reorganize themselves to form various new structures, many of which might be promising for applications in catalysis, electronic, magnetic, optical and thermoelectronic devices. They also allow the formation and isolation of phases that may not be accessible at higher temperatures because of their metastable nature.

Although some solvothermal processes involve supercritical solvents, most simply take advantage of the increased solubility and reactivity of metal salts and complexes at elevated temperatures and pressures without bringing the solvent to its critical point. The metal complexes are decomposed thermally either by boiling the contents in an inert atmosphere or by using an autoclave. A suitable capping agent or stabilizer such as a long-chain amine, thiol, trioctylphosphine oxide (TOPO), etc. is added to the reaction contents at a suitable point to hinder the growth of the particles and hence stabilize them against agglomeration. The stabilizers also help in dissolution of the particles in different solvents. Unlike the cases of co-precipitation and sol-gel methods, solvothermal processes also allow substantially reduced reaction temperatures, and the products of solvothermal reactions are usually crystalline and do not require post-annealing treatments.

3.2 **The synthesis of catalyst by flame processes** (Strobel, Baiker and Pratsinis 2006: 457-461)

Various aerosol reactors and methods have been developed for the synthesis of a wide variety of metal and metal oxide particles. Compared to wet-chemical routes with various post-treatment steps, such as filtration, washing, drying and calcination, gas-phase processes allow the preparation of the desired material without any further post-processing. Flame processes for catalyst preparation also have the advantage that multicomponent forms of catalysts can be readily prepared and their mixing can be controlled to obtain different distributions to prepare tailor made nanocomposites.

The processes for aerosol flame synthesis (AFS) are classified first depending on the precursor state fed to the flame in vapor-fed AFS (VAFS) and liquid-fed AFS

(LAFS). In the latter, if the liquid precursor solution drives the flame process (contributes more than 50% of the energy) it is called flame spray pyrolysis (FSP). If a non-combustible solution is fed into the flame then LAFS is called flame-assisted spray pyrolysis (FASP).

3.2.1 VAFS

This is the most common industrial flame process for synthesis of various ceramic commodities. In this process volatile metal precursors are evaporated and fed into a flame that either supports the process or ignites the process as in pigmentary TiO_2 production (Figure 1A). The metal precursor is converted into the metal oxide and starts to form particles by nucleation from the gas phase (Figure 2). This is a simple and scalable process. However, a drawback is the need for volatile precursors, which limits the application of VAFS to a few products where volatile precursors are available for a reasonable price.

3.2.2 FASP

In FASP a non-combustible liquid precursor is dispersed into fine droplets that are evaporated and pyrolyzed by an external flame. Instead of an electrically heated tube as in conventional spray pyrolysis, an external hydrogen or hydrocarbon flame is used as the energy source during FASP (Figure 1B). In general, aqueous solutions of metal salts are sprayed in the external flame where the solvent evaporates from the droplets and metal precursors are converted in products. Supplying the energy by an external vapor flame allows much higher process temperatures and cooling rates compared to electrically heated hot-wall reactors where temperatures are usually relatively low (below 2000°C) and residence times longer (up to a few seconds). Depending on process conditions, hollow, micron- or nano-sized particles are formed when the precursor reacts in the droplet or gas phase, respectively (Figure 2).

3.2.3 FSP

In FSP the metal precursor is a combustible liquid that is sprayed and ignited, resulting in product nanoparticles. Although this method was developed as early as

1977 by Sokolowski *et al*. for the synthesis of Al_2O_3, it took nearly two decades until other used it for the synthesis of nanoparticles. The organic precursor solution is dispersed either ultrasonically or by gas convection through a nozzle forming a fine spray which is ignited (Figure 1C). The metal precursors evaporate in this spray flame and are combusted. Particles are then formed by nucleation from the gas phase (Figure 2). The process features short residence times (a few milliseconds) and high maximum process temperatures (up to 3000 K). The main advantage of FSP over FASP is the formation of generally homogeneous, nano-sized particles through control of the precursor-solvent composition.

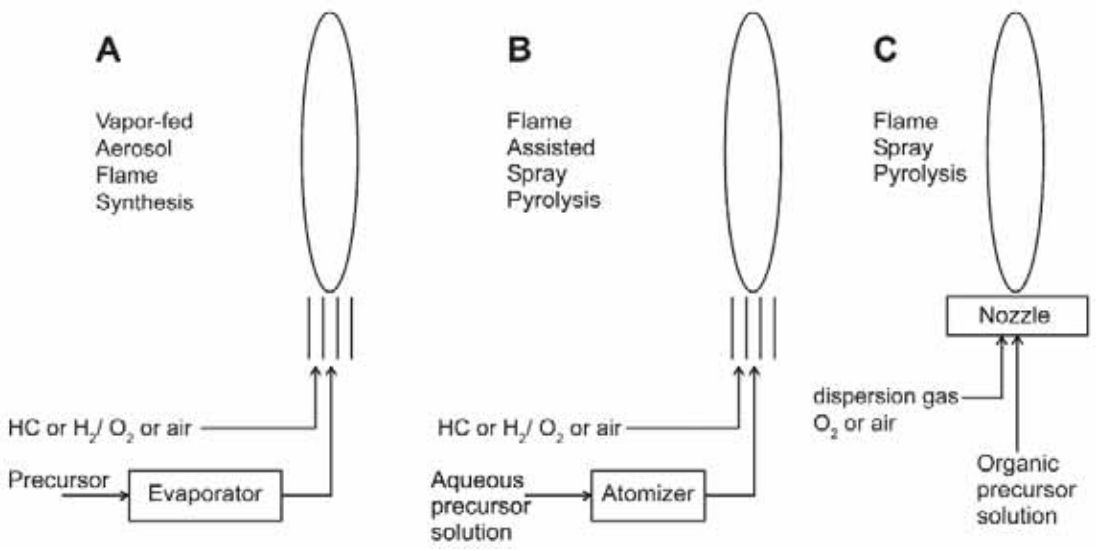

Figure 1 Schematic of selected flame configurations used for the synthesis of heterogeneous catalysts. (A) VAFS, (B) FASP and (C) FSP (Strobel, Baiker and Pratsinis 2006: 457-461).

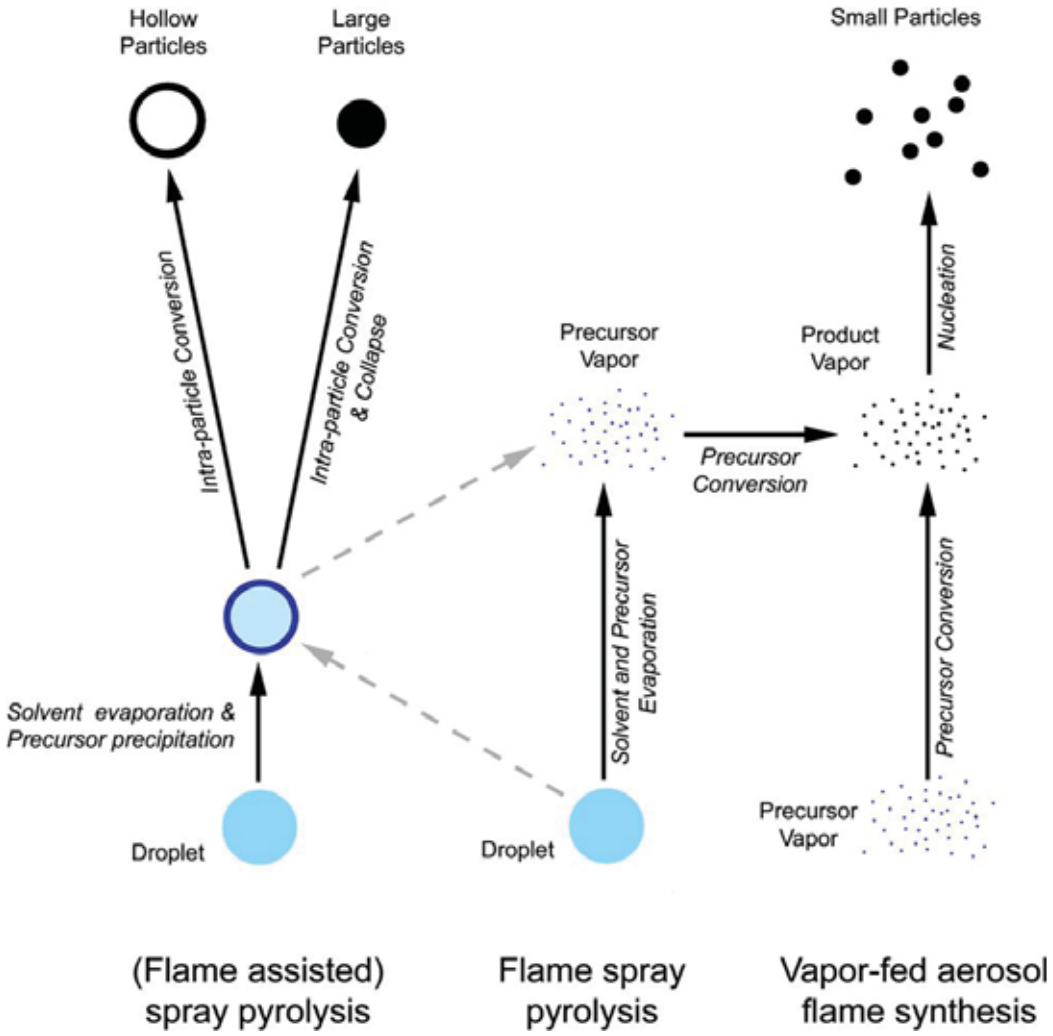

Figure 2 Schematic of the particle formation processes occurring during spray pyrolysis, FSP and VAFS. Two basic particle formation processes can be observed: particle formation in a droplet leading to large or hollow particles (spray pyrolysis and partly in FSP) and particle formation from the gas phase giving small nano-sized particles (VAFS, FSP and partly spray pyrolysis) (Strobel, Baiker and Pratsinis 2006: 457-461).

3.3 The hydrogenation of cinnamaldehyde reaction

One of the oldest and most diverse catalytic processes is the selective hydrogenation of functional groups contained in organic molecules to produce (1) fine chemicals, (2) intermediates used in the pharmaceutical industry, (3) monomers for the production of various polymers, and (4) fats and oils for producing edible and nonedible products. Indeed, there are more hydrogenation catalysts available commercially than any other type, and for good reason, because hydrogenation is one of the most useful, versatile, and environmentally acceptable reaction routes available for organic synthesis (Burwell 1983; 411-465).

The selective hydrogenation of α,β-unsaturated carbonyls is a key step in the manufacture of pharmaceuticals, flavors and fragrances (Gallezot and Richard 1998: 81, Kijenski and Winiarek 2000: L1, Delbecq and Sautet 1995: 217). The hydrogenation of C=C bond to yield saturated carbonyls is thermodynamically favored and can be readily achieved with high selectivity. However, the selective hydrogenation of C=O bond to provide unsaturated alcohols is much more difficult to achieve (Gallezot and Richard 1998: 81). Cinnamaldehyde selective hydrogenation is one such important commercial reaction, which gives cinnamyl alcohol, hydrocinnamaldehyde and hydrocinnamyl alcohol as products in Figure 3. Cinnamyl alcohol is a valuable chemical in the perfumery industry for its odour and fixative properties. It is also used as an intermediate in the pharmaceuticals for the synthesis of antibiotic-chloromycetin (Eilerman 1996: 349). Recently, hydrocinnamaldehyde has been found to be an important intermediate in the preparation of pharmaceuticals used in the treatment of HIV (Muller and Bowers 1999). Although various attempts have been made in the literature to develop a suitable catalytic system for selective hydrogenation of cinnmaldehyde to cinnamyl alcohol or hydrocinnamaldehyde, the selectivity is still an important issue (Lashdaf et al. 2003: 65, Breen et al. 2004: 267). Industrial relevance of unsaturated alcohols in conjunction with economically constraining methods based on chemical reduction of unsaturated carbonyl compounds calls for the development of new catalysts for selective preparation of unsaturated alcohols (Hajek et al 2003: 295).

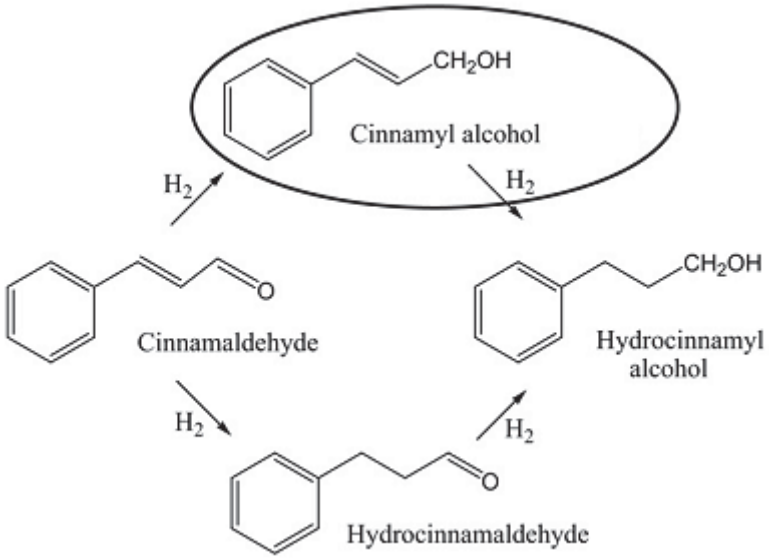

Figure 3 Reaction pathway of the hydrogenation of cinnamaldehyde (Plomp et al. 2008: 13)

CHAPTER 4

EXPERIMENTAL

This chapter describes the experimental procedures for synthesis of nanosized Pt and Pt-Sn catalysts for cinnamaldehyde hydrogenation reaction. This chapter consists three parts such as catalyst preparation, catalyst characterization and catalytic evaluation.

The first part explains catalyst preparation by impregnation method and flame spray pyrolysis and includes the details of chemicals and apparatuses. The second part explains characterization techniques containing N_2-physisorption, X-ray diffraction (XRD), transmission electron microscope (TEM), CO-chemisorption and temperature programmed reduction (H_2-TPR). The last part details the procedure for catalytic evaluation and analyzes reaction products in cinnamaldehyde hydrogenation reaction.

4.1 Catalyst Preparation

For this study, supported platinum and platinum-tin catalysts are synthesized by two methods. The first method, these catalysts are prepared by incipient wetness impregnation which its supports are prepared by glycothermal method (Gly-Imp). And the second method, other catalysts are prepared by flame spray pyrolysis (FSP). The both methods are detailed as follows above.

4.1.1 Synthesis supported platinum and platinum-tin catalysts by impregnation method (Gly-Imp)

Prior to the start of this method, the supports were prepared by glycothermal method. After support preparation, platinum and tin were impregnated on the supports. The obtained catalysts were supported platinum and supported platinum-tin

catalyst. The chemicals for this preparation were listed in Table 1.

Table 1 Chemicals used in glycothermal method and incipient wetness impregnation

Chemical	Supplier
Zirconium (IV) butoxide, 80% solution in 1-butanol	Aldrich
Titanium (IV) butoxide, 97%	Aldrich
1,4-butanediol, > 99%	Merck
Methanol, 99.8 %	QRëC
Hydrogen hexachloroplatinate (IV) hydrate, ca 40% Pt	Acros
Tin (II) chloride, > 99.99%	Aldrich

Glycothermal method

1. Mixed 15 g of Zirconium (IV) butoxide or Titanium (IV) butoxide with 1,4-butanediol to 100 ml in beaker and placed in a 300 ml autoclave (Figure 4).
2. The gap between the beaker and the autoclave was replaced with 30 ml of 1,4-butanediol.
3. The autoclave was purged with nitrogen for three and pressurized pressurized with nitrogen to 5 bar.
4. The mixture was heated to 300°C and held for 2 h after that cooled down to room temperature.
5. Took it to wash with methanol and separated with centrifuge for several times.
6. Dried in oven at 110°C and calcined in air zero at 400°C for 2h.
7. The obtained supports were zirconia (ZrO_2) and titania (TiO_2), respectively.

Figure 4 Autoclave for support preparation (Parr Instrument 2009)

Incipient wetness impregnation

Platinum and tin were deposited on the metal oxide supports by incipient wetness impregnation using water as the solvent, hydrogen hexachloroplatinate (IV) hydrate and tin (II) chloride as metal precursors. The detail of calculation was explained in Appendix A.

1. Dropped water into 2 g of the obtained support (ZrO_2 or TiO_2) in flask with dropper until it was not quite dry to estimate the total pore volume and dried in oven at 110°C.
2. 2 g of the support (ZrO_2 or TiO_2) was gradually dropped with metal precursors that solute in water (0.5 wt% Pt and 0.5, 1.0 and 1.5 wt% Sn solution) and shook it continuously until the volume equal the total pore volume that can estimate.
3. Dried in oven at 110°C and calcined in air zero at 500°C for 2h.
4. The obtained catalysts were supported platinum as follow in Table 2.

Table 2 The symbol of the supported platinum obtained from glycothermal and impregnation method

Symbol	Meaning
0.5%Pt/TiO_2 (Gly-Imp)	The TiO_2 support was prepared by glycothermal and 0.5 wt% Pt was loaded by impregnation
0.5%Pt-0.5%Sn/TiO_2 (Gly-Imp)	The TiO_2 support was prepared by glycothermal and 0.5 wt% Pt and 0.5 wt% Sn were loaded by impregnation
0.5%Pt-1.0%Sn/TiO_2 (Gly-Imp)	The TiO_2 support was prepared by glycothermal and 0.5 wt% Pt and 1.0 wt% Sn were loaded by impregnation
0.5%Pt-1.5%Sn/TiO_2 (Gly-Imp)	The TiO_2 support was prepared by glycothermal and 0.5 wt% Pt and 1.5 wt% Sn were loaded by impregnation
0.5%Pt/ZrO_2 (Gly-Imp)	The ZrO_2 support was prepared by glycothermal and 0.5 wt% Pt was loaded by impregnation
0.5%Pt-0.5%Sn/ZrO_2 (Gly-Imp)	The ZrO_2 support was prepared by glycothermal and 0.5 wt% Pt and 0.5 wt% Sn were loaded by impregnation
0.5%Pt-1.0%Sn/ZrO_2 (Gly-Imp)	The ZrO_2 support was prepared by glycothermal and 0.5 wt% Pt and 1.0 wt% Sn were loaded by impregnation
0.5%Pt-1.5%Sn/ZrO_2 (Gly-Imp)	The ZrO_2 support was prepared by glycothermal and 0.5 wt% Pt and 1.5 wt% Sn were loaded by impregnation

4.1.2 Synthesis supported platinum and platinum-tin catalysts by flame spray pyrolysis

The chemicals for this preparation were listed in Table 3

Table 3 Chemicals used in flame spray pyrolysis

Chemical	Supplier
Platinum (II) acetylacetonate, 99.99%	Aldrich
Zirconium (IV) butoxide, 80% solution in 1-butanol	Aldrich
Titanium (IV) butoxide, 97%	Aldrich
Tin (II) 2-ethylhexanoate, 95%	Sigma
Xylene, 99.8%	Merck

Platinum (II) acetylacetonate, Zirconium (IV) butoxide, Titanium (IV) butoxide and Tin (II) 2-ethylhexanoate were used as the feed precursor. They were dissolved in xylene to 0.3 M solution. The detail of calculation was explained in Appendix A.

1. The spray was ignited by supporting flamelets fed with oxygen (3 l/min) and methane (1.5 l/min).
2. During particle synthesis, 5 ml/min of liquid precursor were fed to the flame by a syringe pump and dispersed with 5 l/min oxygen forming fine spray droplets.
3. The pressure drop at the capillary tip was maintained at 1.5 bar by adjusting the orifice gap area at the nozzle.
4. The product particles were collected on a glass fiber filter (Whatman GF/C, 15 cm in diameter) with the aid of a vacuum pump.
5. Flame spray pyrolysis apparatus was shown in Figure 5 and the obtained catalysts were detailed as follow in Table 4.

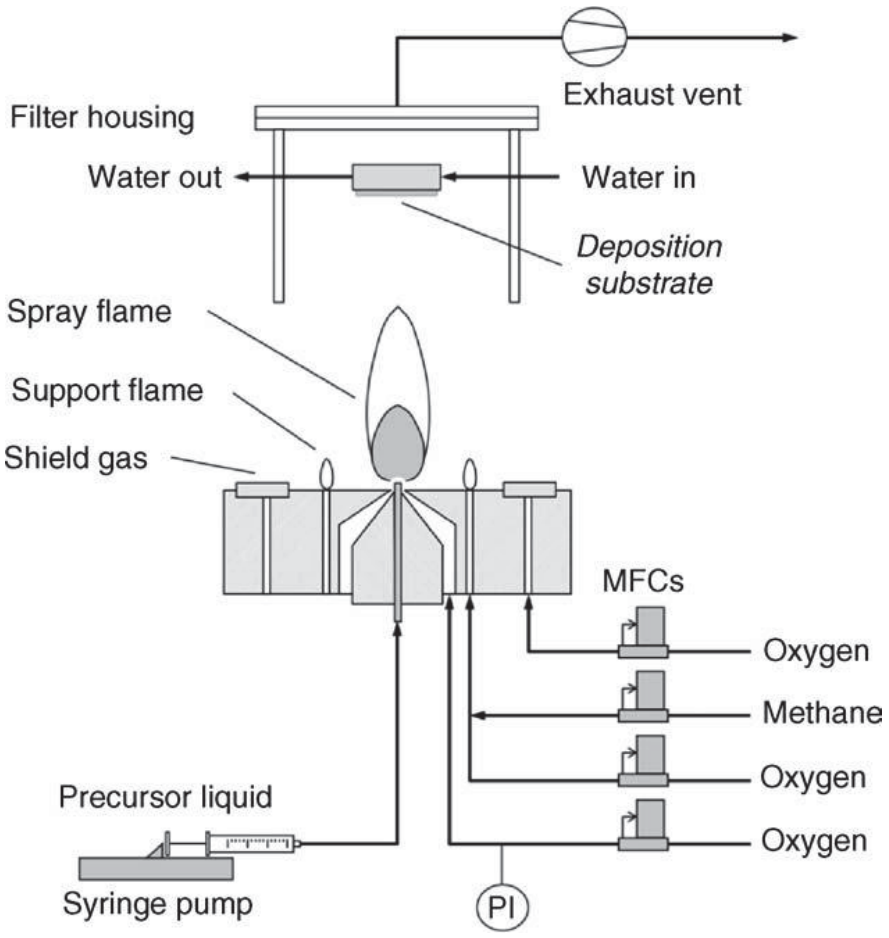

Figure 5 Flame spray pyrolysis for catalyst synthesis (Mädler et al. 2006: 285)

Table 4 The symbol of the supported platinum obtained from flame spray pyrolysis

Symbol	Meaning
0.5%Pt/TiO_2 (FSP)	0.5 wt% Pt support on TiO_2 was prepared by flame spray pyrolysis
0.5%Pt-0.5%Sn/TiO_2 (FSP)	0.5 wt% Pt and 0.5 wt% Sn support on TiO_2 were prepared by flame spray pyrolysis
0.5%Pt-1.0%Sn/TiO_2 (FSP)	0.5 wt% Pt and 1.0 wt% Sn support on TiO_2 were prepared by flame spray pyrolysis
0.5%Pt-1.5%Sn/TiO_2 (FSP)	0.5 wt% Pt and 1.5 wt% Sn support on TiO_2 were prepared by flame spray pyrolysis
0.5%Pt/ZrO_2 (FSP)	0.5 wt% Pt support on ZrO_2 was prepared by flame spray pyrolysis
0.5%Pt-0.5%Sn/ZrO_2 (FSP)	0.5 wt% Pt and 0.5 wt% Sn support on ZrO_2 were prepared by flame spray pyrolysis
0.5%Pt-1.0%Sn/ZrO_2 (FSP)	0.5 wt% Pt and 1.0 wt% Sn support on ZrO_2 were prepared by flame spray pyrolysis
0.5%Pt-1.5%Sn/ZrO_2 (FSP)	0.5 wt% Pt and 1.5 wt% Sn support on ZrO_2 were prepared by flame spray pyrolysis

4.2 Catalyst Characterization

The prepared catalysts will be characterized by several techniques:

4.2.1 N_2-physisorption

The BET surface area, average pore size diameter and pore size distribution were determined by N_2-physisorption using Belsorp Mini II. The catalysts were firstly pretreated in helium gas flow of 50 ml/min at 150°C for 3 h for removing water bound to the particle surface from air moisture. After cooled down to the ambient temperature, the weight of dried catalyst was collected. Sample cell was installed to the adsorption part. The requisite data was input to the software before the measurement. The sample cell was dipped in the dewar containing liquid N_2. The volume of N_2 was measured at -196 °C using the different N_2 partial pressure.

4.2.2 X-ray diffraction (XRD)

The X-ray diffraction (XRD) patterns of powder were obtained using an X-ray diffractometer SIEMENS D5000 connected with a computer with Diffract ZT version 3.3 program for fully control of the XRD analyzer. The experiments were carried out using Ni-filtered CuKα radiation. Scans were performed over the 2θ ranges from 20° to 80°. The crystalline size was estimated from line broadening according to the Scherrer equation and α-alumina was used as standard. This instrument has located at Center of Excellence on Catalysis and Catalytic Reaction, Chulalongkorn University.

4.2.3 Transmission electron microscope (TEM)

Transmission Electron Microscope (TEM) is a conventional method to give detailed information about the shapes, the mean particle size and the size distribution of metallic dispersions. The catalyst sample will be observed using JEOL-JEM 200CX transmission electron microscope operated at 100 kV. This instrument has located at Central Laboratory and Greenhouse Complex, Kasetsart University.

4.2.4 CO-chemisorption

The active sites and relative percentages dispersion of platinum catalyst were determined by CO-pulse chemisorption technique using a Micromeritics Pulse ChemiSorb 2700 instrument at Center of Excellence on Catalysis and Catalytic Reaction, Chulalongkorn University.

0.1 g of a catalyst sample was placed in a quartz tubular reactor. Under H_2 atmosphere at a flow rate of 50 ml/min, the catalyst sample was heated up to 500°C at a heating rate of 10°C/min and held for 1 h at this temperature in order to reduce catalyst. After the reduction, the system was cooled down to room temperature by helium at flow rate of 30 ml/min. At this temperature, the catalyst sample was ready to be measured the metal active sites, 86 µL of the ultra purity CO gas was injected to adsorb on the metal surface of the catalyst sample. Injection of CO was continuously repeated until saturation. The amount of the metal active sites of the catalyst sample and percentages of platinum dispersion was calculated according to description in Appendix C.

4.2.5 Temperature programmed reduction (H_2-TPR)

Temperature programmed reduction was used to determine the reducibility of catalysts. The hydrogen consumption was measured by using a Micrometritics Pulse Chemisorb 2700 instrument at Center of Excellence on Catalysis and Catalytic Reaction, Chulalongkorn University.

0.1 g of a catalyst sample was placed in a quartz tubular reactor. Under N_2 atmosphere at a flow rate of 25 ml/min, the catalyst sample was heated up to 250°C at a heating rate of 10 °C/min and held for 1 h at this temperature in order to eliminate the adsorbed water. After the pretreatment, the system was cooled down to room temperature. The reduction step was performed under 10% H_2 in Ar flow of 25 ml/min from room temperature to 800°C at heating rate of 10°C/min. It was noted that during the reduction step the water produced in this process was trapped by the liquid N_2.

4.3 Catalytic evaluation

The catalysts were tested for their catalytic activity in the selective hydrogenation of cinnamaldehyde using a high pressure stainless steel (SS) made hydrogenation reactor of capacity 300 ml provided with gas inlet and outlet valves, pressure gauge, thermocouple, stirrer and sampling valve (Figure 6).

1. 0.15 g of catalyst was reduced at 500°C for 1 h with 30 ml/min of H_2 gas.
2. Catalyst was activated at 100°C using H_2 pressure (50 bar) for about 3 h in 40 ml of ethanol in the reactor and cooled down to room temperature.
3. 0.01 mol (or 1.3349 g) of cinnamaldehyde and 45 ml of ethanol were taken in the reactor.
4. The reactor was purged with hydrogen for three times and pressurized with hydrogen to 50 bar.
5. The hydrogenation reaction was performed at 60°C for 2 h.
6. Products were withdrawn from the reactor periodically every 15 min for GC analysis.
7. The operating condition of GC was shown in Table 5.
8. 0.05 µl of sample was injected into the GC and the raw data of chromatograms were modified by using calibration curve.

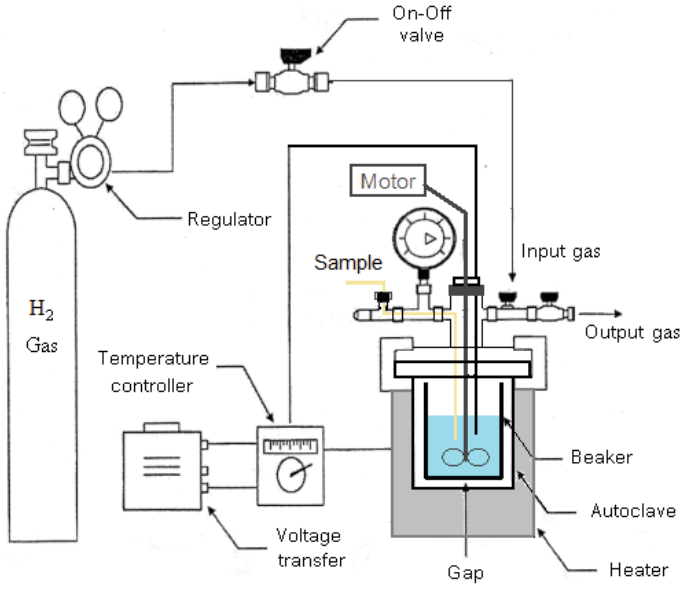

Figure 6 The reactor for hydrogenation of cinnamaldehyde

Table 5 Operating conditions of gas chromatography

Gas chromatography Shimadzu GC14B	
Operating conditions	
Capillary column	DB-1
Length of column	60 m
Purge	10 ml/min
Split	80 ml/min
Carrier	150 kPa
Make up	50 kPa
H_2	60 kPa
Air	50 kPa
Injection temperature	270°C
Column temperature	140°C 30 min, heating rate 5°C/min, 180°C 15 min
Detector temperature	150°C

CHAPTER 5

RESULTS AND DISCUSSION

The main topic of this research involves the use of the supported Pt-Sn catalysts in the hydrogenation of cinnamaldehyde reaction. The results and discussion in this chapter are divided into two sections. In the first section, the physical and chemical properties of catalysts are determined by various characterization techniques. The catalytic performance for cinnamaldehyde hydrogenation is evaluated in the second section. It contains mainly the conversion of cinnamaldehyde and the selectivity of cinnamyl alcohol.

5.1 The physical and chemical properties of the supported Pt-Sn catalysts

In the part, the catalytic properties were characterized by various methods. The phase identification and the average crystallite size were determined by the X-ray diffraction technique. The N_2 physisorption showed the BET surface area, the mean pore diameter, the pore volume and the particle size diameter. The shapes, particle size distribution and mean particle size were obtained by transmission electron microscope (TEM). The platinum active sites and metal dispersion were obtained by CO chemisorptions technique. The temperature programmed reduction of H_2 exhibited the reduction behavior of catalysts.

5.1.1 X-ray diffraction (XRD)

Figure 7 shows the XRD patterns of TiO_2 and TiO_2 supported catalyst prepared by impregnation method (Gly-Imp). All the catalyst samples exhibited only the characteristic peaks of anatase phase of TiO_2. They were assigned by the peak at 25º, 38º, 48º, 54º, 55º, 62º and 75º (JCDPS No.21-1272) (Kang 2003: 177).

The additional peaks corresponding to Pt, Sn and other titania phases were not observed due probably to low amount of Pt and Sn loaded and/or high dispersion of those metals on the TiO_2 supports.

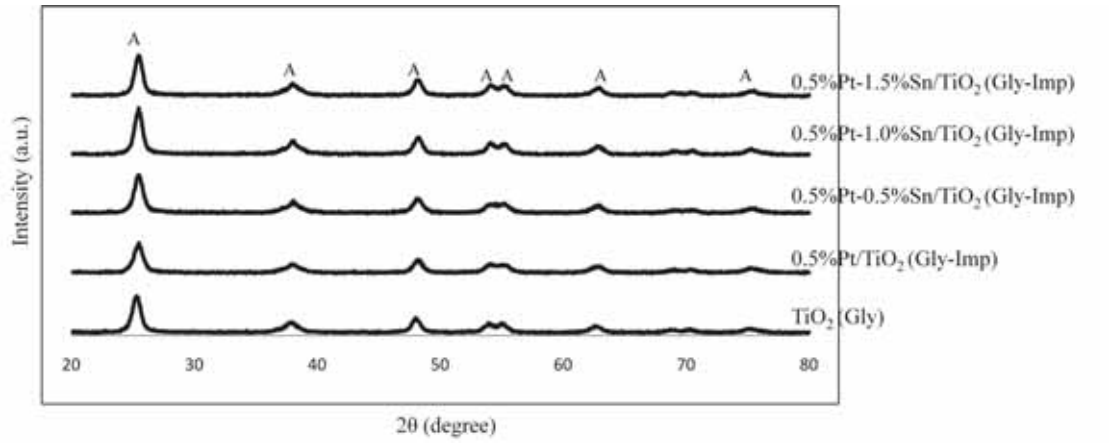

Figure 7 XRD patterns of TiO_2 supported catalysts prepared by impregnation method (Gly-Imp) (A = anatase)

Figure 8 shows the XRD patterns of TiO_2 and TiO_2 supported catalyst prepared by FSP. All catalyst samples exhibited the main characteristic peaks of anatase TiO_2 with small contamination of rutile phase (the peak at 27º) (Chang et al. 2008: 285-286). The additional peaks corresponding to Pt and Sn were not observed too.

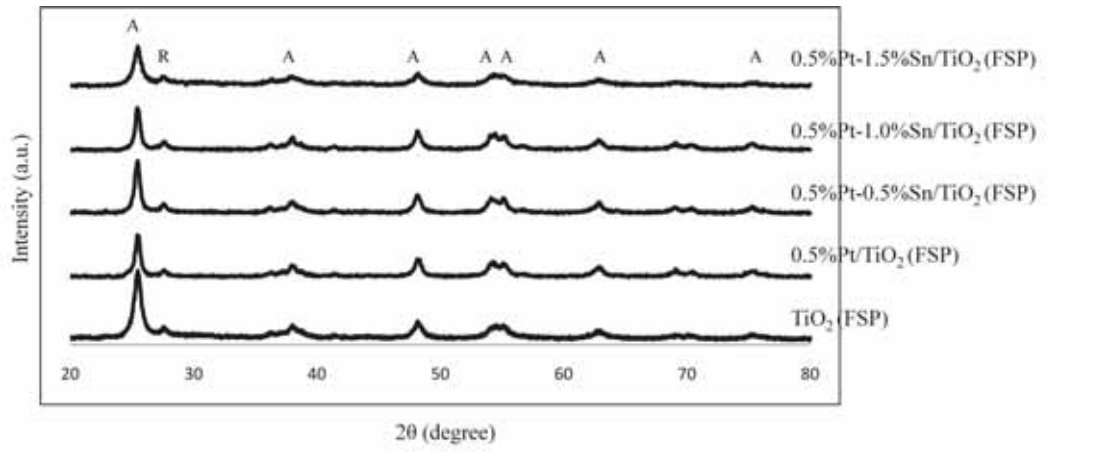

Figure 8 XRD patterns of TiO_2 supported catalysts prepared by FSP (A = anatase, R = rutile)

Figure 9 shows the XRD patterns of ZrO_2 and ZrO_2 supported catalyst prepared by impregnation method (Gly-Imp). The XRD profiles matched well the standard diffraction data of tetragonal phase of ZrO_2 (JCDPS No. 42-1164) (Kongwudthiti et al. 2003: 808). They were assigned by the peak at 30º, 35º, 50º and 60º. The additional peaks corresponding to Pt, Sn and other zirconia phases were not observed as same as TiO_2 supported catalysts prepared by the same method.

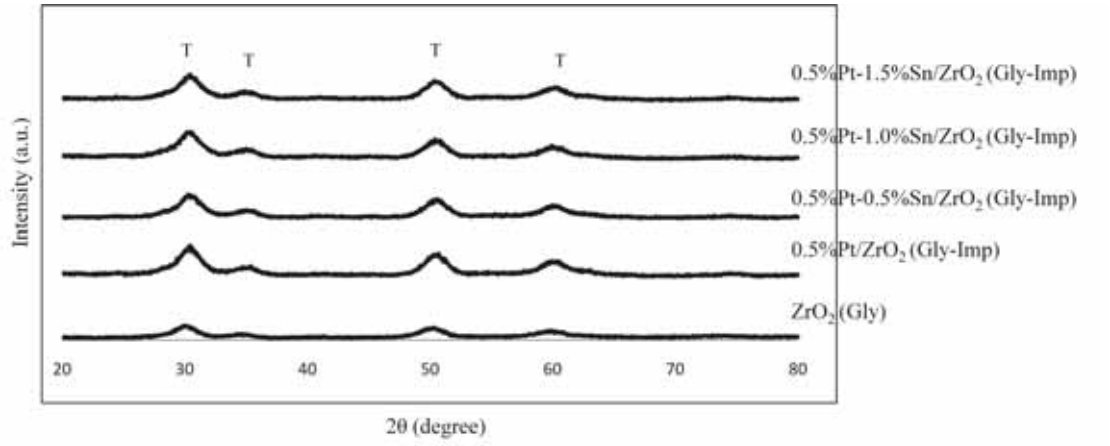

Figure 9 XRD patterns of ZrO_2 supported catalysts prepared by impregnation method (Gly-Imp) (T = tetragonal)

Figure 10 shows the XRD patterns of ZrO_2 and ZrO_2 supported catalyst prepared by FSP. All the catalyst samples did not exhibit only the characteristic peaks of tetragonal phase of ZrO_2 (JCDPS No. 50-1089) but they also showed monoclinic ZrO_2 (JCDPS No.37-1484) (Burakorn et al. 2008: 352-358). Pt and Sn peak were not observed too.

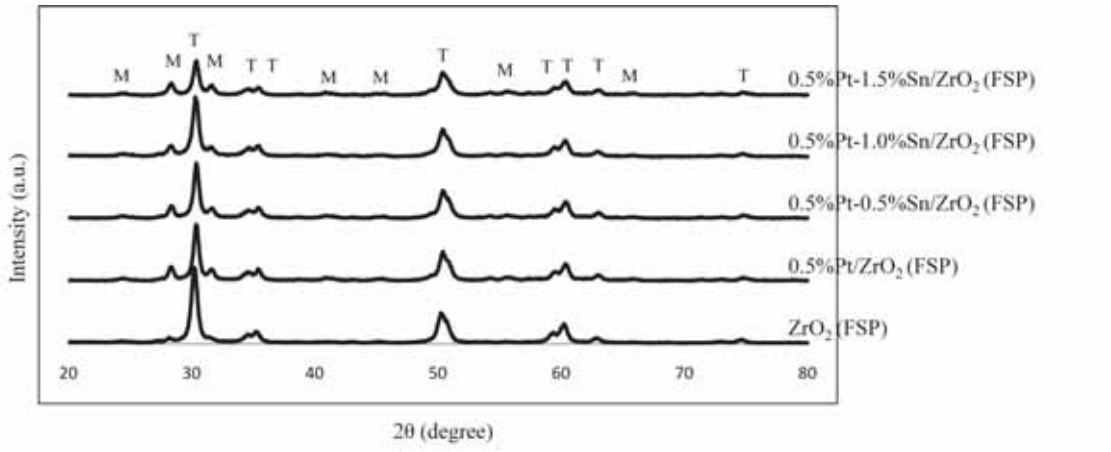

Figure 10 XRD patterns of ZrO_2 supported catalysts prepared by FSP (T = tetragonal, M = momoclinic)

The crystallite sizes of catalysts calculated from Scherrer's equation are summarized in Table 6. It was found that TiO_2 supported catalysts prepared by impregnation method (Gly-Imp) had crystallite sizes of anatase phase of TiO_2 ranged between 7.9 to 12.2 nm, while the TiO_2 crystallite sizes of supported catalysts prepared by FSP were ranged between 8.5 to 13.3 nm for anatase phase and 8.4 to 13.7 nm for rutile phase. ZrO_2 supported catalysts prepared by impregnation method (Gly-Imp) had the crystallite sizes of tetragonal ZrO_2 about 2.9-3.4 nm, while the ones prepared by FSP has crystallite sizes of tetragonal ZrO_2 about 13.7-17.6 nm and crystallite sizes of monoclinic phase about 6.8-13.1 nm.

For the present of tin, the crystallite sizes of TiO_2 supported catalysts prepared by impregnation method (Gly-Imp) increased from 7.9 to 12.2 nm as the amounts of Sn loading increased from 0 to 1.5 wt%. In the case of FSP-made catalyst, the

crystallite size increased from 11.2 to 13.3 nm as the Sn loading increased from 0 to 1.0 wt% and then decreased to 8.5 nm after the addition of Sn further increased to 1.5 wt%. The crystallite sizes of ZrO_2 supported catalysts prepared by impregnation method (Gly-Imp) decreased from 3.4 to 2.9 nm as the amounts of Sn loading increased from 0 to 1.0 wt% and then increased to 3.4 nm after the addition of Sn further increased to 1.5 wt%. In the case of FSP-made catalyst, the crystallite size increased from 14.7 to 17.6 nm as the Sn loading increased from 0 to 0.5 wt% and then decreased to 13.7 nm after the addition of Sn further increased to 1.5 wt%.

Table 6 The crystallite size of catalysts

Catalysts	Crystallite size (nm)
0.5%Pt/TiO_2 (Gly-Imp)	(A) 7.9
0.5%Pt-0.5%Sn/TiO_2 (Gly-Imp)	(A) 11.2
0.5%Pt-1.0%Sn/TiO_2 (Gly-Imp)	(A) 10.4
0.5%Pt-1.5%Sn/TiO_2 (Gly-Imp)	(A) 12.2
0.5%Pt/TiO_2 (FSP)	(A) 11.2, (R) 11.3
0.5%Pt-0.5%Sn/TiO_2 (FSP)	(A) 11.2, (R) 11.3
0.5%Pt-1.0%Sn/TiO_2 (FSP)	(A) 13.3, (R) 8.4
0.5%Pt-1.5%Sn/TiO_2 (FSP)	(A) 8.5, (R) 13.7
0.5%Pt/ZrO_2 (Gly-Imp)	(T) 3.4
0.5%Pt-0.5%Sn/ZrO_2 (Gly-Imp)	(T) 3.3
0.5%Pt-1.0%Sn/ZrO_2 (Gly-Imp)	(T) 2.9
0.5%Pt-1.5%Sn/ZrO_2 (Gly-Imp)	(T) 3.4
0.5%Pt/ZrO_2 (FSP)	(T) 14.7, (M) 6.8
0.5%Pt-0.5%Sn/ZrO_2 (FSP)	(T) 17.6, (M) 7.1
0.5%Pt-1.0%Sn/ZrO_2 (FSP)	(T) 15.4, (M) 9.5
0.5%Pt-1.5%Sn/ZrO_2 (FSP)	(T) 13.7, (M) 13.1

A = Anatase, R= Rutile, T = Tetragonal, M = Monoclinic

5.1.2 N_2 physisorption

The BET surface area, mean pore diameter and total pore volume of the supported Pt and Pt-Sn catalysts were determined by N_2 physisorption technique and the result are shown in Table 7. It was observed that the catalyst prepared by impregnation method (Gly-Imp) had larger BET surface area than the catalyst preparation by FSP. When loading of tin increased, the BET surface area of TiO_2 supported catalysts prepared by impregnation method (Gly-Imp) decreased from 110 to 95 m^2/g due to blocking of tin in the catalyst pore but the BET surface area of TiO_2 supported catalysts prepared by FSP was remained constant (71 m^2/g). BET surface area of ZrO_2 supported catalysts prepared by impregnation method (Gly-Imp) decreased from 151 to 143 m^2/g when loading of tin increased while the BET surface area of ZrO_2 supported catalysts prepared by FSP were constant around 50-52 m^2/g.

The mean pore sizes of catalysts prepared by impregnation method (Gly-Imp) were smaller than catalysts prepared by FSP. The mean pore sizes of TiO_2 supported catalysts prepared by impregnation method (Gly-Imp) had diameter about 16.1-24.4 nm while by FSP had diameter about 24.9-30.9 nm. And the mean pore sizes of ZrO_2 supported catalysts by Gly-Imp had diameter about 4.6-4.9 nm while by FSP had diameter about 24.1-41.4 nm.

The total pore volume of TiO_2 supported catalysts prepared by impregnation method (Gly-Imp) were about 0.44-0.57 cm^3(STP)/g and by FSP were about 0.43-0.55 cm^3(STP)/g. For the total pore volume of ZrO_2 supported catalysts prepared by impregnation method (Gly-Imp) were about 0.17-0.18 cm^3(STP)/g but by FSP were about 0.32-0.54 cm^3(STP)/g

Table 7 The BET surface area, mean pore diameter, total pore volume and particle size diameter

Catalysts	BET surface area[a] (m^2/g)	Mean pore diameter[a] (nm)	Total pore volume[a] (cm^3(STP)/g)	Particle size diameter[b] (nm)
0.5%Pt/TiO_2 (Gly-Imp)	110	16.1	0.44	12.9
0.5%Pt-0.5%Sn/TiO_2 (Gly-Imp)	103	17.9	0.46	13.8
0.5%Pt-1.0%Sn/TiO_2 (Gly-Imp)	94	24.4	0.57	15.1
0.5%Pt-1.5%Sn/TiO_2 (Gly-Imp)	95	22.6	0.54	14.9
0.5%Pt/TiO_2 (FSP)	71	30.9	0.55	20.0
0.5%Pt-0.5%Sn/TiO_2 (FSP)	71	30.8	0.55	20.0
0.5%Pt-1.0%Sn/TiO_2 (FSP)	71	24.9	0.44	20.0
0.5%Pt-1.5%Sn/TiO_2 (FSP)	71	26.4	0.43	20.0
0.5%Pt/ZrO_2 (Gly-Imp)	151	4.6	0.18	7.0
0.5%Pt-0.5%Sn/ZrO_2 (Gly-Imp)	148	4.7	0.18	7.1
0.5%Pt-1.0%Sn/ZrO_2 (Gly-Imp)	147	4.7	0.17	7.2
0.5%Pt-1.5%Sn/ZrO_2 (Gly-Imp)	143	4.9	0.17	7.4
0.5%Pt/ZrO_2 (FSP)	52	41.4	0.54	20.3
0.5%Pt-0.5%Sn/ZrO_2 (FSP)	52	40.7	0.53	20.3
0.5%Pt-1.0%Sn/ZrO_2 (FSP)	53	24.1	0.32	19.9
0.5%Pt-1.5%Sn/ZrO_2 (FSP)	50	27.6	0.34	21.1

[a]Using N_2 physisorption at -196ºC, Error of measurement ± 5%

[b]Particle diameter = 6/(density ×BET surface area)

The nature of pore of catalyst was studied using N_2 adsorption/desortion isotherms and pore size distribution curve. Figure 11- Figure 14 shows the N_2 adsorption/desorption isotherm and the pore size distribution of the TiO_2 supported Pt-Sn catalysts from impregnation method (Gly-Imp). It was found that hysteresis loop indicating the presence of opened pores and associated with a cylinder mesoporous (Eberhardt et al. 2004: 137). Figure 15- Figure 18 shows isotherms of the TiO_2 supported Pt-Sn catalysts prepared by FSP mehod. It was found that the typical

adsorption-desorption isotherms of agglomerated flame-synthesized materials characterized by nonporous primary nanoparticles (Piacentini et al. 2006: 45-46). Figure 19- Figure 22 shows the N_2 adsorption/desorption isotherm and the pore size distribution of the ZrO_2 supported Pt-Sn catalysts from impregnation method (Gly-Imp). It was found that hysteresis loop indicating the presence of closed or opened pores and associated with ink-bottle pores where entrance to the pore was narrower than the body. Figure 23- Figure 26 shows the N_2 adsorption/desorption isotherm and the pore size distribution of the ZrO_2 supported Pt-Sn catalysts from FSP. It was found that hysteresis loop indicating the typical adsorption-desorption isotherms of agglomerated flame-synthesized materials characterized by very small nonporous primary particles with interstitial volumes between the particles (Piacentini, Maciejewski and Baiker 2006: 128-130).

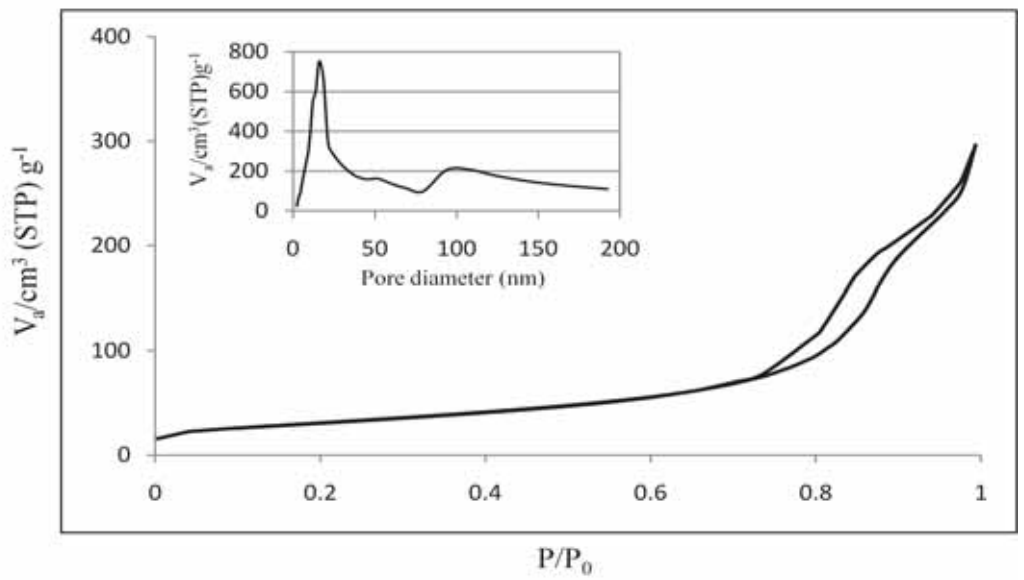

Figure 11 The N_2 adsorption/desorption isotherm and the pore size distribution of 0.5%Pt/TiO_2 (Gly-Imp)

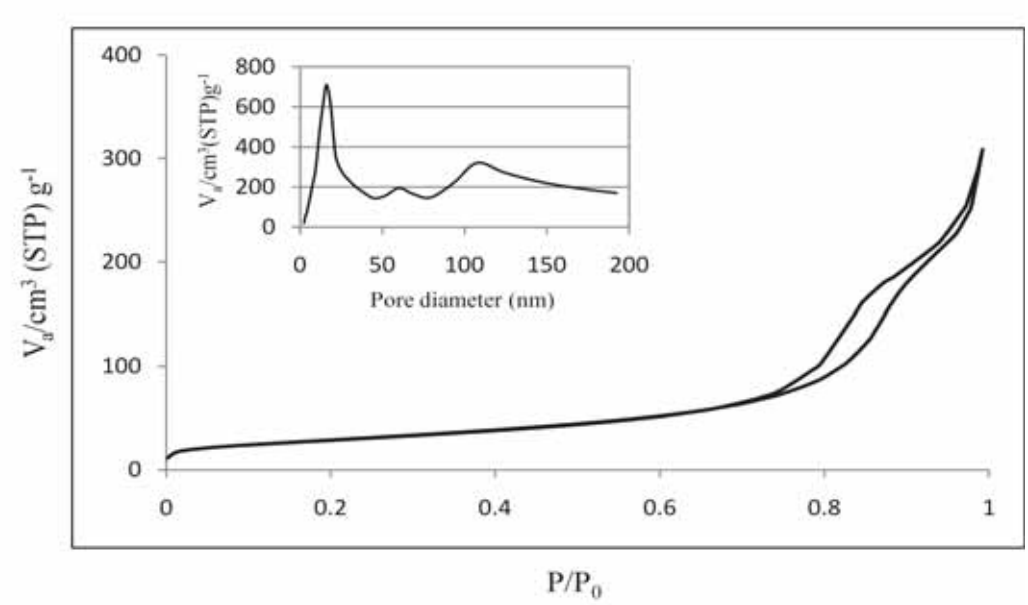

Figure 12 The N_2 adsorption/desorption isotherm and the pore size distribution of 0.5%Pt-0.5%Sn/TiO_2 (Gly-Imp)

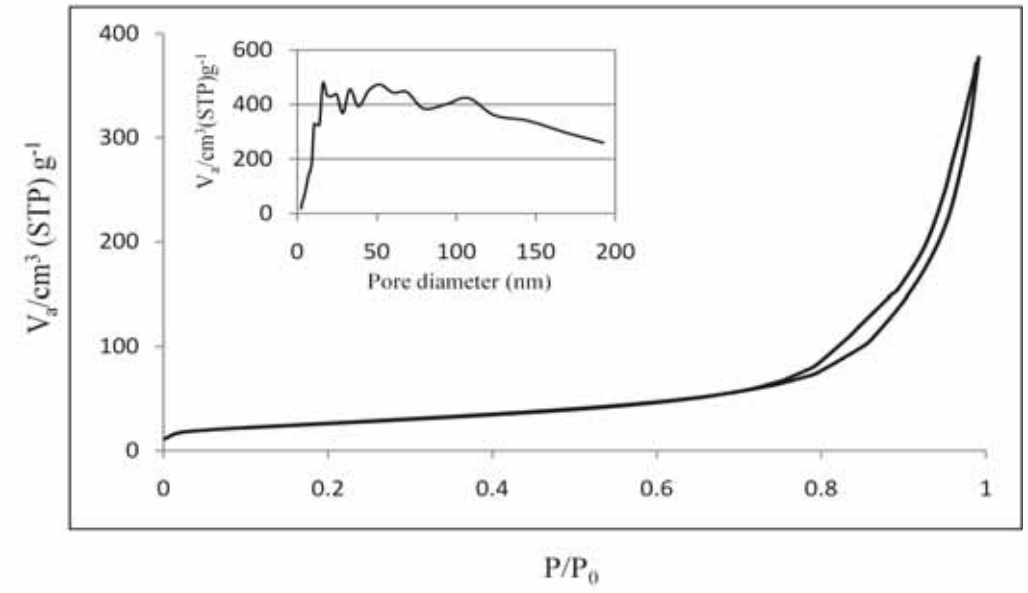

Figure 13 The N_2 adsorption/desorption isotherm and the pore size distribution of 0.5%Pt-1.0%Sn/TiO_2 (Gly-Imp)

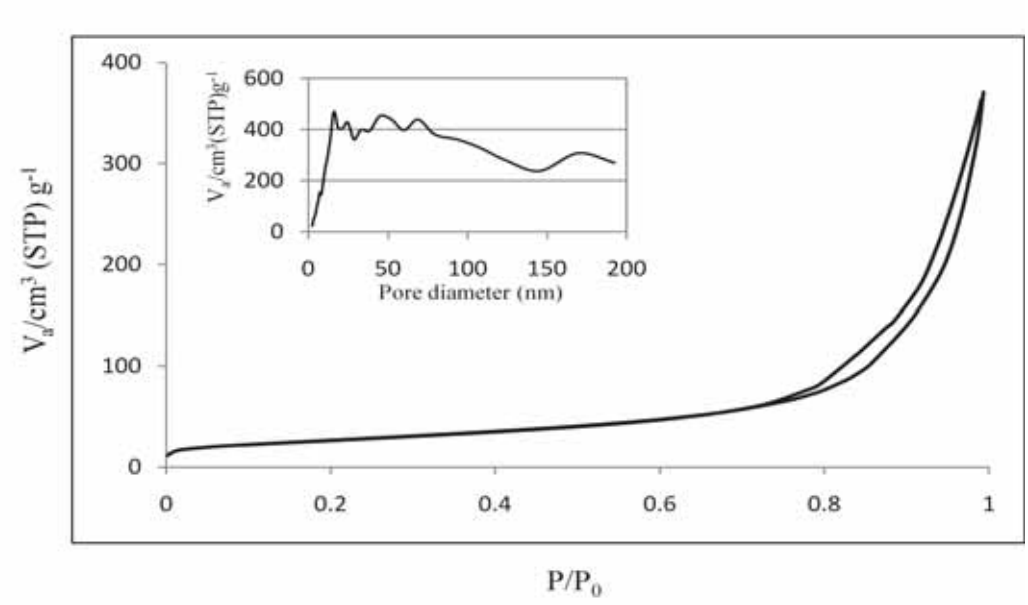

Figure 14 The N_2 adsorption/desorption isotherm and the pore size distribution of 0.5%Pt-1.5%Sn/TiO_2 (Gly-Imp)

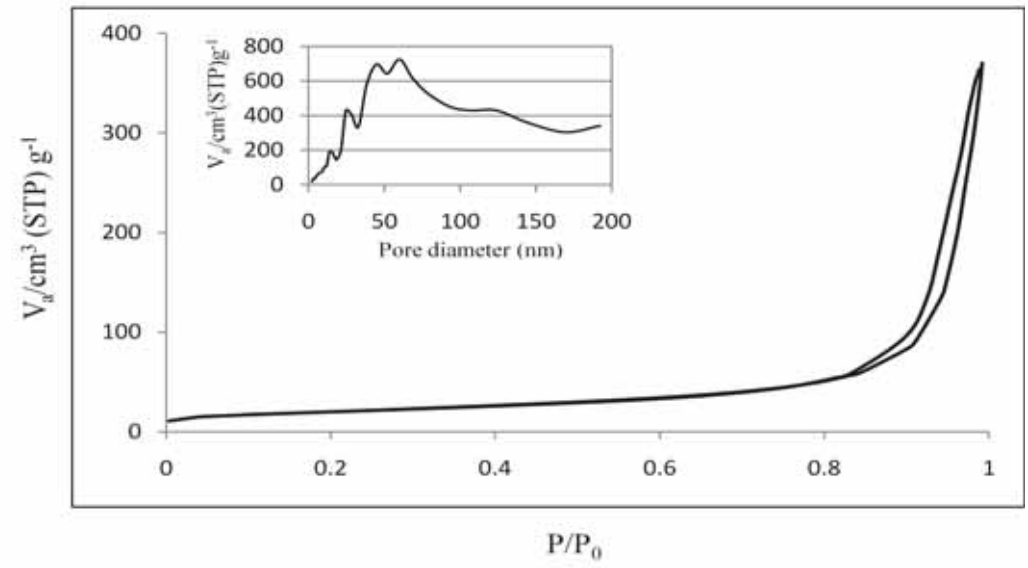

Figure 15 The N_2 adsorption/desorption isotherm and the pore size distribution of 0.5%Pt/TiO_2 (FSP)

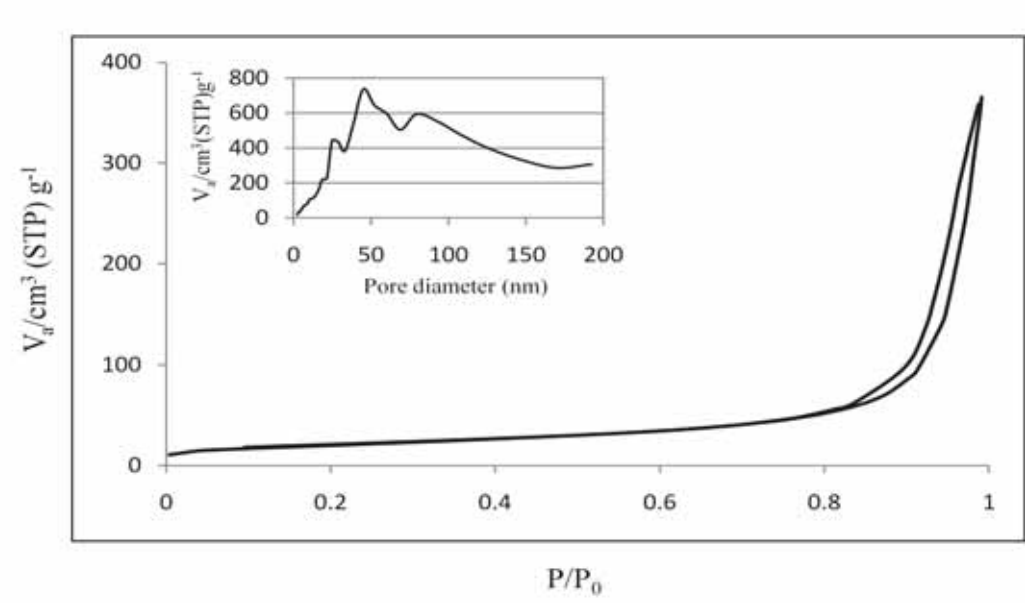

Figure 16 The N_2 adsorption/desorption isotherm and the pore size distribution of 0.5%Pt-0.5%Sn/TiO_2 (FSP)

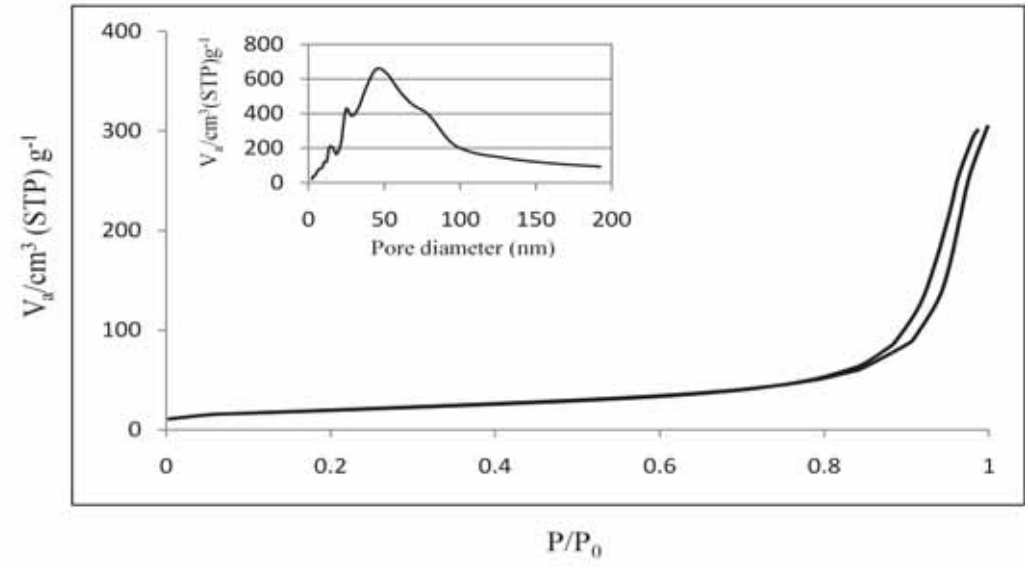

Figure 17 The N_2 adsorption/desorption isotherm and the pore size distribution of 0.5%Pt-1.0%Sn/TiO_2 (FSP)

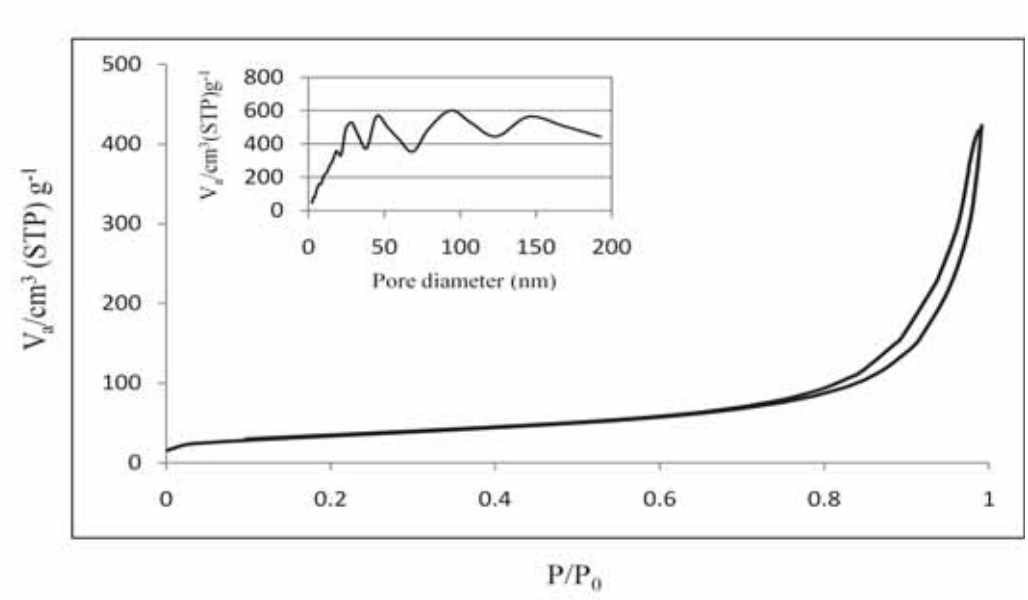

Figure 18 The N_2 adsorption/desorption isotherm and the pore size distribution of 0.5%Pt-1.5%Sn/TiO_2 (FSP)

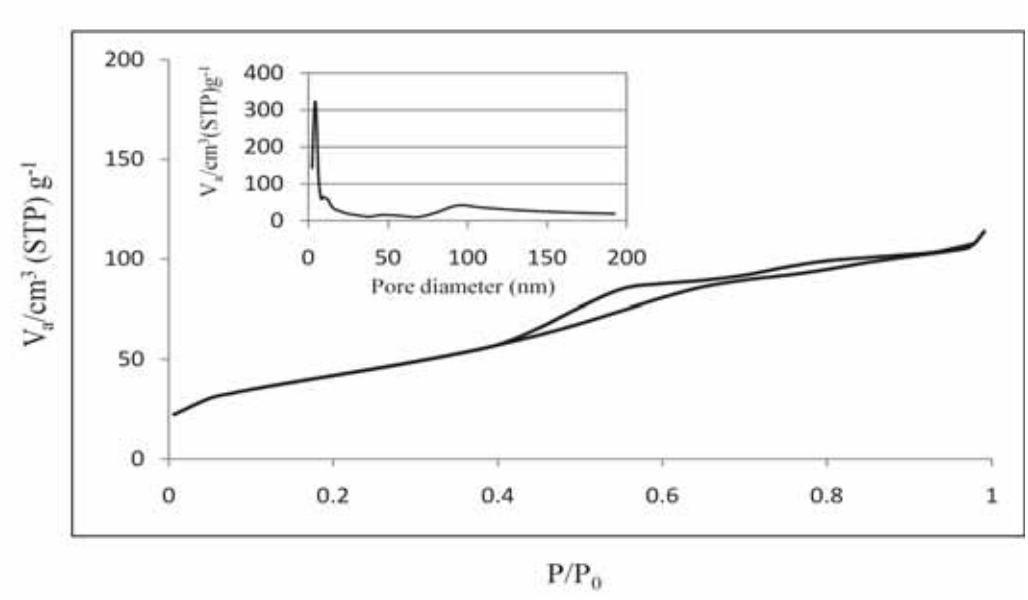

Figure 19 The N_2 adsorption/desorption isotherm and the pore size distribution of 0.5%Pt/ZrO_2 (Gly-Imp)

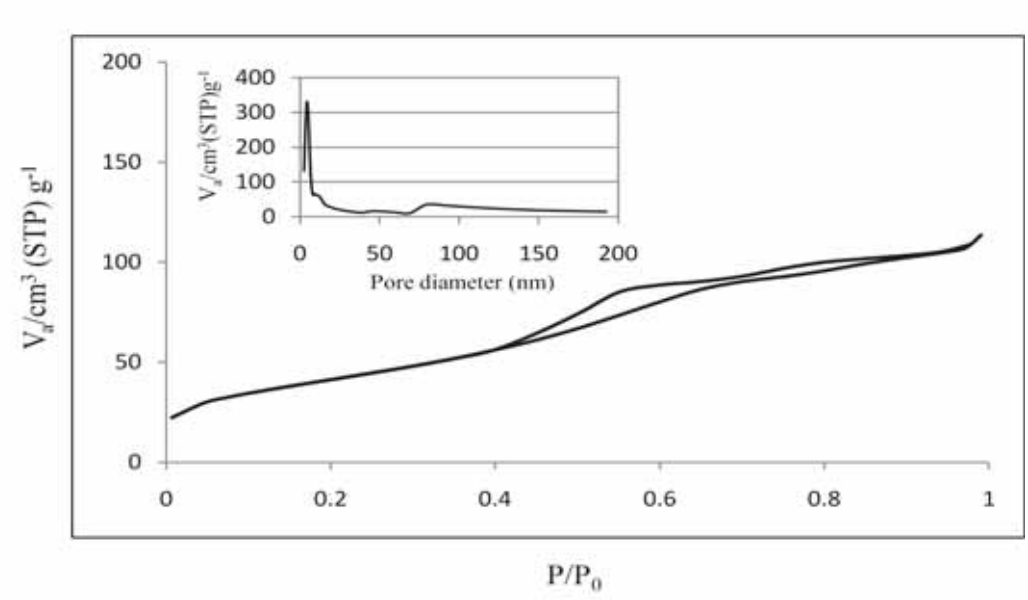

Figure 20 The N_2 adsorption/desorption isotherm and the pore size distribution of 0.5%Pt-0.5%Sn/ZrO_2 (Gly-Imp)

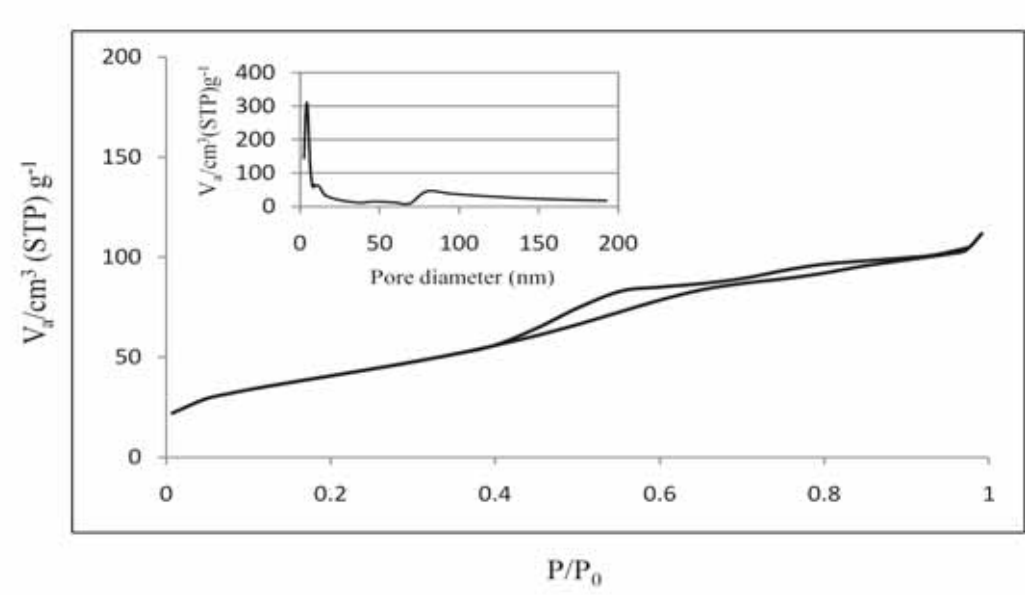

Figure 21 The N_2 adsorption/desorption isotherm and the pore size distribution of 0.5%Pt-1.0%Sn/ZrO_2 (Gly-Imp)

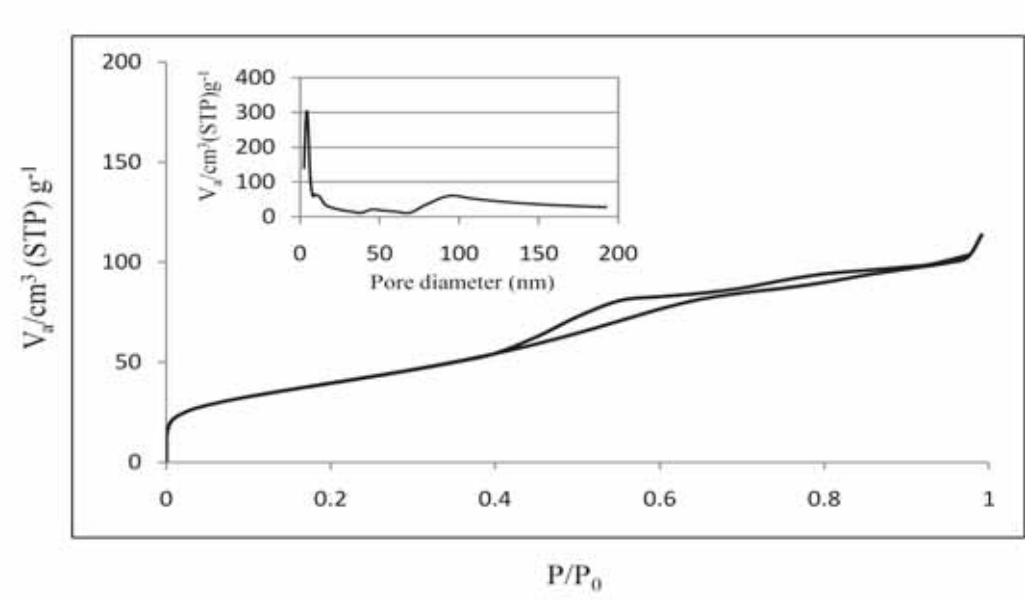

Figure 22 The N_2 adsorption/desorption isotherm and the pore size distribution of 0.5%Pt-1.5%Sn/ZrO_2 (Gly-Imp)

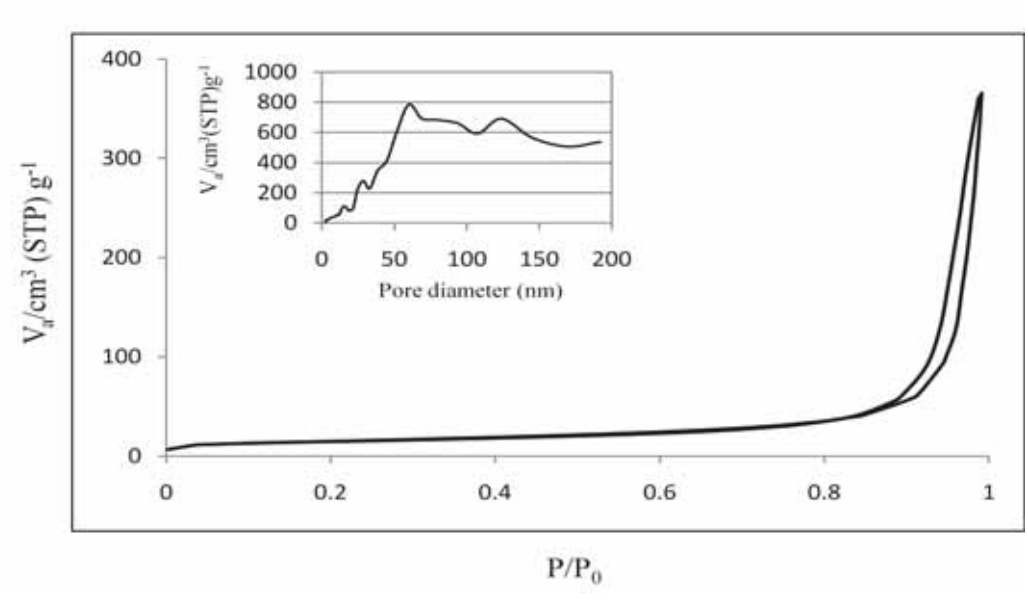

Figure 23 The N_2 adsorption/desorption isotherm and the pore size distribution of 0.5%Pt/ZrO_2 (FSP)

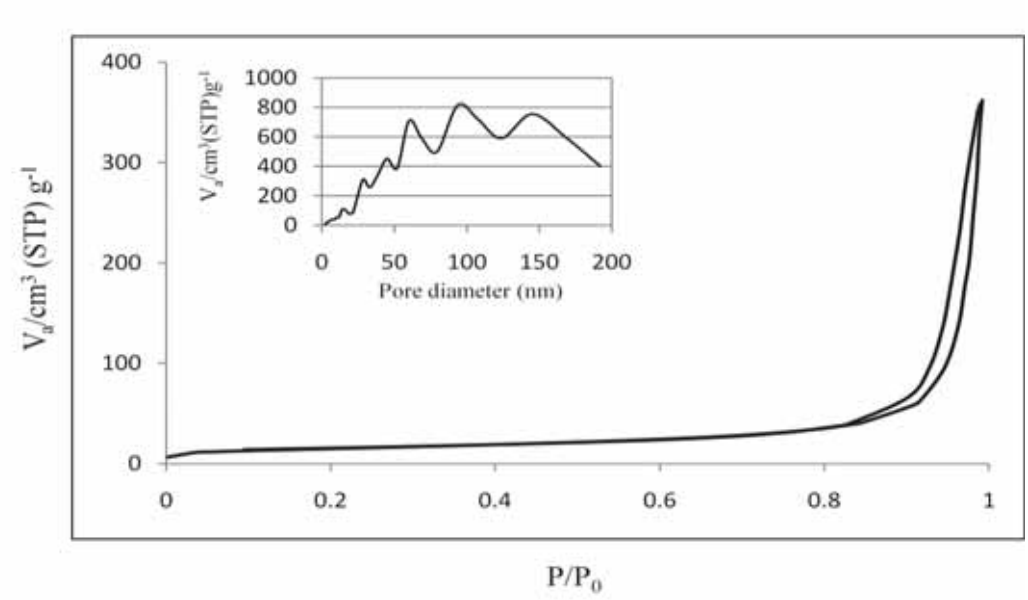

Figure 24 The N_2 adsorption/desorption isotherm and the pore size distribution of 0.5%Pt-0.5%Sn/ZrO_2 (FSP)

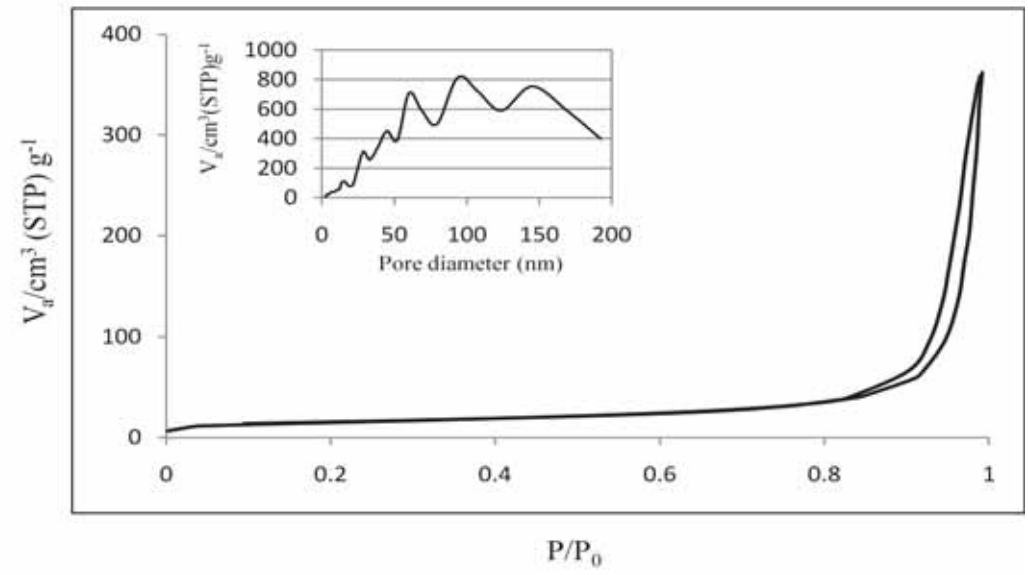

Figure 25 The N_2 adsorption/desorption isotherm and the pore size distribution of 0.5%Pt-1.0%Sn/ZrO_2 (FSP)

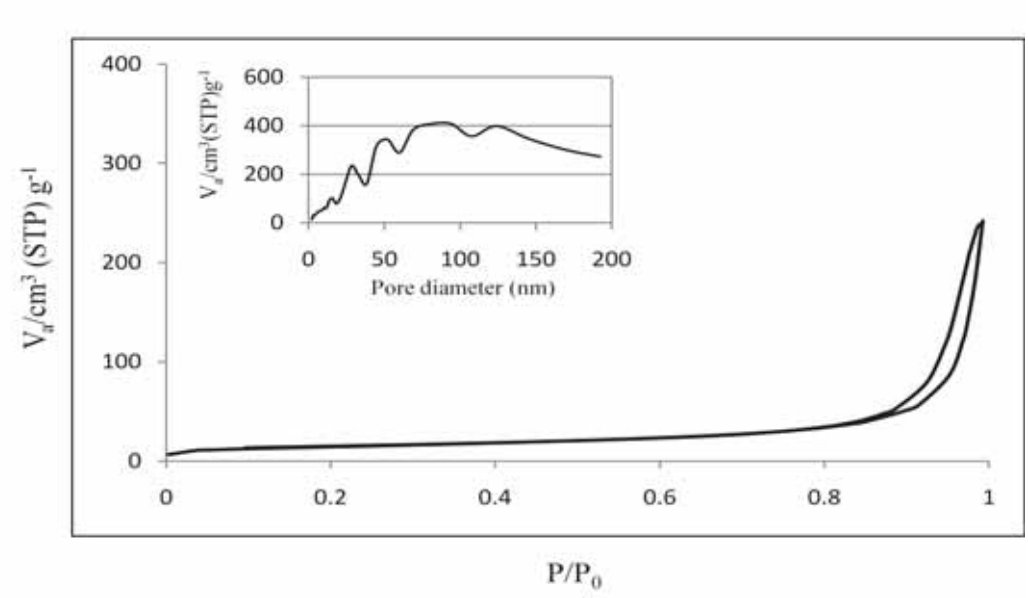

Figure 26 The N_2 adsorption/desorption isotherm and the pore size distribution of 0.5%Pt-1.5%Sn/ZrO_2 (FSP)

5.1.3 Transmission electron microscope (TEM)

Transmission electron microscope (TEM) is a conventional method to give detailed information about the shape, particle size distribution and mean particle size of the catalysts. Figure 27- Figure 58 show the TEM images and particle size distribution of catalysts where mean particle size (μ) and standard deviation (σ) were calculated from these TEM images as show in Table 8. It could be seen that catalysts were rather sphere particle. The particle size and the width of distribution curve of catalysts prepared by FSP were larger than the catalysts prepared by impregnation method (Gly-Imp). Addition of tin onto the catalysts, it was found that mean particle size of TiO_2 supported catalysts prepared by impregnation method (Gly-Imp) decreased from 12.6 nm to 11.1 nm as the amounts of Sn loading increased from 0 to 0.5 wt% and then increased to 13.0 nm after the addition of Sn further increased to 1.5 wt%. In the case of FSP-made catalyst, the mean particle size increased from 16.6 to 22.7 nm as the Sn loading increased from 0 to 1.0 wt% and then decreased to 16.7 nm after the addition of Sn further increased to 1.5 wt%. The mean particle sizes of ZrO_2

supported catalysts prepared by impregnation method (Gly-Imp) were constant around 13.0-15.6 nm. In the case of FSP-made catalyst, the mean particle sizes were constant around 19.0-21.1 nm.

Table 8 The mean particle size of the catalysts from TEM

Catalysts	Mean particle size (nm)	Standard deviation
0.5%Pt/TiO_2 (Gly-Imp)	12.6	2.7
0.5%Pt-0.5%Sn/TiO_2 (Gly-Imp)	11.1	1.4
0.5%Pt-1.0%Sn/TiO_2 (Gly-Imp)	12.4	2.4
0.5%Pt-1.5%Sn/TiO_2 (Gly-Imp)	13.0	2.4
0.5%Pt/TiO_2 (FSP)	16.6	3.7
0.5%Pt-0.5%Sn/TiO_2 (FSP)	21.7	4.6
0.5%Pt-1.0%Sn/TiO_2 (FSP)	22.7	3.7
0.5%Pt-1.5%Sn/TiO_2 (FSP)	16.7	4.0
0.5%Pt/ZrO_2 (Gly-Imp)	13.0	1.8
0.5%Pt-0.5%Sn/ZrO_2 (Gly-Imp)	14.0	1.9
0.5%Pt-1.0%Sn/ZrO_2 (Gly-Imp)	15.6	2.2
0.5%Pt-1.5%Sn/ZrO_2 (Gly-Imp)	14.1	1.6
0.5%Pt/ZrO_2 (FSP)	20.0	3.2
0.5%Pt-0.5%Sn/ZrO_2 (FSP)	19.9	4.4
0.5%Pt-1.0%Sn/ZrO_2 (FSP)	21.1	2.8
0.5%Pt-1.5%Sn/ZrO_2 (FSP)	20.4	3.8

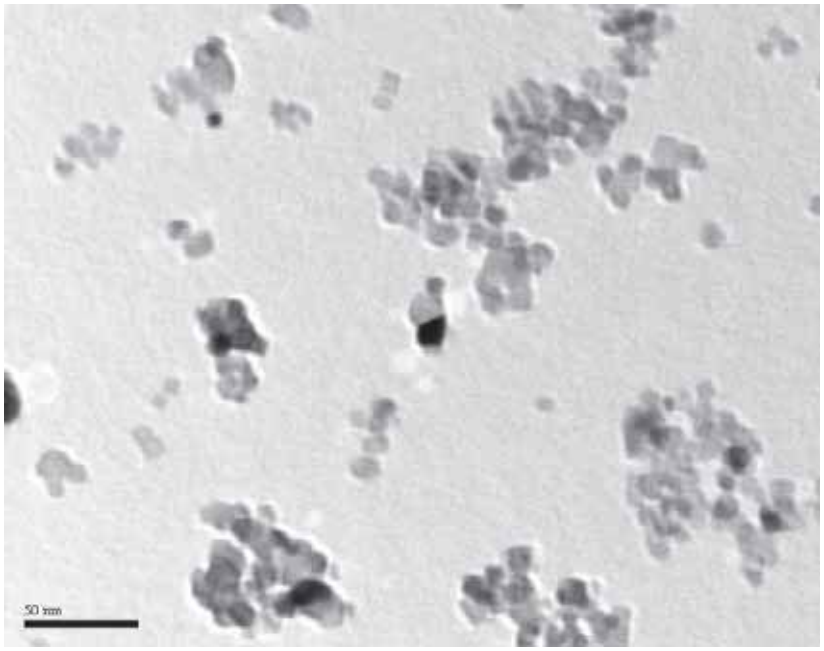

Figure 27 TEM image of 0.5%Pt /TiO_2 (Gly-Imp)

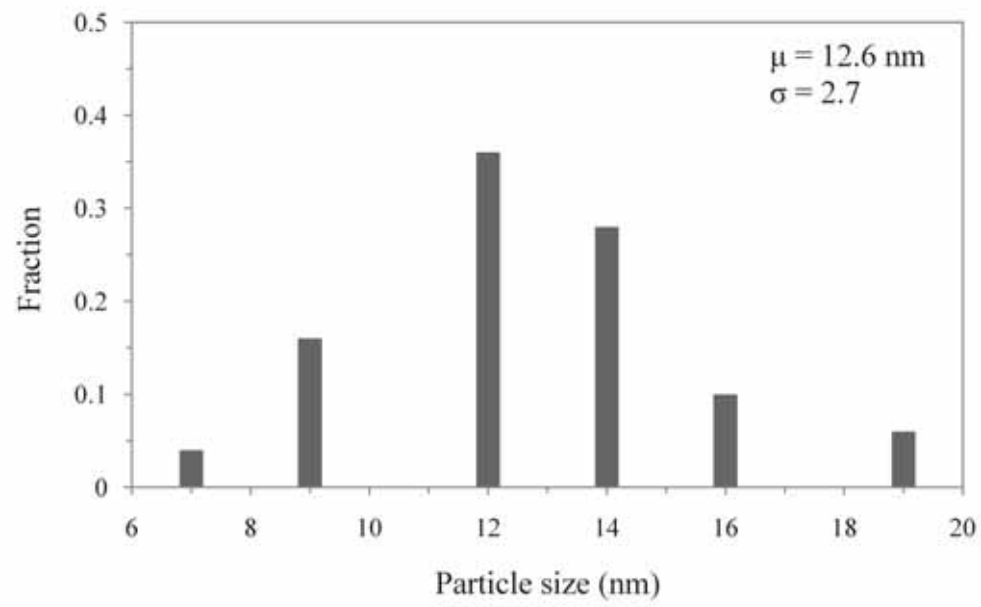

Figure 28 Particle size distribution of 0.5%Pt /TiO_2 (Gly-Imp)

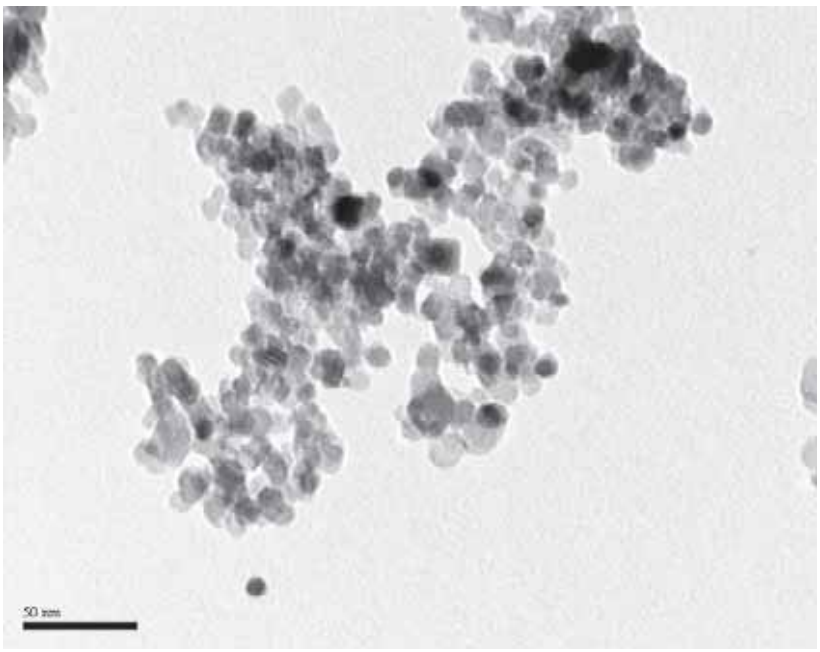

Figure 29 TEM image of 0.5%Pt-0.5%Sn/TiO_2 (Gly-Imp)

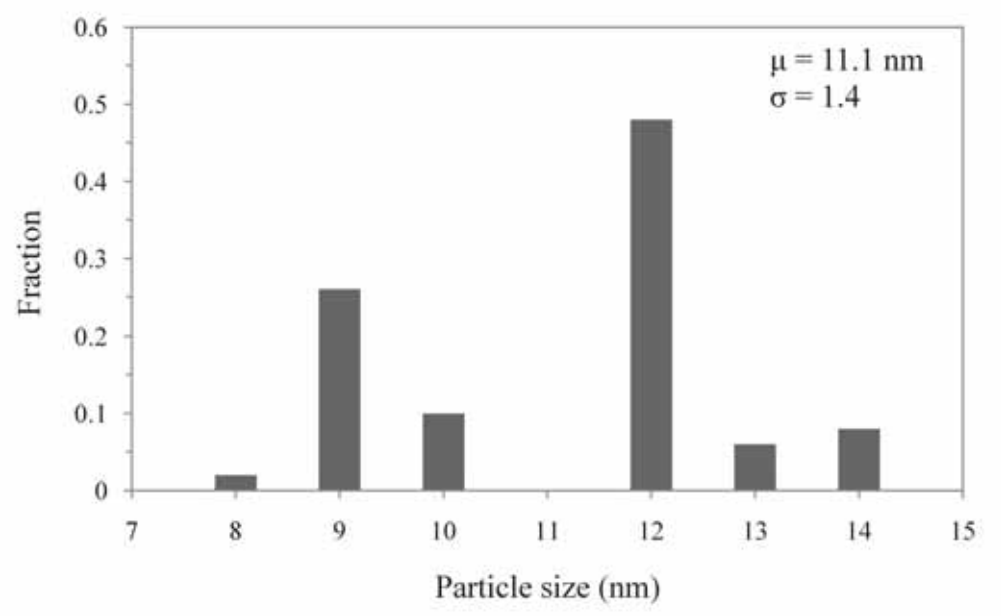

Figure 30 Particle size distribution of 0.5%Pt-0.5%Sn/TiO_2 (Gly-Imp)

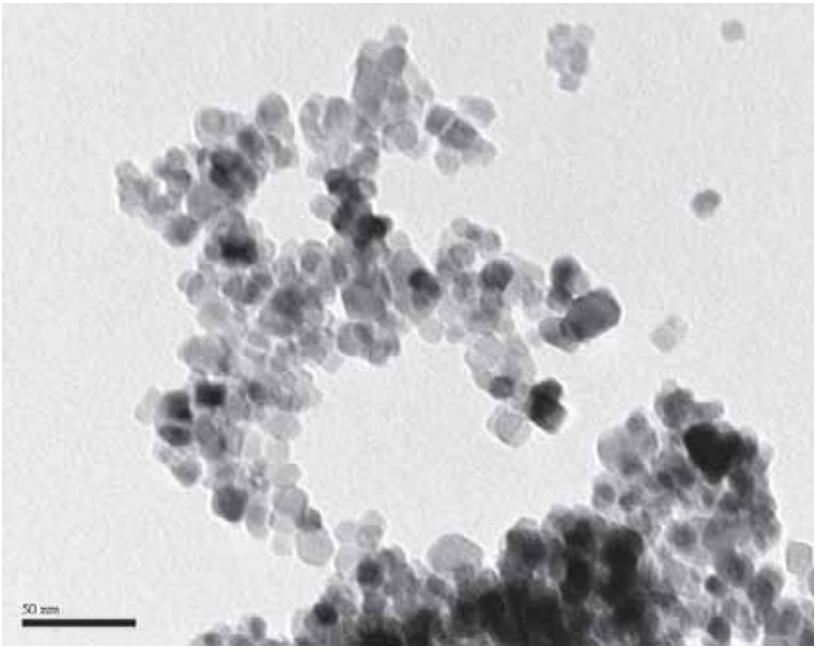

Figure 31 TEM image of 0.5%Pt-1.0%Sn/TiO_2 (Gly-Imp)

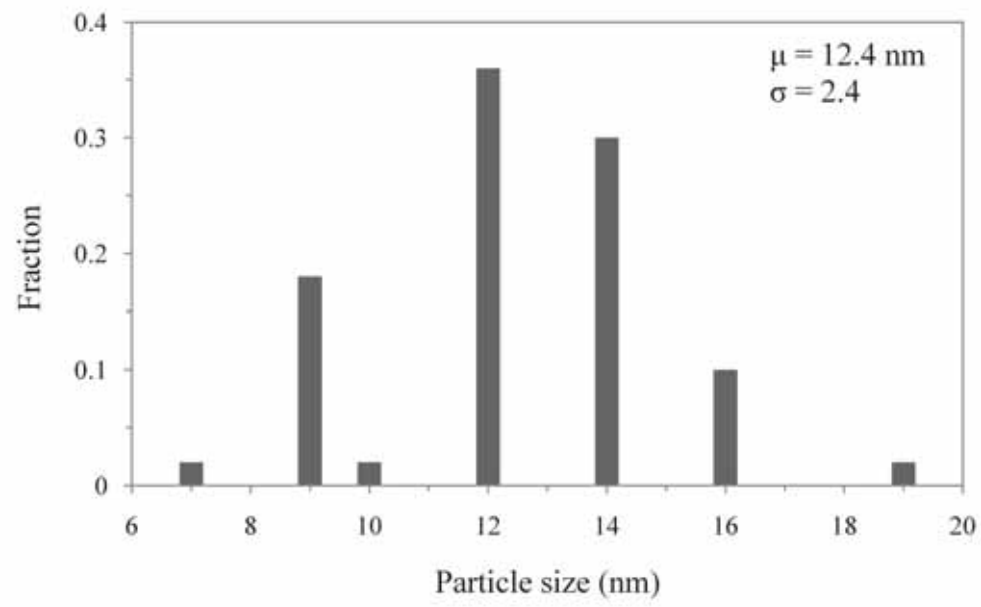

Figure 32 Particle size distribution of 0.5%Pt-1.0%Sn/TiO_2 (Gly-Imp)

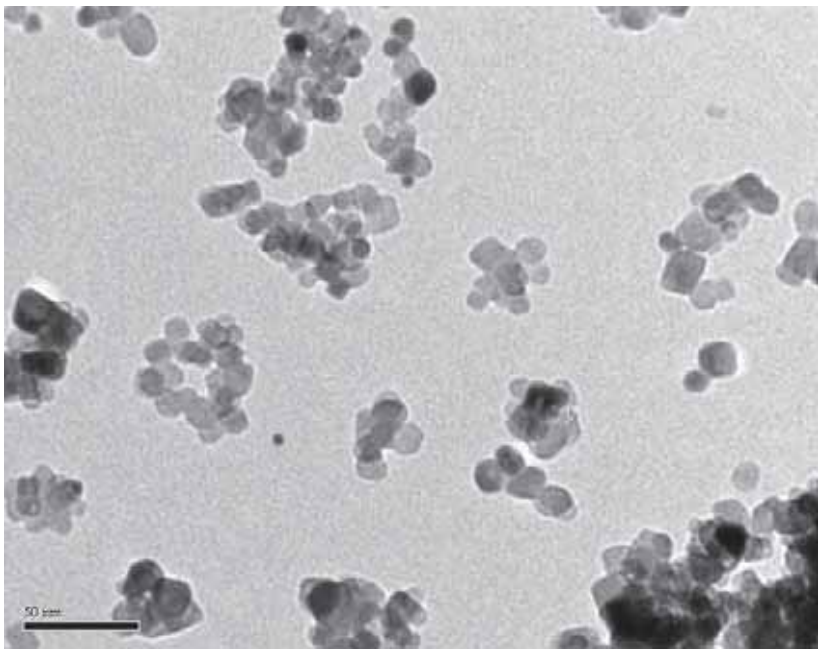

Figure 33 TEM image of 0.5%Pt-1.5%Sn/TiO_2 (Gly-Imp)

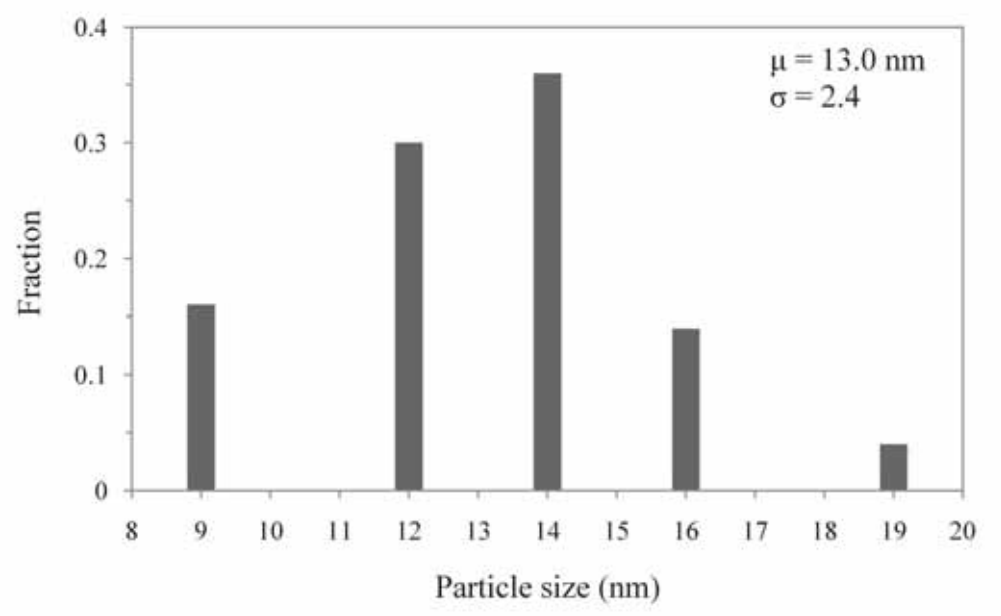

Figure 34 Particle size distribution of 0.5%Pt-1.5%Sn/TiO_2 (Gly-Imp)

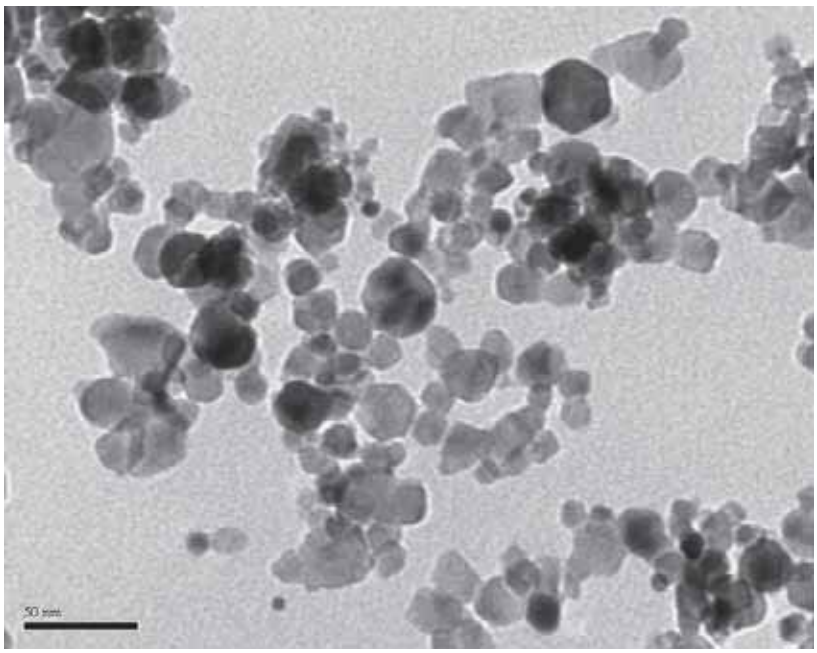

Figure 35 TEM image of 0.5%Pt/TiO_2 (FSP)

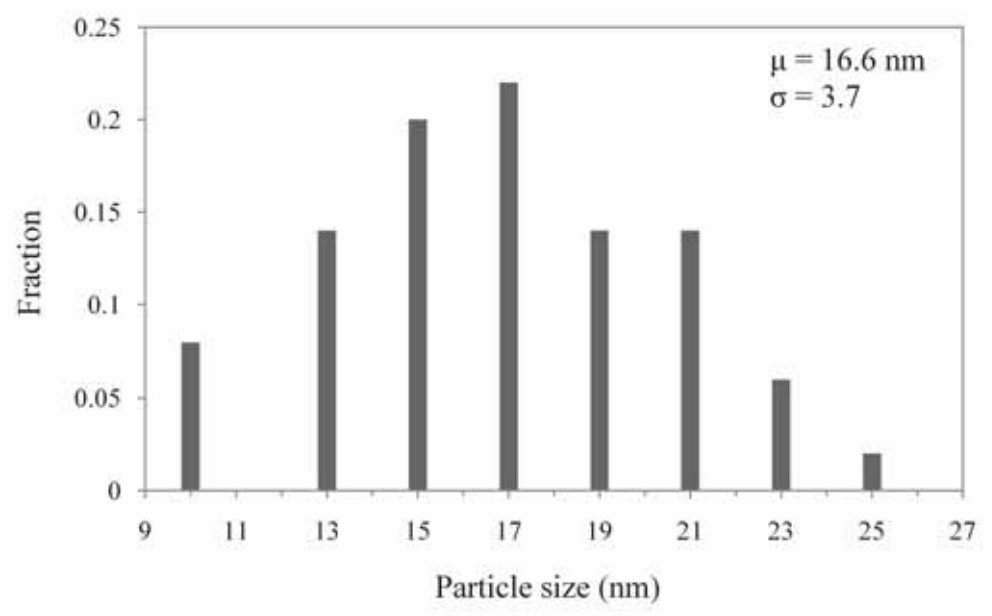

Figure 36 Particle size distribution of 0.5%Pt/TiO_2 (FSP)

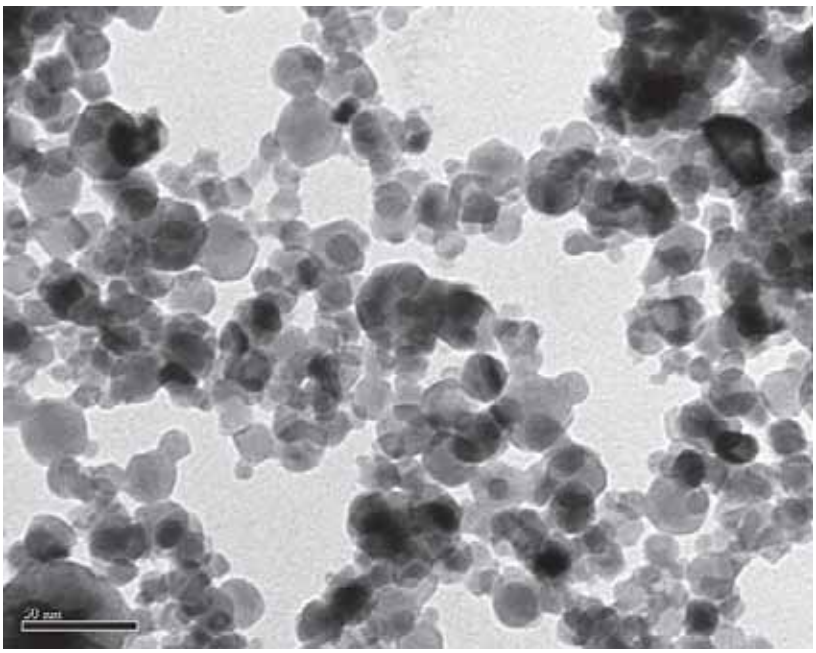

Figure 37 TEM image of 0.5%Pt-0.5%Sn/TiO_2 (FSP)

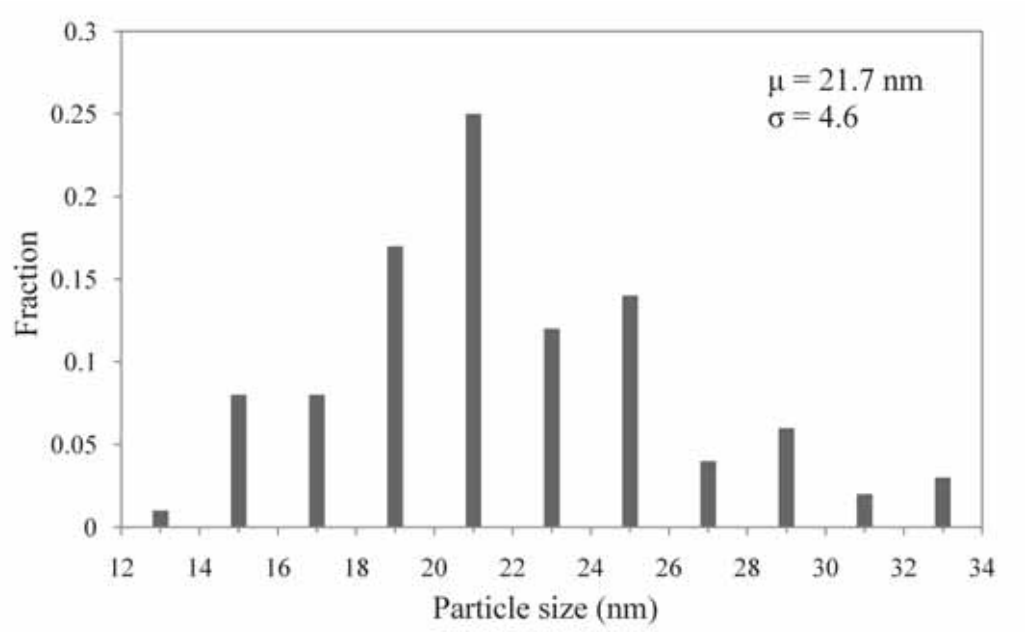

Figure 38 Particle size distribution of 0.5%Pt-0.5%Sn/TiO_2 (FSP)

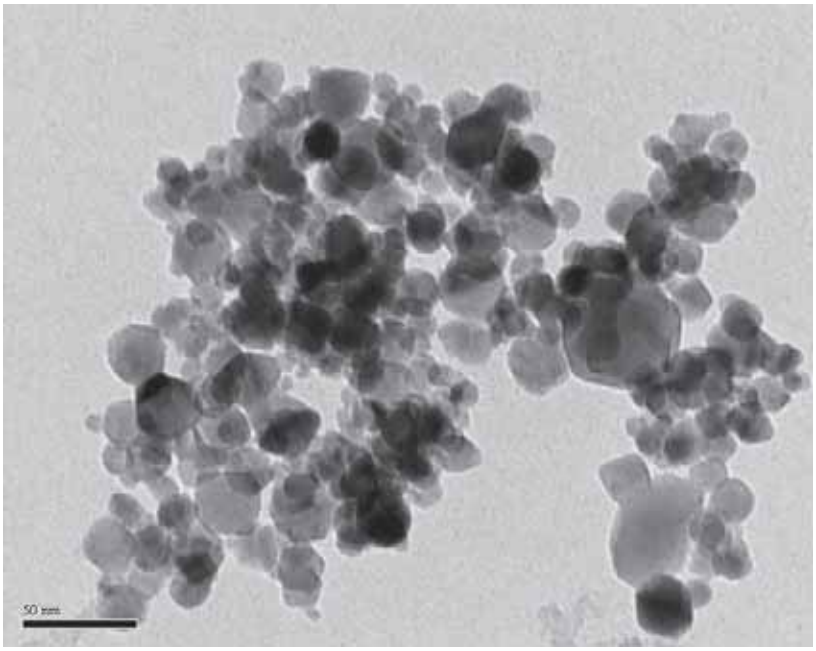

Figure 39 TEM image of 0.5%Pt-1.0%Sn/TiO_2 (FSP)

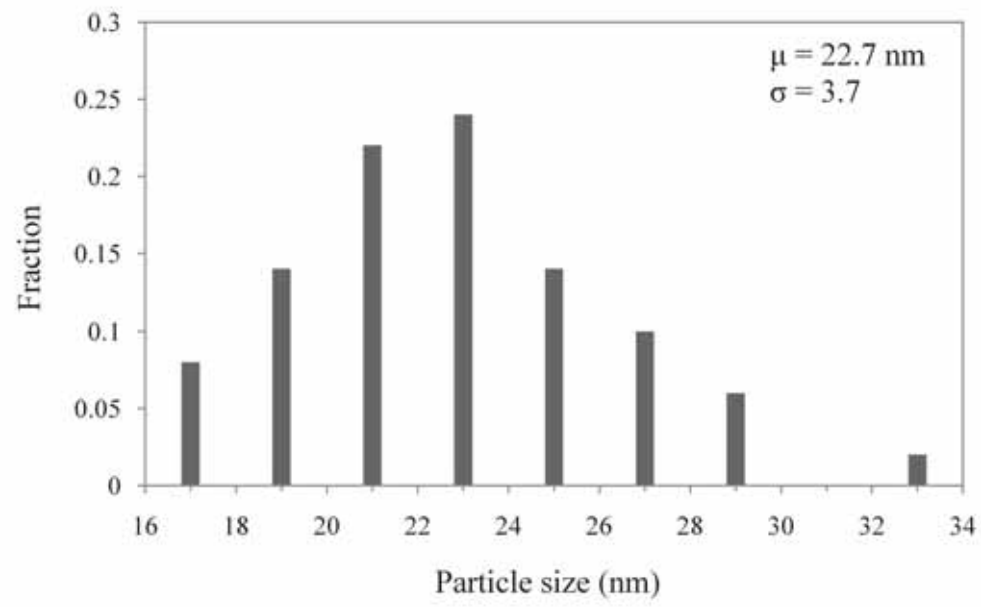

Figure 40 Particle size distribution of 0.5%Pt-1.0%Sn/TiO_2 (FSP)

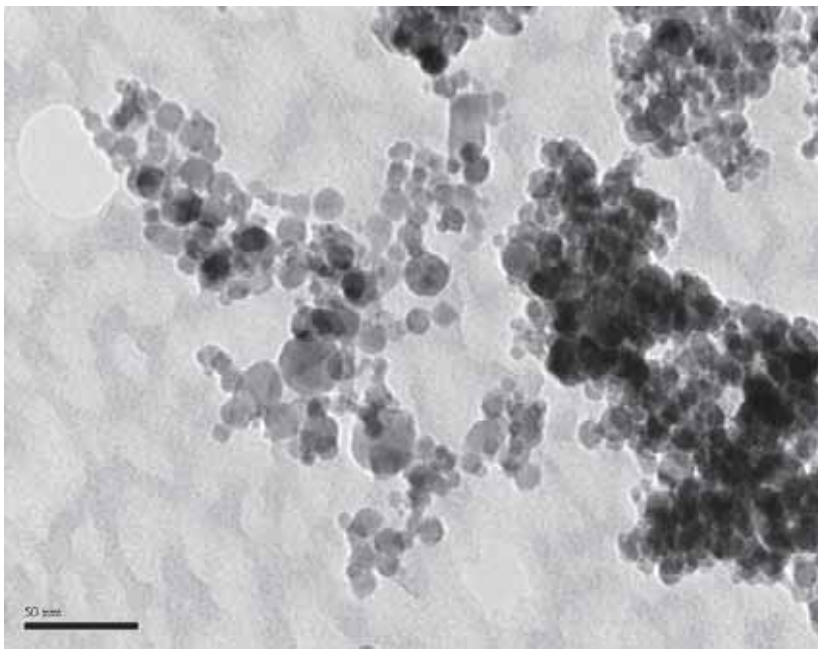

Figure 41 TEM image of 0.5%Pt-1.5%Sn/TiO_2 (FSP)

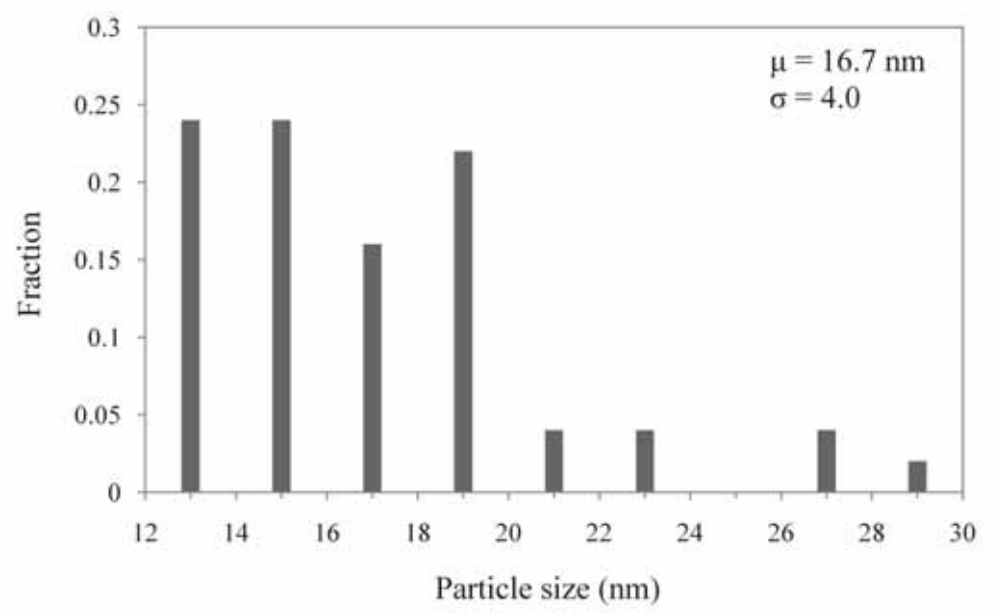

Figure 42 Particle size distribution of 0.5%Pt-1.5%Sn/TiO_2 (FSP)

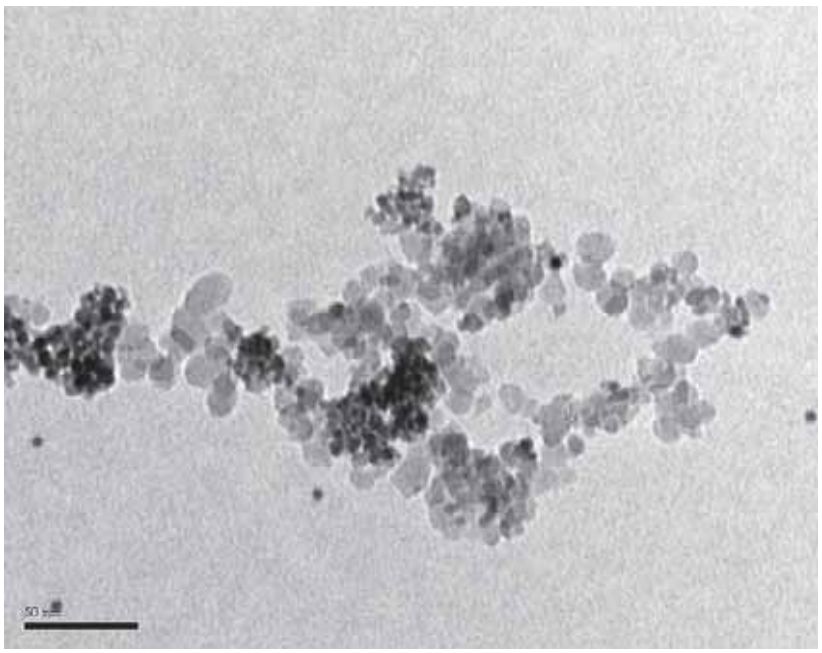

Figure 43 TEM image of 0.5%Pt /ZrO_2 (Gly-Imp)

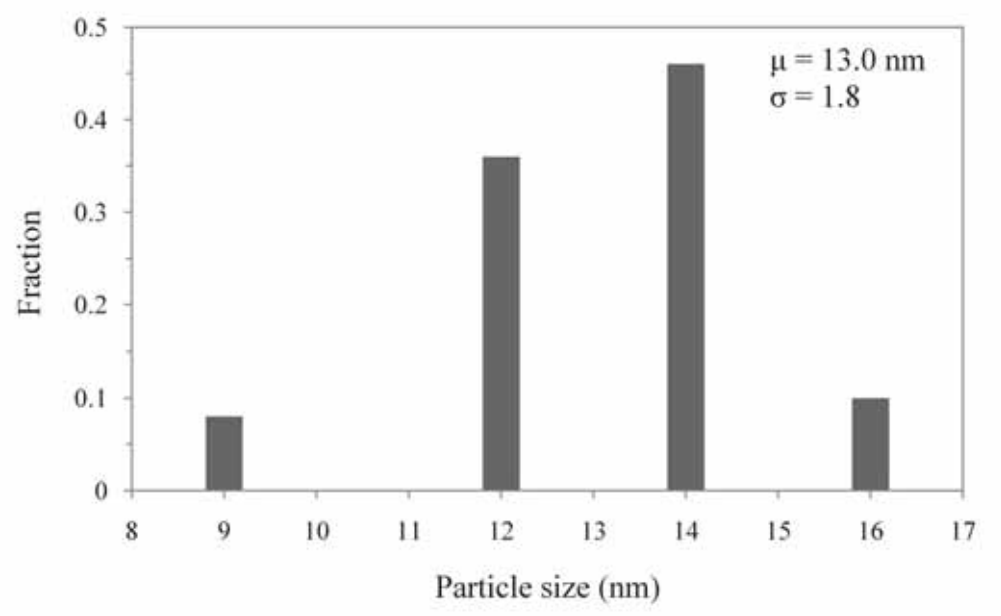

Figure 44 Particle size distribution of 0.5%Pt /ZrO_2 (Gly-Imp)

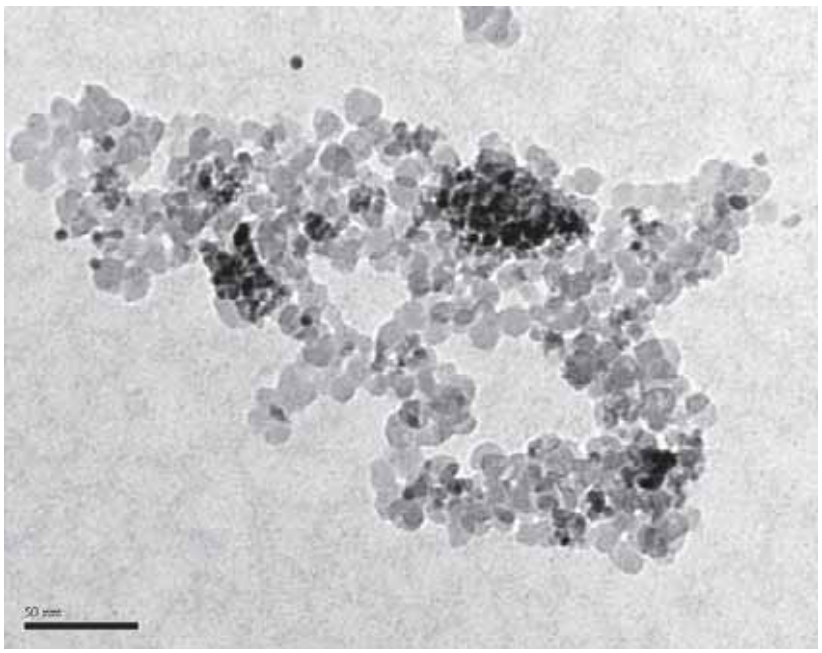

Figure 45 TEM image of 0.5%Pt-0.5%Sn/ZrO_2 (Gly-Imp)

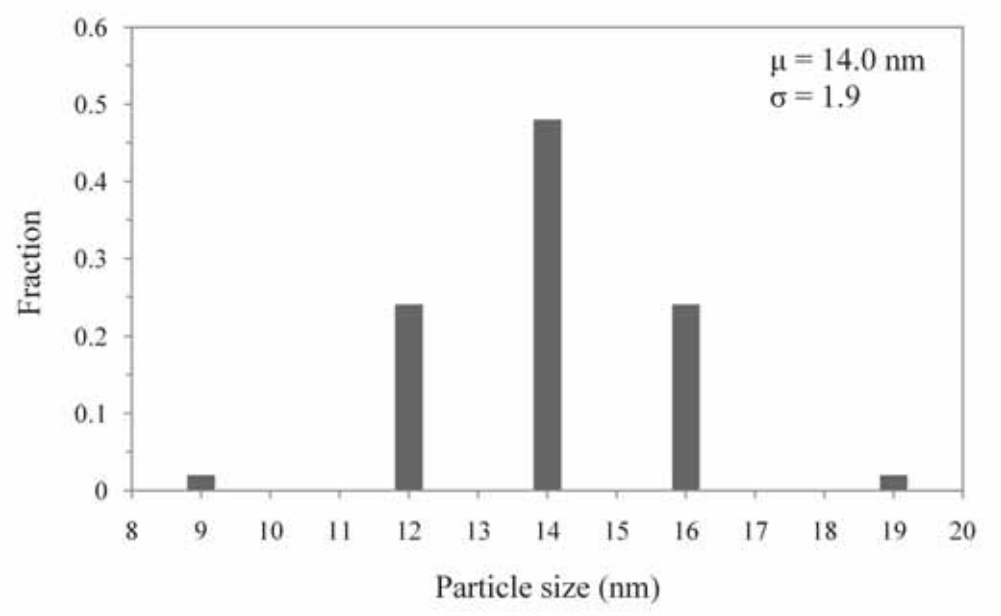

Figure 46 Particle size distribution of 0.5%Pt-0.5%Sn/ZrO_2 (Gly-Imp)

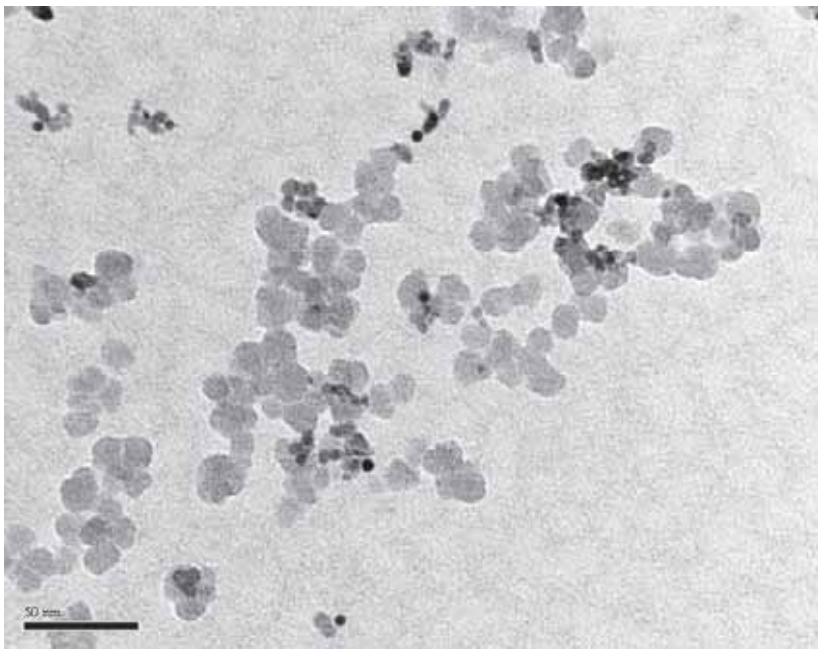

Figure 47 TEM image of 0.5%Pt-1.0%Sn/ZrO_2 (Gly-Imp)

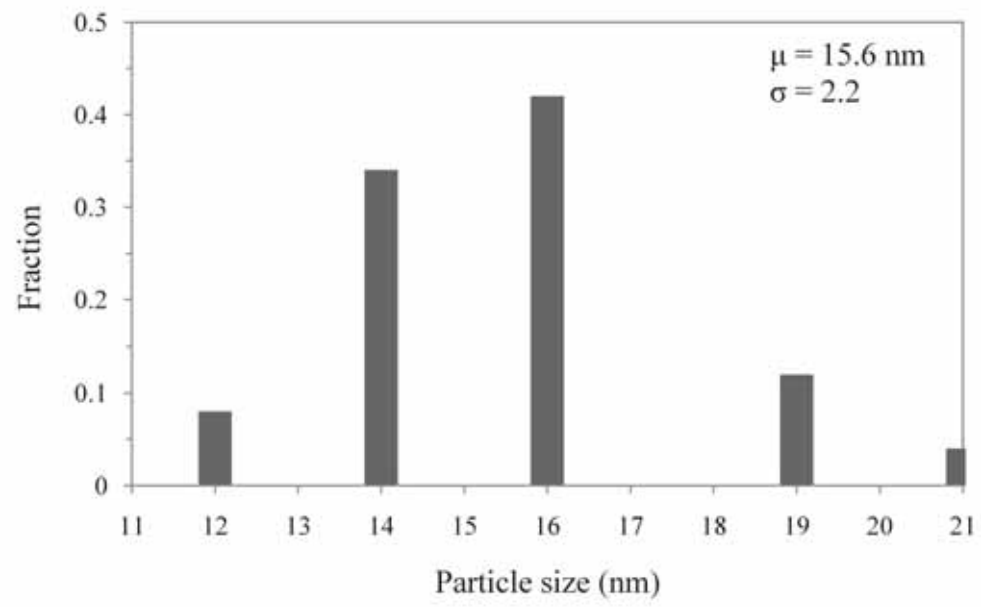

Figure 48 Particle size distribution of 0.5%Pt-1.0%Sn/ZrO_2 (Gly-Imp)

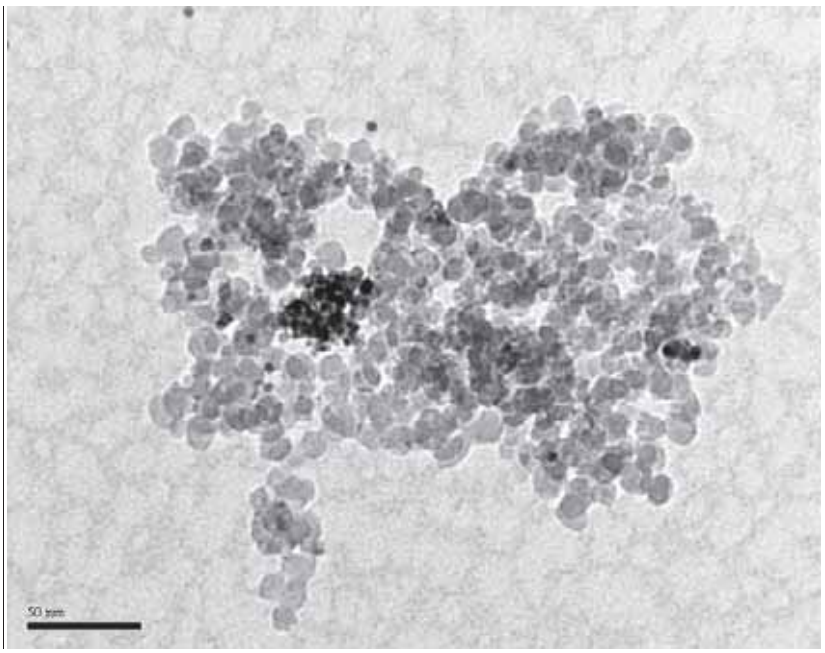

Figure 49 TEM image of 0.5%Pt-1.5%Sn/ZrO_2 (Imp-Gly)

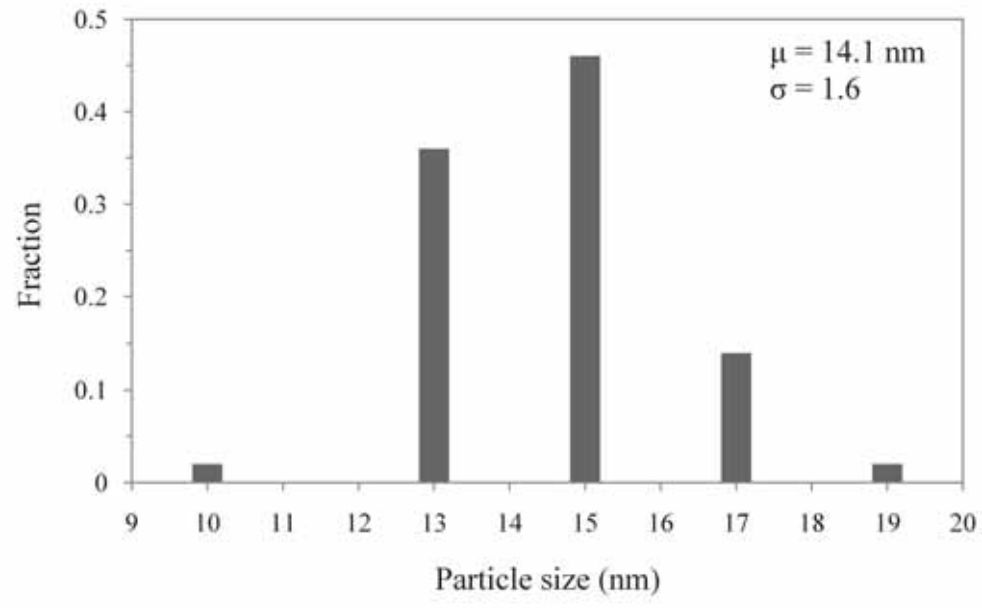

Figure 50 Particle size distribution of 0.5%Pt-1.5%Sn/ZrO_2 (Imp-Gly)

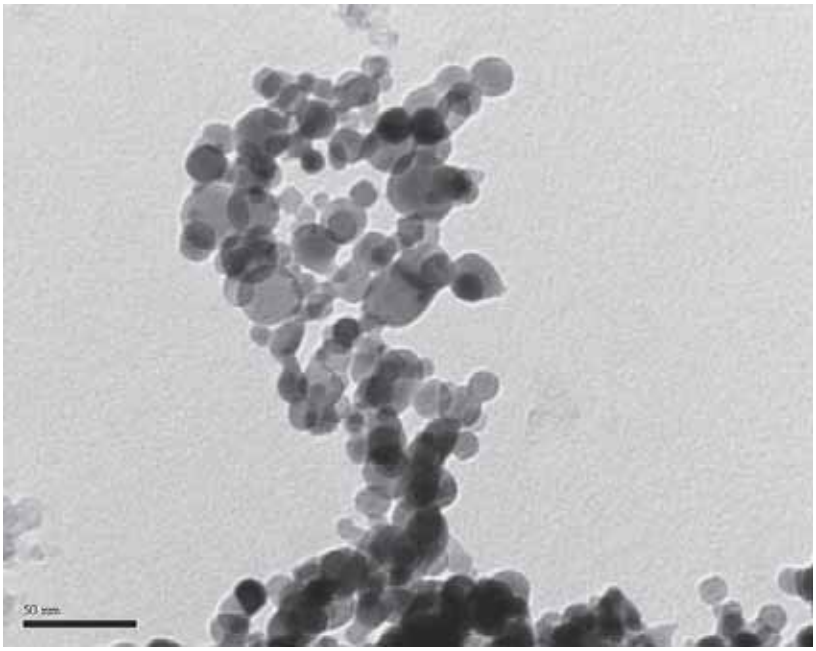

Figure 51 TEM image of 0.5%Pt /ZrO_2 (FSP)

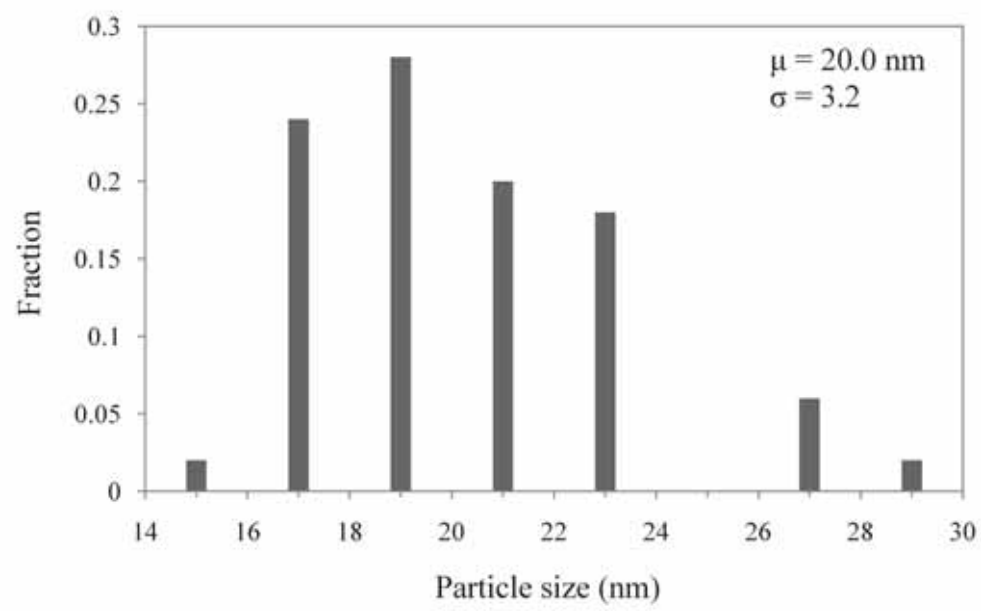

Figure 52 Particle size distribution of 0.5%Pt /ZrO_2 (FSP)

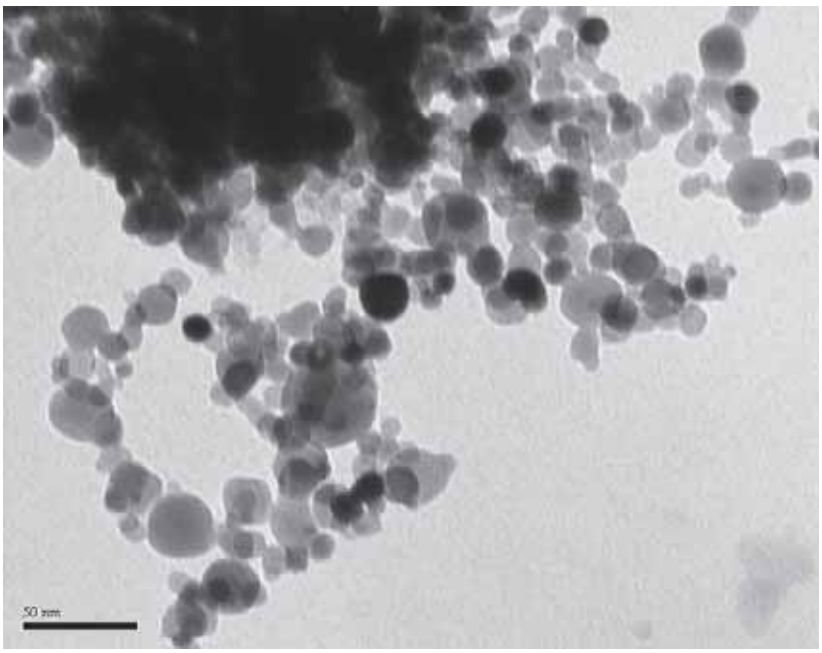

Figure 53 TEM image of 0.5%Pt-0.5%Sn/ZrO_2 (FSP)

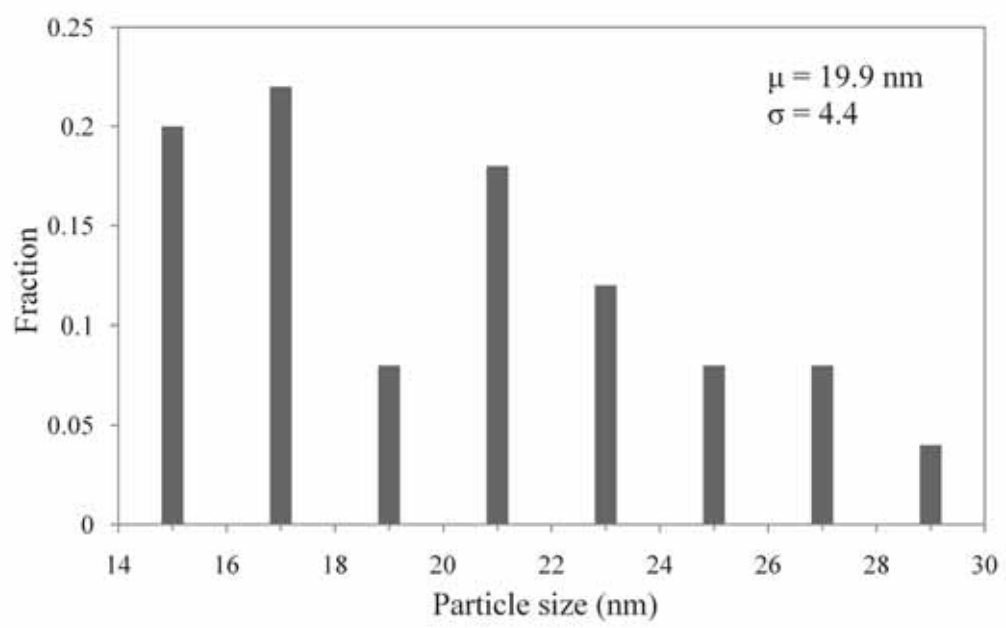

Figure 54 Particle size distribution of 0.5%Pt-0.5%Sn/ZrO_2 (FSP)

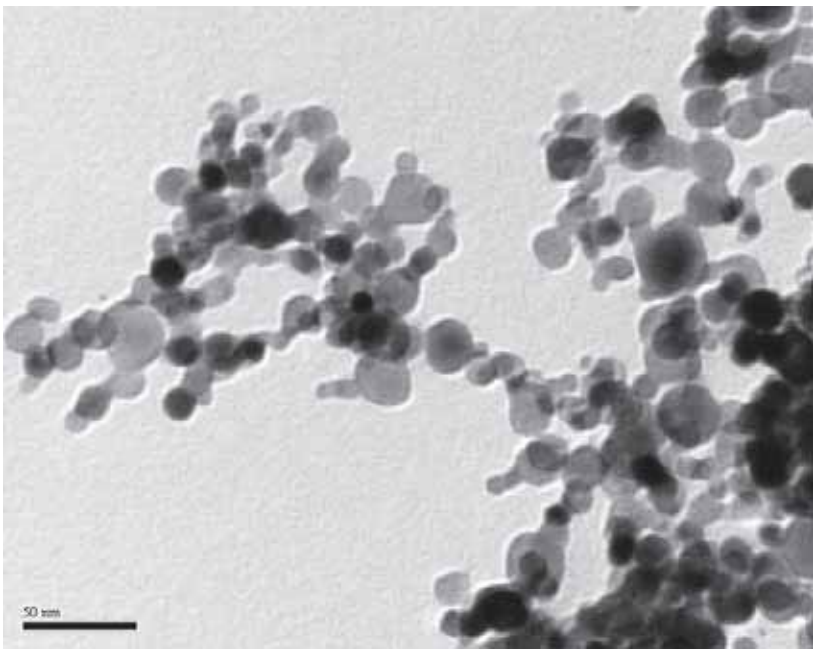

Figure 55 TEM image of 0.5%Pt-1.0%Sn/ZrO_2 (FSP)

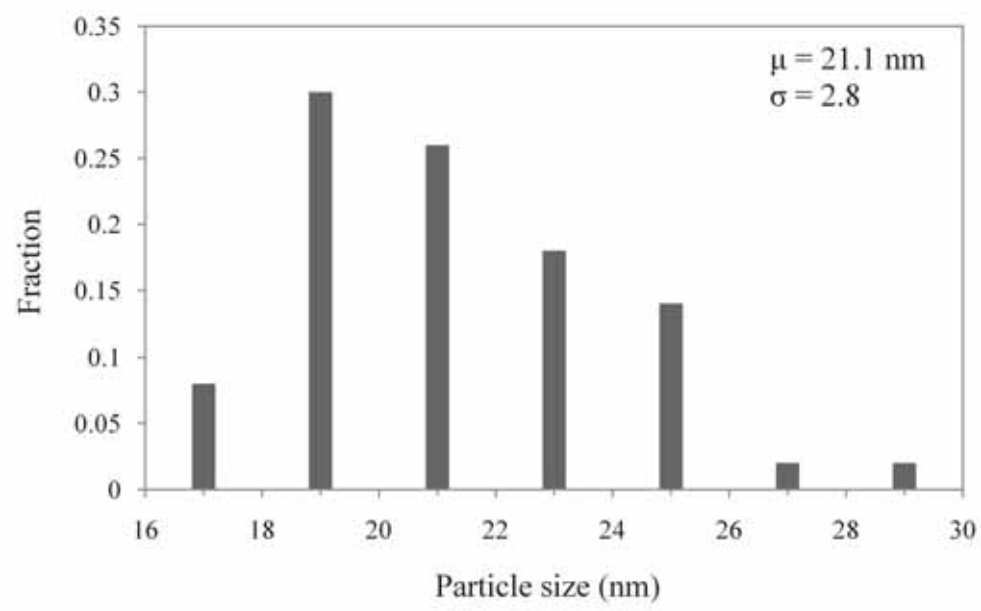

Figure 56 Particle size distribution of 0.5%Pt-1.0%Sn/ZrO_2 (FSP)

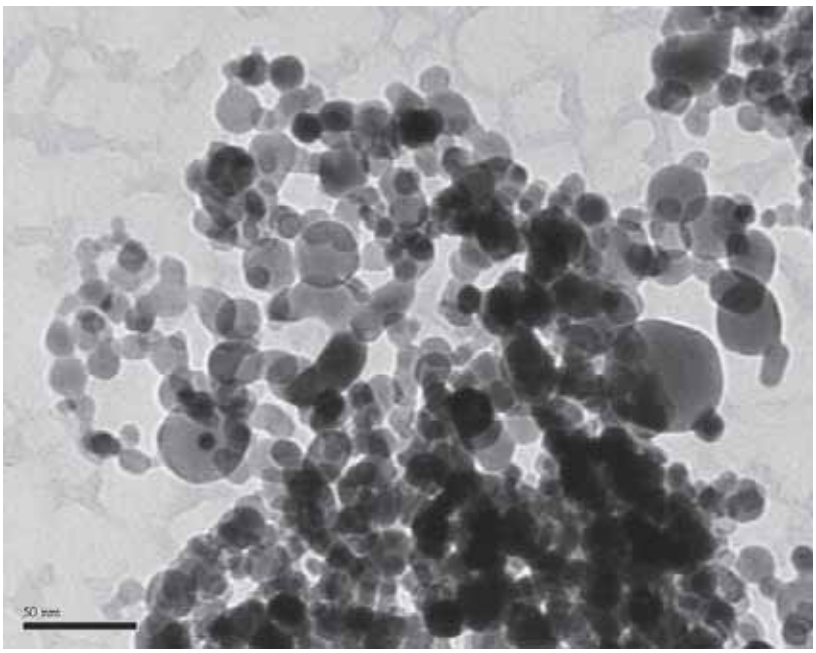

Figure 57 TEM image of 0.5%Pt-1.5%Sn/ZrO_2 (FSP)

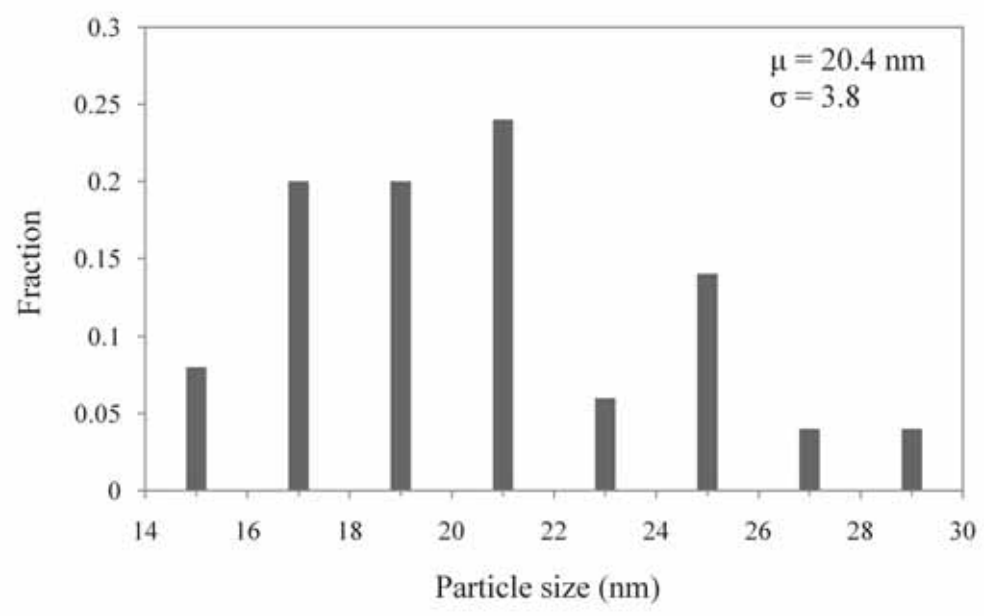

Figure 58 Particle size distribution of 0.5%Pt-1.5%Sn/ZrO_2 (FSP)

5.1.4 CO chemisorptions

The relative amounts of active platinum metal sites on the catalyst samples were calculated from CO chemisorptions which provided the information on the number of platinum active sites, platinum dispersion and mean diameter size of platinum metal. In this research, chemisorptions measurements are based on the assumption of the stoichiometry of 1:1 for CO adsorption and regardless of the particle size. These results are shown in Table 9. It was found that catalysts prepared by FSP had higher platinum active sites than catalysts prepared by impregnation method (Gly-Imp) (except 0.5%Pt-1.0%Sn/ZrO_2), corresponding to the larger of platinum dispersion. Platinum active sites of TiO_2 supported catalysts prepared by impregnation method (Gly-Imp) increased from trace to 2.5×10^{18} molecule/g catalyst after the Sn content increased from 0 to 1.0 wt% but they decreased to 0.9×10^{18} molecule/g when Sn loading content was 1.5 wt%. ZrO_2 supported catalysts prepared by impregnation method (Gly-Imp) had not trend clearly. While ZrO_2 supported catalysts prepared by FSP decreased from 13.2 to 15.2 molecule/g catalyst after the Sn content increased from 0 to 0.5 wt% but they decreased to 5.5 molecule/g when Sn loading content was 1.5 wt%. Stagg et al. (Stagg et al. 1997: 75-94) point to platinum active sites and % platinum dispersion decreased when increasing of tin content due to the formation of Pt-Sn ensembles or alloys that not adsorb CO.

Table 9 The results from CO Chemisorptions

Catalysts	**Active site[a]$\times10^{-18}$ (molecule/g catalyst)**	**Platinum dispersion[b] (%)**	**Platinum size[c] (nm)**
0.5%Pt/TiO_2 (Gly-Imp)	trace	n.d.	n.d.
0.5%Pt-0.5%Sn/TiO_2 (Gly-Imp)	1.5	9.5	11.4
0.5%Pt-1.0%Sn/TiO_2 (Gly-Imp)	2.5	16.1	6.7
0.5%Pt-1.5%Sn/TiO_2 (Gly-Imp)	0.9	5.9	18.3
0.5%Pt/TiO_2 (FSP)	5.0	32.3	3.3
0.5%Pt-0.5%Sn/TiO_2 (FSP)	5.5	36.0	3.0

Catalysts	Active site[a]×10^{-18} (molecule/g catalyst)	Platinum dispersion[b] (%)	Platinum size[c] (nm)
0.5%Pt-1.0%Sn/TiO_2 (FSP)	3.2	20.5	5.3
0.5%Pt-1.5%Sn/TiO_2 (FSP)	3.5	22.6	4.8
0.5%Pt/ZrO_2 (Gly-Imp)	5.0	32.3	3.3
0.5%Pt-0.5%Sn/ZrO_2 (Gly-Imp)	1.7	10.9	9.9
0.5%Pt-1.0%Sn/ZrO_2 (Gly-Imp)	5.2	34.0	3.2
0.5%Pt-1.5%Sn/ZrO_2 (Gly-Imp)	4.2	27.3	4.0
0.5%Pt/ZrO_2 (FSP)	13.2	85.7	1.3
0.5%Pt-0.5%Sn/ZrO_2 (FSP)	15.2	98.5	1.1
0.5%Pt-1.0%Sn/ZrO_2 (FSP)	5.0	32.4	3.3
0.5%Pt-1.5%Sn/ZrO_2 (FSP)	5.5	36.0	3.0

[a]Error of measurement = ±5%

[b]Platinum dispersion (%) = $\frac{\text{The } amount \;\; of \;\; Pt \;\; measured \;\; by \;\; CO \;\; chemisorpt \;\; ion}{The \;\; amount \;\; of \;\; Pt \;\; loaded \;\; in \;\; catalyst} \times 100$

[c]Metallic platinum diameter = 108/(% Platinum dispersion)

5.1.5 Temperature programmed reduction (H_2-TPR)

H_2-TPR is a power tool to study reduction behavior of metal oxides. A wide range of variables such as metal oxide particle size, interaction between metal and support had an influence on the reduction behavior of platinum catalysts resulting in the observation of different location of TPR peaks. Reduction of platinum in the oxide form PtO_2 or PtO_x to Pt^0 metal involved two steps. The PtO_2 was first reduced to PtO_x and subsequently to Pt^0 metal. In addition, reduction of tin in the oxide form SnO_2 or SnO_x to Sn^0 metal also involved two steps. The SnO_2 was first reduced to SnO_x and subsequently to Sn^0 metal (Salmones et al. 2002: 209-211; Zhang et al. 2006: 84-85). On the other hand, an appearance of TPR peaks at high temperature, usually above 400°C, can imply an interaction between metal and support materials.

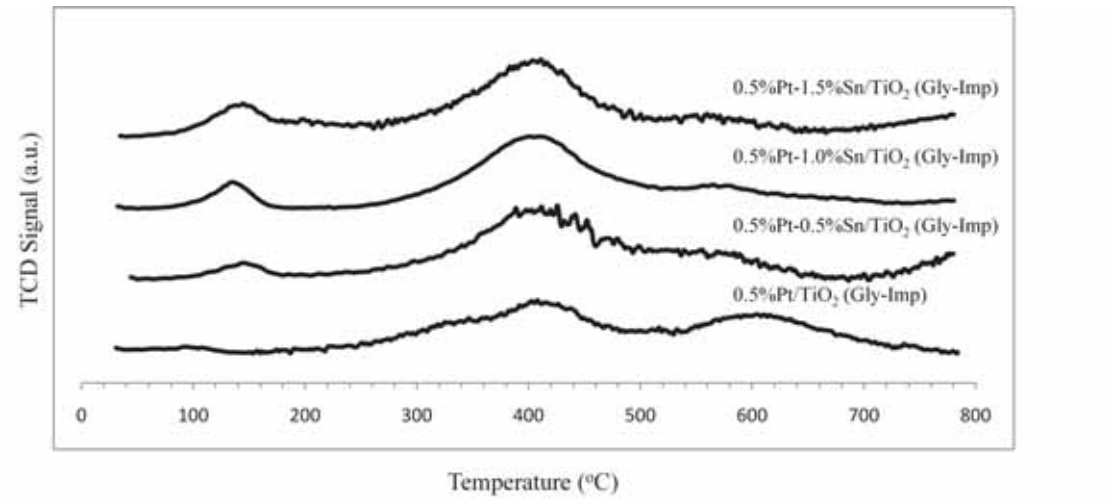

Figure 59 TPR profiles of the TiO_2 supported catalysts prepared by impregnation method (Gly-Imp)

Figure 59 showed the TPR profile of TiO_2 supported catalysts prepared by impregnation method (Gly-Imp). 0.5%Pt/TiO_2 showed two main peaks of strong reduction located at ca. 400°C and 600°C. Two steps of the reduction of PtO_x to Pt^0 metal were occurred in the first peak and the second peak referred interaction between metal and support. TPR pattern of the 0.5%Pt-1.5%Sn/TiO_2 was rather similar to the 0.5%Pt-1.0%Sn/TiO_2 and 0.5%Pt-0.5%Sn/TiO_2. There were one small peak and two main peaks occurred at ca. 140°C, 400°C and 580°C, respectively. The first peak at 140°C was reduction of PtO_2 (SnO_2) to PtO_x (SnO_x). And two main peak was the reduction of PtO_x (SnO_x) to Pt^0 (Sn^0) and the interaction between metal and support. Addition of the impregnated Sn could not only reduce the interaction between metal and support but also showed peak at located 140°C compared to the 0.5%Pt/TiO_2.

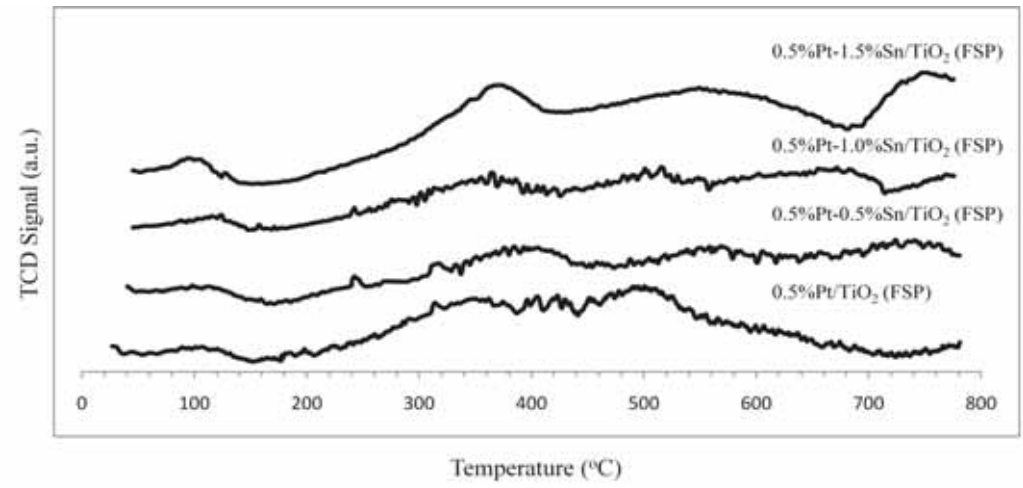

Figure 60 TPR profiles of the TiO_2 supported catalysts prepared by FSP

Figure 60 showed the TPR profile of TiO_2 supported catalysts prepared by FSP. 0.5%Pt/TiO_2 showed three peaks of the reduction located at ca. 100°C, 350°C and 500°C. Two steps of the reduction of PtO_2 to PtO_x were occurred in the first peak and the second peak was the reduction of PtO_x to Pt^0 metal. The last peak referred interaction between metal and support. TPR pattern of the 0.5%Pt-1.5%Sn/TiO_2 was rather similar to the 0.5%Pt-0.5%Sn/TiO_2 and 0.5%Pt-1.0%Sn/TiO_2. There were four peaks. The first peak at 110°C was reduction of PtO_2 (SnO_2) to PtO_x (SnO_x). The second peak at 360°C-400°C was the reduction of PtO_x (SnO_x) to Pt^0 (Sn^0). The third peak was the interaction between metal and support. And the last peak was probably the reduction of TiO_2 support. It was seen that the addition of tin could occurred the reduction of TiO_2 support. And when we compared between TPR profiles of the ZrO_2 supported catalysts from impregnation method (Gly-Imp) and FSP, it was found that the second and third peak of catalysts prepared by FSP shifted to lower temperature and it could be assigned to the reduction of TiO_2 support.

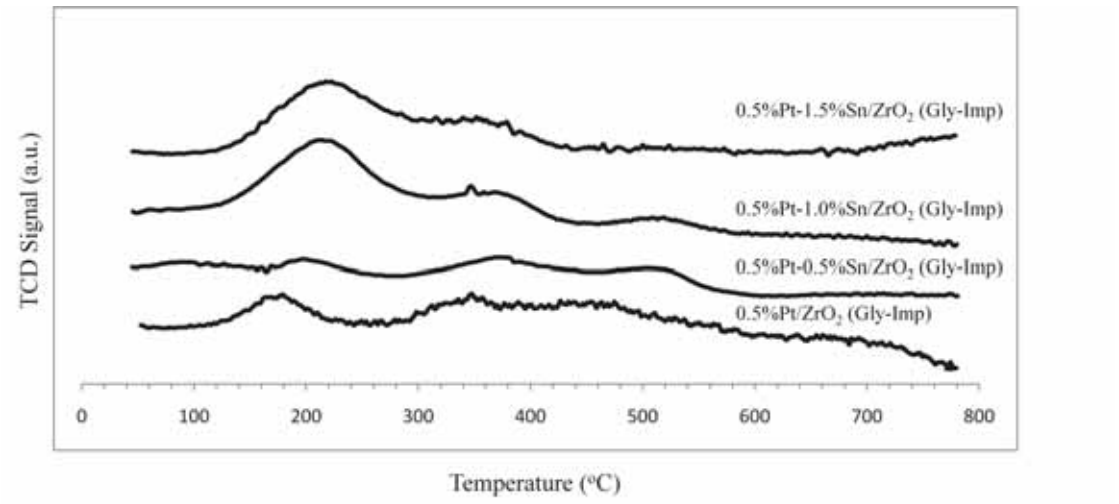

Figure 61 TPR profiles of the ZrO_2 supported catalysts prepared by impregnation method (Gly-Imp)

Figure 61 showed the TPR profile of ZrO_2 supported catalysts prepared by impregnation method (Gly-Imp). 0.5%Pt/ZrO_2 showed three main peaks of reduction located at ca. 170°C, 300°C and 460°C. Two steps of the reduction of PtO_2 to PtO_x were occurred in the first peak and the second peak was the reduction of PtO_x to Pt^0 metal. The third peak referred interaction between metal and support. TPR pattern of 0.5%Pt-1.0%Sn/ZrO_2 was rather similar to the 0.5%Pt-0.5%Sn/ZrO_2 but intensity of first peak of 0.5%Pt-0.5%Sn/ZrO_2 was less. There were three main peaks of reduction. The first peak at 200°C was reduction of PtO_2 (SnO_2) to PtO_x (SnO_x). The second peak at 350°C was reduction of PtO_x (SnO_x) to Pt^0 (Sn^0) and the last peak was the interaction between metal and support. TPR pattern of the 0.5%Pt-1.5%Sn/ZrO_2 was rather similar to the 0.5%Pt-1.0%Sn/ZrO_2 but the last peak of the 0.5%Pt-1.5%Sn/ZrO_2 was not occurred. It was seen that addition of the impregnated Sn increased the interaction between metal and support for 0.5%Pt-0.5%Sn/ZrO_2 and 0.5%Pt-1.0%Sn/ZrO_2 catalyst.

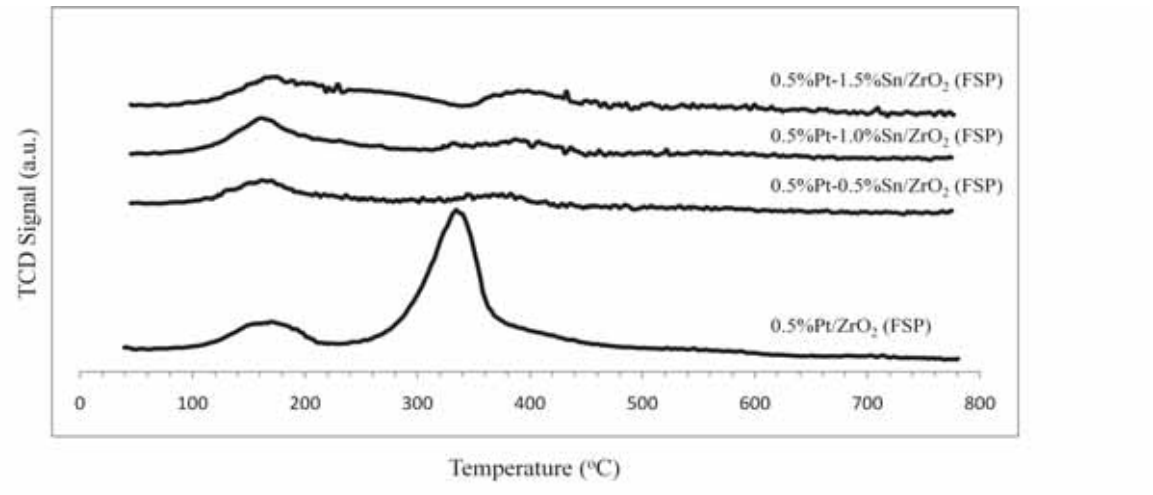

Figure 62 TPR profiles of the ZrO_2 supported catalysts prepared by FSP

Figure 62 showed the TPR profile of ZrO_2 supported catalysts prepared by FSP. 0.5%Pt/ZrO_2 showed two main peaks of strong reduction located at ca. 170°C and 330°C. Two steps of the reduction of PtO_2 to PtO_x were occurred in the first peak and the second peak was the reduction of PtO_x to Pt^0 metal. TPR pattern of the 0.5%Pt-1.5%Sn/ZrO_2 was rather similar to the 0.5%Pt-1.0%Sn/ZrO_2 and 0.5%Pt-0.5%Sn/ZrO_2. There were two main peaks. The first peak at 160°C was reduction of PtO_2 (SnO_2) to PtO_x (SnO_x). The second peak at 380°C-400°C was reduction of PtO_x (SnO_x) to Pt^0 (Sn^0). Addition of tin increased the temperature reduction of PtO_x to Pt^0 metal and the interaction between metal and support. So the reduction occurred more difficult.

5.2 Catalytic activity of the supported Pt-Sn catalysts for cinnamaldehyde hydrogenation

The hydrogenation of cinnamaldehyde is a parallel and consecutive reduction of different functional groups present in the same starting substrate, i.e., C=C and C=O. The products obtained in the hydrogenation of cinnamaldehyde were cinnamyl alcohol, hydrocinnamaldehyde and 3-phenyl-1-propanol. Other possible reaction

products such as methylstyrene, phenylpropane and acetals were not detected in the present work. The conversion and selectivity were defined as:

$$Conversion\ (t) = \frac{[CMA(0)] - [CMA(t)]}{[CMA(0)]} \times 100\%$$

$$Selectivity\ (t) = \frac{CMO(t)}{[CMA(0)] - [CMA(t)]} \times 100\%$$

Note: *CMA* = Cinnamaldehyde

CMO = Cinnamyl alcohol

Table 10 showed the conversion of cinnamaldehyde and the selectivity of cinnamyl alcohol for cinnamaldehyde hydrogenation reaction at reaction condition as 0.01 mol of cinnamaldehyde, 85 ml of C_2H_5OH, 50 bar of H_2 for 120 min. It was found that the conversion of cinnamaldehyde for the TiO_2 supported catalysts prepared by FSP increased from 20.4% to 38.0% as the amounts of Sn loading increased from 0 to 0.5 wt% and then decreased to 26.4% after the addition of Sn further increased to 1.5 wt%. The conversion of cinnamaldehyde for the ZrO_2 supported catalysts prepared by impregnation method (Gly-Imp) decreased from 30.9% to 27.0% as the amounts of Sn loading increased from 0 to 0.5 wt% and then increased to 41.9% after the addition of Sn further increased to 1.5 wt%. For the TiO_2 supported catalysts prepared by impregnation method (Gly-Imp) and the ZrO_2 supported catalysts prepared by FSP, the conversion of cinnamaldehyde had trend no obviously.

For the selectivity of cinnamyl alcohol, the TiO_2 supported catalysts prepared by impregnation method (Gly-Imp) increased from 2.47% to 3.44% as the amounts of Sn loading increased from 0 to 0.5 wt% and then decreased to 1.88% after the addition of Sn further increased to 1.5 wt%. In the case of FSP-made catalyst, the selectivity of cinnamyl alcohol increased from 4.47% to 7.50% as the amounts of Sn loading increased from 0 to 0.5 wt% and then decreased to 4.49% after the addition of

Sn further increased to 1.5 wt%. The ZrO_2 supported catalysts prepared by FSP decreased from 5.32% to 2.32% as the amounts of Sn loading increased from 0 to 1.0 wt% and then increased to 5.20% after the addition of Sn further increased to 1.5 wt%. For the ZrO_2 supported catalysts prepared by impregnation method (Gly-Imp), the conversion of cinnamaldehyde had not trend obviously.

Table 10 The hydrogenation of cinnamaldehyde over Pt-Sn catalysts

Catalysts	Conversion (%)	Selectivity (%)			
		HCMA	HCMO	CMO	Other
0.5%Pt/TiO_2 (Gly-Imp)	40.8	3.09	2.41	2.47	92.03
0.5%Pt-0.5%Sn/TiO_2 (Gly-Imp)	38.9	1.94	2.13	3.44	92.49
0.5%Pt-1.0%Sn/TiO_2 (Gly-Imp)	29.1	1.72	2.42	2.47	93.39
0.5%Pt-1.5%Sn/TiO_2 (Gly-Imp)	35.5	1.63	2.21	1.88	94.27
0.5%Pt/TiO_2 (FSP)	20.4	2.03	2.30	4.47	91.19
0.5%Pt-0.5%Sn/TiO_2 (FSP)	38.0	4.19	2.35	7.50	85.95
0.5%Pt-1.0%Sn/TiO_2 (FSP)	28.4	2.33	2.27	5.51	89.89
0.5%Pt-1.5%Sn/TiO_2 (FSP)	26.4	2.00	2.15	4.49	91.36
0.5%Pt/ZrO_2 (Gly-Imp)	30.9	2.68	2.19	3.97	91.16
0.5%Pt-0.5%Sn/ZrO_2 (Gly-Imp)	27.0	1.89	2.41	3.67	92.03
0.5%Pt-1.0%Sn/ZrO_2 (Gly-Imp)	33.3	2.10	2.34	4.94	90.62
0.5%Pt-1.5%Sn/ZrO_2 (Gly-Imp)	41.9	2.03	2.30	4.47	91.19
0.5%Pt/ZrO_2 (FSP)	18.7	5.88	3.04	5.32	85.76
0.5%Pt-0.5%Sn/ZrO_2 (FSP)	42.4	3.44	2.42	4.67	89.48
0.5%Pt-1.0%Sn/ZrO_2 (FSP)	35.2	2.76	2.33	2.32	92.59
0.5%Pt-1.5%Sn/ZrO_2 (FSP)	38.2	2.93	2.23	5.20	89.64

Hydrocinnamaldehyde (HCMA), 3-Phenyl-1-propanal (HCMO), Cinnamyl alcohol (CMO)
Reaction condition: 0.01 mol CMA, 85 ml C_2H_5OH, 50 bar, 120 min

CHAPTER 6

CONCLUSIONS

In this study, the nanosized Pt and Pt-Sn catalysts were prepared by two methods for the hydrogenation of cinnamaldehyde. In the first method, the support was prepared by glycothermal and then platinum and tin were added onto the support by impregnation (Gly-Imp). In the second method, the catalysts were prepared by flame spray pyrolysis (FSP). The supports for preparation of catalysts were titania (TiO_2) and zirconia (ZrO_2). The obtained catalysts were characterized by X-ray diffraction (XRD), N_2 physisorption, transmission electron microscopy (TEM), CO chemisorption and temperature programmed reduction (H_2-TPR). The conclusions of these results were summarized as follows:

1. Nanosized Pt and Pt-Sn catalysts were successfully prepared by impregnation method (Gly-Imp) and FSP method.
2. For TiO_2 supported catalysts, the catalyst preparation by FSP method obtained both anatase and rutile phase for titania while the catalyst preparation by impregnation method (Gly-Imp) obtained only anatase phase.
3. For ZrO_2 supported catalysts, the catalyst preparation by FSP method obtained both tetragonal and monoclinic phase for zirconia while the catalyst preparation by impregnation method (Gly-Imp) obtained only tetragonal phase.
4. The catalyst preparation by impregnation method (Gly-Imp) showed larger the BET surface area than the catalyst preparation by FSP method.
5. Addition of tin onto the catalysts prepared by impregnation method (Gly-Imp), the BET surface area decreased with increasing the tin loading into catalysts because blocking of tin in the catalyst pore. While the addition of tin onto the catalysts prepared by FSP method, the BET surface area was remained constant.

6. The TiO_2 supported catalysts preparation by impregnation method (Gly-Imp) gave the mean pore size about 16.1-22.6 nm while preparation by FSP gave the mean pore size about 24.9-30.9 nm.

7. The ZrO_2 supported catalysts preparation by impregnation method (Gly-Imp) gave the mean pore size about 4.6-4.9 nm while preparation by FSP method gave the mean pore size about 24.1-41.4 nm.

8. The TiO_2 supported catalysts preparation by impregnation method (Gly-Imp) gave the total pore volume about 0.44-0.57 cm^3(STP)/g while preparation by FSP method gave the total pore volume about 0.43-0.55 cm^3(STP)/g.

9. The ZrO_2 supported catalysts preparation by impregnation method (Gly-Imp) gave the total pore volume about 0.17-0.18 cm^3(STP)/g while preparation by FSP method gave the total pore volume about 0.32-0.54 cm^3(STP)/g.

10. The catalysts preparation by impregnation method (Gly-Imp) gave rather narrow pore size distribution.

11. The TiO_2 supported catalysts preparation by impregnation method (Gly-Imp) gave the mean particle size (from TEM) about 11.1-13.0 nm while preparation by FSP method gave the mean particle size about 16.6-22.7 nm

12. The ZrO_2 supported catalysts preparation by impregnation method (Gly-Imp) gave the mean particle size (from TEM) about 13.0-15.6 nm while preparation by FSP method gave the mean particle size about 19.9-21.1 nm

13. The catalysts preparation by FSP method had higher platinum active sites and platinum dispersion than catalysts prepared by impregnation method (Gly-Imp) except 0.5%Pt-1.0%Sn/ZrO_2.

14. For catalytic activity had not trend obviously but it can run reaction.

Bibliography

Antos, G.J., M.D. Moser and M.P. Lapinski. "The New Generation of Commercial Catalytic Naphtha-Reforming Catalysts" In Catalytic Naphtha Reforming, 335. Edited by G.J. Antos and A.M. Aitani . New York: Marcel Dekker, 2004.

Audo et al. "Synthesis of platinum-tin/alumina reforming catalysts from a well-defined platinum-tin precursor complex." Catalysis Today 65 (2001): 157.

Bednarova, L. et al. "Effect of Support on the Size and Composition of Highly Dispersed Pt-Sn Particles." Journal of Catalysis. 211 (2002): 335.

Beltramini, J. and D.L. Trimm. "Catalytic reforming of n-heptane on platinum, tin and platinum-tin supported on alumina." Applied Catalysis. 31 (1987):113-118.

Breen, J. P. et al. "Steric effects in the selective hydrogenation of cinnamaldehyde to cinnamyl alcohol using an Ir/C catalyst." Applied Catalysis A: General 268 (2004): 267.

Burakorn, T. et al. "Characterization of cobalt dispersed on the mixed nanoscale alumina and zirconia supports" Journal of Materials Processing Technology 206 (2008): 352-358.

Burch, R. and L.C. Garl. "Platinum-tin reforming catalysts: II. Activity and selectivity in hydrocarbon reactions." Journal of Catalysis 71 (1981): 360.

Burwell, R. "Hydrogenation and dehydrogenation of organic compounds." In Fundamentals of Industrial Catalytic Processes, 411-465. Edited by C. H. Bartholomew and R. J. Farrauto. London: Blackie Academic & Professional, 1983.

Chang, H. et al. "Synthetic routes for titania nanoparticles in the flame spray pyrolysis." Colloids and Surfaces A: Physicochem. Eng. Aspects 313-314 (2008): 282-287.

Chatterjee, M. et al. "Effect of synthesis variables on the hydrogenation of cinnamaldehyde over Pt-MCM-48 in supercritical CO_2 medium" Applied Catalysis A: General 262 (2004): 93-100.

Che, M. and C.O. Bennett. "The Influence of Particle Size on the Catalytic Properties of Supported Metals." Advances in Catalysis. 36 (1989): 55.

Coloma, F. et al. "Crotonaldehyde hydrogenation over bimetallic Pt-Sn catalysts supported on pregraphitized carbon black. Effect of the preparation method." Applied Catalysis A: General 148 (1996) 63.

Delbecq, F. and Sautet P. "Competitive C=C and C=O Adsorption of α, β-Unsaturated Aldehydes on Pt and Pd Surfaces in Relation with the Selectivity of Hydrogenation Reactions: A Theoretical Approach." Journal of Catalysis 152 (1995): 217-236.

Eberhardt, M. et al. "Fundamental investigations of thermal aging phenomena of model NO_x storage systems." Topics in Catalysis 30/31 (2004): 137.

Eilerman, R. E. In Kirk-Othmer Encyclopedia of Chemical Technology, 349. Edited by J. I. Kroschwitz and M. Howe-Grant. Vol. 6, Wiley, New York, 1996.

Fujikawa, T., F.H. Ribeiro and G.A. Somorjai. "The Effect of Sn on the Reactions of n-Hexane and Cyclohexane Over Polycrystalline Pt Foils." Journal of Catalysis 178 (1998): 58.

Gallezot, P. and D. Richard. "Selective Hydrogenation of α,β-Unsaturated Aldehydes." Catalysis Reviews 40 (1998): 81-126.

Hajek, J. et al. "Impact of Catalyst Reduction Mode on Selective Hydrogenation of Cinnamaldehyde over Ru-Sn Sol-Gel Catalysts." Industrial and Engineering Chemistry Research 42 (2003): 295.

Homs et al. "Vapour phase hydrogenation of crotonaldehyde over magnesia-supported platinum-tin catalysts." Physical Chemistry Chemical Physics 3 (2001): 1782-1788

Jackson, S. David and Justin S. J. Hargreaves. Metal oxide catalysis. Vol. 1, Wiley-VCH, 2008.

Kang, Misook. "Synthesis of Fe/TiO_2 photocatalyst with nanometer size by solvothermal method and the effect of H_2O addition on structural stability and photodecomposition of methanol." Journal of Molecular Catalysis A: Chemical 197 (2003): 173-183.

Kappenstein, C. et al. "Characterisation and activity in *n*-hexane rearrangement reactions of metallic phases on $Pt–Sn/Al_2O_3$ catalysts of different preparations." Faraday Trans. 94 (1998): 2463.

Karthikeyan, J. et al. "Nano material powders and deposits prepared by flame spray processing of liquid precursors." Nanostructured Materials 8 (1997): 61-74.

Kijenski , Jacek and Piotr Winiarek. "Selective hydrogenation of α,β-unsaturated aldehydes over Pt catalysts deposited on monolayer supports." Applied Catalysis A: General 193 (2000): L1–L4.

Kogan, S.B. and M. Herskowitz. "Selective propane dehydrogenation to propylene on novel bimetallic catalysts." Catalysis Communications. 2 (2001): 179.

Kongwudthiti, S. et al. "Influence of synthesis conditions on the preparation of zirconia powder by the glycothermal method" Ceramics International 29 (2003): 807-814.

Koo-amornpattana, W. and J.M. Winterbottom. "Pt and Pt-alloy catalysts and their properties for the liquid-phase hydrogenation of cinnamaldehyde." Catalysis Today 66 (2001): 277-287.

Lashdaf, M. et al. "Behaviour of palladium and ruthenium catalysts on alumina and silica prepared by gas and liquid phase deposition in cinnamaldehyde hydrogenation." Applied Catalysis A: General 241(2003): 65-75.

Lashdaf, M. et al. "Role of acidity in hydrogenation of cinnamaldehyde on platinum beta zeolite." Microporous and Mesoporous Materials 75 (2004): 149-158.

Letizia, C.S. et al. "Fragrance material review on cinnamyl alcohol." Food and Chemical Toxicology 43 (2005): 837-866.

Li, Yan, Peng-Fei Zhu and Ren-Xian Zhou. "Selective hydrogenation of cinnamaldehyde to cinnamyl alcohol with carbon nanotubes supported Pt-Co catalysts." Applied Surface Science 254 (2008): 2609-2614.

Llorca, J. et al. "Supported Pt-Sn catalysts highly selective for isobutane dehydrogenation: preparation, characterization and catalytic behavior." Applied Catalysis A: General 189 (1999): 77.

Mädler, L. "Direct formation of highly porous gas-sensing films by in situ thermophoretic deposition of flame-made Pt/SnO_2 nanoparticles." Sensors and Actuators: B 114 (2006): 283-295.

Mahata, N. et al. "Selective hydrogenation of cinnamaldehyde to cinnamyl alcohol over mesoporous carbon supported Fe and Zn promoted Pt catalyst." Applied Catalysis A: General 339 (2008): 159-168.

Margìtfalvi et al. "Characterization of Sn-Pt/SiO_2 Catalysts Used in Selective Hydrogenation of Crotonaldehyde by Mössbauer Spectroscopy." Journal of Catalysis 190 (2000): 474

Muller, A. and J. Bowers, WO Patent Application WO 99/08989, First Chemical Corporation, 1999.

Okuyama, Kikuo and I. Wuled Lenggoro. "Preparation of nanoparticles via spray route." Chemical Engineering Science 58 (2003): 537-547.

Palazov, A. et al. "Adsorption and hydrogenation of ethylene, 1-hexene, and benzene and CO adsorption on $Pt/Al_2O_3$and$Pt-Sn/Al_2O_3$ catalysts." Journal of Catalysis 103 (1987): 249.

Parr Instrument. Series 4590 Micro Bench Top Reactors [Online]. Accessed 20 March 2009. Available from http://www.parrinst.com/default.cfm?Page_ID=187

Piacentini, M. et al. "Flame-made $Pt–Ba/Al_2O_3$ catalysts: Structural properties and behavior in lean-NO_x storage-reduction." Journal of Catalysis 243 (2006): 45-46.

Piacentini, M., M. Maciejewski and A. Baiker. "Supported Pt-Ba NO_x storage-reduction catalysts: Influence of support and Ba loading on stability and storage efficiency of Ba-containing species." Applied Catalysis B: Environmental 66 (2006): 128-130.

Plomp, A.J. et al. "Particle size effects for carbon nanofiber supported platinum and ruthenium catalysts for the selective hydrogenation of cinnamaldehyde." Applied Catalysis A: General 351 (2008): 9-15.

Praserthdam, P., N. Grisdanurak and W. Yuangsawatdikul. "Coke formation over $Pt-Sn-K/Al_2O_3$ in C_3, C_5-C_8 alkane dehydrogenation." Chemical Engineering journal 77 (2000): 215.

Rangel, M.C. et al. "n-octane reforming over alumina-supported Pt, Pt-Sn and Pt-W catalysts." Catalysis Letters. 64 (2000): 171

Salmones, J. et al. "H_2 reduction behaviors and catalytic performance of bimetallic tin-modified platinum catalysts for propane dehydrogenation." Journal of Molecular Catalysis A: Chemical 184 (2002): 209-211.

Stagg, S. M. et al. "Isobutane Dehydrogenation on $Pt-Sn/SiO_2$ Catalysts: Effect of Preparation Variables and Regeneration Treatments." Journal of Catalysis 168 (1997): 75-94.

Strobel, Reto, Alfons Beiker, and Sotiris E. Pratsinis. "Aerosol flame synthesis of catalysts." Advanced Powder Technology 17 (2006): 457-480.

Xi, Chunyi et al. "Hydrogenation of cinnamaldehyde over Pt/RHCs in supercritical carbon dioxide-Influence of support pretreatment and phase behavior." Catalysis Communications 9 (2008): 140-145.

Zavala, A. Vázquez et al. "Characterization of structure and catalytic activity of Pt-Sn catalysts supported in Al_2O_3, SiO_2 and TiO_2." Applied Surface Science. 136 (1998): 62.

Zhang, Y. et al. "Properties of the metallic phase of zinc-doped platinum catalysts for propane dehydrogenation." Journal of Molecular Catalysis A: Chemical 266 (2006): 80-87.

Zhang, Z. et al. "High-yield solvothermal formation of magnetic CoPt alloy nanowires." Journal American Chemical Society 125 (2003): 7528.

APPENDIX

APPENDIX A

APPENDIX A

CALCULATION FOR CATALYST PREPARATION

Calculation of catalysts preparation from incipient wetness impregnation

Table 11 Precursors were used in incipient wetness impregnation

Precursors	Molecular formula	MW of precursor (g/mol)	Metal	MW of metal (g/mol)	Metal content (wt %)
Hydrogen hexachloroplatinate (IV) hydrate	H_2PtCl_6	409.82	Pt	195.23	40
Tin (II) chloride	$SnCl_2$	189.6	Sn	118.71	60

Example A1: Calculation preparation of 0.5%Pt/ZrO_2 catalyst for incipient wetness impregnation

Based on 100 g of catalyst, the composition of the catalyst will be as follow:

Pt = 0.5 g

ZrO_2 = 100 - 0.5 = 99.5 g

For 2 g of support

Pt required = 2 × (0.5/99.5) = 0.01005 g

Thus, Pt 0.01005 g was prepared from 40 wt% Pt of H_2PtCl_6

$$H_2PtCl_6 = 0.01005\,gPt\left(\frac{100\,gH_2PtCl_6}{40\,gPt}\right) = 0.025125 \text{ g}$$

Example A2: Calculation preparation of 0.5%Pt-0.5%Sn/ZrO_2 catalyst incipient wetness impregnation

Based on 100 g of catalyst, the composition of the catalyst will be as follow:

Pt = 0.5 g

Sn = 0.5 g

ZrO_2 = 100 - 0.5 - 0.5 = 99.0 g

For 2 g of support

Pt required = 2 × (0.5/99.0) = 0.0101g

Sn required = 2 × (0.5/99.0) = 0.0101 g

Thus, Pt 0.0101 g was prepared from 40 wt% Pt of H_2PtCl_6

$$H_2PtCl_6 = 0.0101\,gPt\left(\frac{100\,gH_2PtCl_6}{40\,gPt}\right) = 0.02525\ g$$

Sn 0.0101 g was prepared from 62.61 wt% Sn of $SnCl_2$

$$SnCl_2 = 0.0101\,gSn\left(\frac{100\,gSnCl_2}{62.61\,gSn}\right) = 0.01613\ g$$

Calculation of catalysts preparation from flame spray pyrolysis

Table 12 Precursors were used in flame spray pyrolysis

Precursors	Molecular formula	MW of precursor (g/mol)	Density (g/ml)	Purity (%)
Platinum (II) acetylacetonate	$C_{10}H_{14}O_4Pt$	393.29	-	99.99
Tin (II) 2-ethylhexanoate	$C_{16}H_{30}O_4Sn$	405.11	1.251	95
Zirconium (IV) butoxide	$C_{16}H_{36}O_4Zr$	383.70	1.049	80
Titanium (IV) butoxide	$C_{16}H_{36}O_4Ti$	340.36	1.000	97

Example A3: Calculation preparation of 0.5%Pt/ZrO_2 catalyst for flame spray pyrolysis

Based on 100 g of catalyst:

	g	MW	Mol
Pt	0.5	195.23	$\frac{0.5}{195.23} = 2.56 \times 10^{-3}$
ZrO_2	99.5	123.22	$\frac{99.5}{123.22} = 0.807$
			0.810

For 0.3 M of solution:

$$\text{Pt required} = \frac{0.3 \times 2.56 \times 10^{-3}}{0.810} = 9.48 \times 10^{-4}\ mol$$

$$ZrO_2 \text{ required} = \frac{0.3 \times 0.807}{0.810} = 0.2989\ mol$$

Basis 1 lite:

Pt 9.48×10^{-4} *mol* was prepared from $C_{10}H_{14}O_4Pt$

$$C_{10}H_{14}O_4Pt = 9.48 \times 10^{-4}\, mol \times \frac{393.29\, g}{1\, mol} \times \frac{1}{0.9999} = 0.3729\, g$$

ZrO_2 0.2989 *mol* was prepared from $C_{16}H_{36}O_4Zr$

$$C_{16}H_{36}O_4Zr = 0.2989\, mol \times \frac{383.7\, g}{1\, mol} \times \frac{1\, ml}{1.049\ \text{g}} \times \frac{1}{0.80} = 136.66\, ml$$

And added xylene to 1,000 ml

Example A4: Calculation preparation of 0.5%Pt-0.5%Sn/ZrO_2 catalyst for flame spray pyrolysis

Based on 100 g of catalyst:

	g	**MW**	**Mol**
Pt	0.5	195.23	$\frac{0.5}{195.23} = 2.56 \times 10^{-3}$
Sn	0.5	118.70	$\frac{0.5}{118.70} = 4.21 \times 10^{-3}$
ZrO_2	99.0	123.22	$\frac{99.0}{123.22} = 0.8034$
			0.8102

For 0.3 M of solution:

$$\text{Pt required} = \frac{0.3 \times 2.56 \times 10^{-3}}{0.8102} = 9.48 \times 10^{-4}\, mol$$

$$\text{Sn required} = \frac{0.3 \times 4.21 \times 10^{-3}}{0.8102} = 1.56 \times 10^{-3}\, mol$$

$$ZrO_2 \text{ required} = \frac{0.3 \times 0.8034}{0.8102} = 0.2975\, mol$$

Basis 1 lite:

Pt $9.48\times10^{-4}\ mol$ was prepared from $C_{10}H_{14}O_4Pt$

$$C_{10}H_{14}O_4Pt = 9.48\times10^{-4}\ mol\times\frac{393.29\ g}{1\ mol}\times\frac{1}{0.9999}=0.3729\ g$$

Sn $1.56\times10^{-3}\ mol$ was prepared from $C_{16}H_{30}O_4Sn$

$$C_{16}H_{30}O_4Sn = 1.56\times10^{-3}\ mol\times\frac{405.11\ g}{1\ mol}\times\frac{1}{0.95}=0.6652\ g$$

ZrO_2 $0.2975\ mol$ was prepared from $C_{16}H_{36}O_4Zr$

$$C_{16}H_{36}O_4Zr = 0.2975\ mol\times\frac{383.7\ g}{1\ mol}\times\frac{1\ ml}{1.049\ \text{g}}\times\frac{1}{0.80}=136.02\ ml$$

And added xylene to 1,000 ml

APPENDIX B

APPENDIX B

CALCULATION OF THE CRYSTALLITE SIZE

Calculation of the crystallite size by Debye-Scherrer equation

The crystallite size was calculated from the half-height width of the diffraction peak of XRD pattern using the Debye-Scherrer equation.

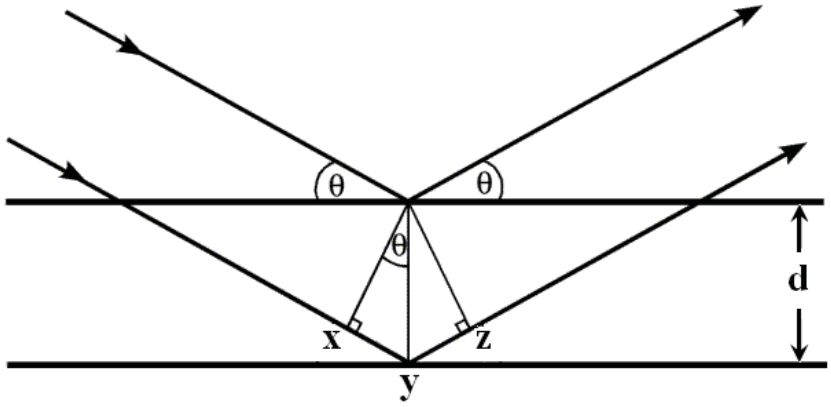

Figure 63 Derivation of Bragg's Law for X-ray diffraction

$$xy = yz = d \sin \theta$$

Thus $$xyz = 2d \sin \theta$$

But $$xyz = n\lambda$$

Therefore $$2d \sin \theta = n\lambda$$ **Bragg's Law**

$$d = \frac{n\lambda}{2 \sin \theta}$$

The Bragg's Law was derived to B.1

$$D = \frac{K\lambda}{\beta \cos\theta} \qquad \text{(B.1)}$$

Where D = Crystallite size, Å

K = Crystallite-shape factor = 0.9

λ = X-ray wavelength, 1.5418 Å for CuKα

θ = Observed peak angle, degree

β = X-ray diffraction broadening, radian

The X-ray diffraction broadening (β) is the pure width of powder diffraction free from all broadening due to the experimental equipment. α-Alumina is used as a standard sample to observe the instrumental broadening since its crystallite size is larger than 2000 Å. The X-ray diffraction broadening (β) can be obtained by using Warren's formula.

From Warren's formula:

$$\beta = \sqrt{B_M^2 - B_S^2} \qquad \text{(B.2)}$$

Where B_M = The measured peak width in radians at half peak height

B_S = The corresponding width of the standard material

Example B1: Calculation of the crystallite size of ZrO_2

The half-height width of 111 diffraction peak = 1.83^o (from Figure 72)

= $(2\pi \times 1.83)/360$

= 0.0319 radian

The corresponding half-height width of peak of α-Alumina (from the B_S value at the 2θ of 30.3^o in Figure 73) = 0.0043 radian

The peak width, $\beta = \sqrt{B_M^2 - B_S^2}$

$\beta = \sqrt{0.0319^2 - 0.0043^2}$

$\beta = 0.0316$ radian

$2\theta = 30.3^o$

$\theta = 15.15^o$

$\lambda = 1.5418$ Å

$K = 0.9$

The crystallite size, $D = \frac{K\lambda}{\beta \cos\theta} = \frac{0.9 \times 1.5418}{0.0316 \cos 15.15}$

$D = 45.49$ Å $= 4.5$ nm

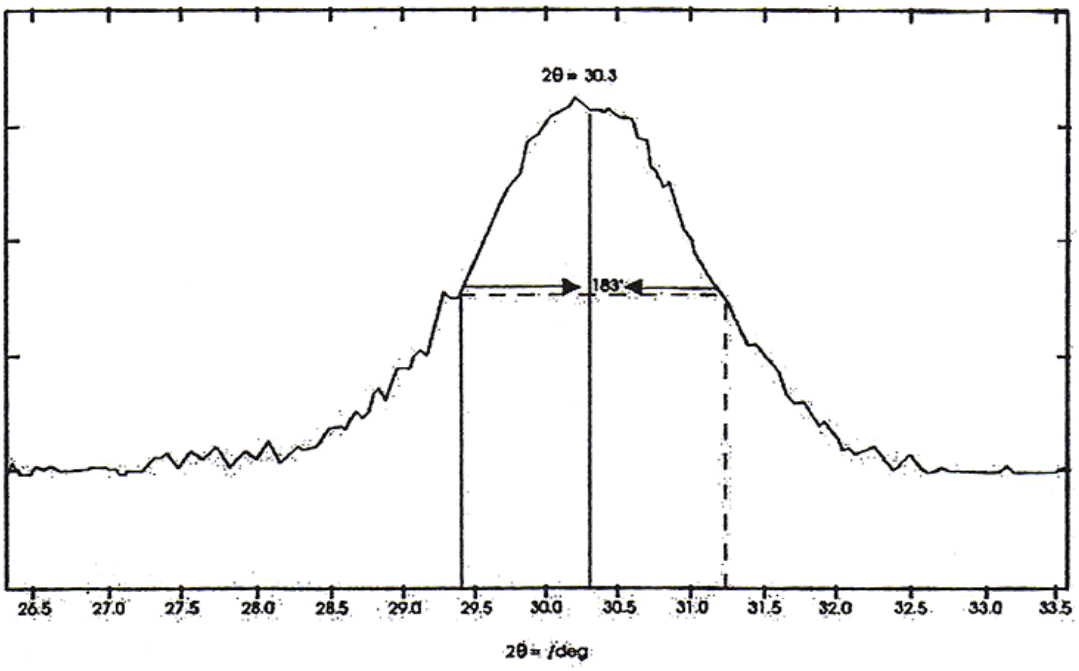

Figure 64 The 111 diffraction peak of ZrO_2 for calculation of the crystalline size

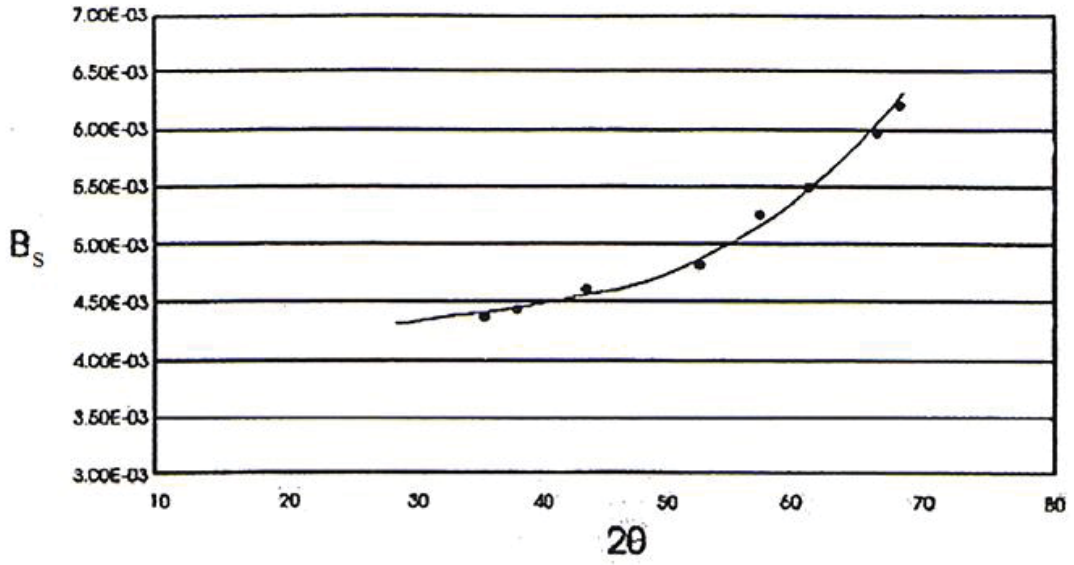

Figure 65 The plot indicating the value of line broadening due to the equipment. The data were obtained by using α-alumina as a standard.

APPENDIX C

APPENDIX C

CALCULATION OF METAL ACTIVE SITES

To calculate the metal active sites of the catalyst measured by CO chemisorptions technique at room temperature. A stoichiometry of CO/Pt = 1 is assumed. The calculation procedure is as follows:

Let the weight of catalyst used	=	W	g
Integral area of CO peak after 1st adsorption	=	A	unit
Integral area of CO peak after 2nd adsorption	=	B	unit
Integral area of CO peak after 3rd adsorption	=	C	unit
Integral area of CO peak after 4th adsorption	=	D	unit
Integral area of 86 µL of standard CO peak	=	(B+C+D)/3	unit
	=	E	unit
Amounts of CO adsorbed on catalyst	=	E - A	unit
Volume of CO adsorbed on catalyst	=	$\left(\frac{E-A}{E}\right)\times 86$	µl
	=	F	µl
Volume of 1 mole of Pt at 30°C	=	24.937×10^{6}	µl
Mole of CO adsorbed on catalyst	=	$\frac{F}{24.937\times10^{6}}$	mole
Molecule of CO adsorbed on catalyst	=	$\left[\frac{F}{24.937\times10^{6}}\right]\left[6.02\times10^{23}\right]$	molecules

Metal active sites

$$= \frac{\left[\frac{F}{24.937\times10^{6}}\right]\left[6.02\times10^{23}\right]}{W} \quad \text{molecules of CO/g of catalyst}$$

In addition, the platinum dispersion, which is the ratio between the apparent platinum molecules observed from the measurement of CO adsorption and the actual platinum molecules obtained from the measurement of atomic adsorption spectroscopy, can also be calculated.

The actual percentage of platinum loading = 0.5 wt%

$$\text{The actual platinum molecules} = \frac{0.005\times6.02\times10^{23}}{195.23}$$

$$= 1.542\times10^{19} \quad \text{molecules/g of catalyst}$$

Therefore,

$$\text{The platinum dispersion} = \frac{\text{Metal active sites}}{1.542\times10^{19}}\times100 \quad \%$$

$$\text{Metal size} = \frac{108}{\%\text{Pt dispersion}} \quad \text{nm}$$

APPENDIX D

APPENDIX D

EXPERIMENTAL DATA

Table 13 The conversion and selectivity from cinnamaldehyde hydrogenation for 0.5%Pt/TiO_2 (Gly-Imp)

Time (min)	Conversion (%)	Selectivity (%)			
		Hydro-cinnamaldehyde	3-Phynyl-1-propanol	Cinnamyl alcohol	Other
0	0.0	0.0	0.0	0.0	0.0
15	33.9	2.8	2.4	1.9	93.0
30	28.5	3.1	2.4	2.0	92.5
45	27.6	3.2	2.4	2.4	92.0
60	38.8	3.0	2.3	2.1	92.7
75	30.5	3.2	2.3	2.5	92.0
90	31.4	3.2	2.4	2.4	92.0
105	44.8	3.1	2.4	2.2	92.4
120	40.8	3.1	2.4	2.5	92.0

Table 14 The conversion and selectivity from cinnamaldehyde hydrogenation for 0.5%Pt-0.5%Sn/TiO_2 (Gly-Imp)

Time (min)	Conversion (%)	Selectivity (%)			
		Hydro-cinnamaldehyde	3-Phynyl-1-propanol	Cinnamyl alcohol	Other
0	0.0	0.0	0.0	0.0	0.0
15	39.8	1.8	2.2	1.9	94.2
30	27.9	1.9	2.3	2.8	93.0
45	31.8	1.9	2.1	2.7	93.3
60	33.8	1.9	2.1	2.8	93.1
75	32.1	2.0	2.1	3.0	92.9
90	24.3	2.0	2.2	4.0	91.9
105	40.0	2.0	2.2	3.4	92.4
120	38.9	1.9	2.1	3.4	92.5

Table 15 The conversion and selectivity from cinnamaldehyde hydrogenation for 0.5%Pt-1.0%Sn/TiO_2 (Gly-Imp)

Time (min)	Conversion (%)	Selectivity (%)			
		Hydro-cinnamaldehyde	3-Phynyl-1-propanol	Cinnamyl alcohol	Other
0	0.0	0.0	0.0	0.0	0.0
15	32.2	2.0	2.8	1.7	93.5
30	41.7	1.7	2.2	2.1	94.0
45	40.8	1.6	2.1	2.1	94.2
60	37.0	2.0	2.5	2.3	93.1
75	33.8	1.9	2.5	2.2	93.5
90	39.6	1.8	2.3	2.0	93.9
105	37.2	1.8	2.4	2.1	93.8
120	29.1	1.7	2.4	2.5	93.4

Table 16 The conversion and selectivity from cinnamaldehyde hydrogenation for 0.5%Pt-1.5%Sn/TiO_2 (Gly-Imp)

Time (min)	Conversion (%)	Selectivity (%)			
		Hydro-cinnamaldehyde	3-Phynyl-1-propanol	Cinnamyl alcohol	Other
0	0.0	0.0	0.0	0.0	0.0
15	26.7	1.7	2.2	1.5	94.7
30	19.9	1.7	2.4	1.7	94.2
45	29.6	1.7	2.4	1.9	94.0
60	32.0	1.6	2.2	1.9	94.3
75	10.6	1.7	2.3	2.4	93.6
90	20.1	1.8	2.4	2.3	93.6
105	16.4	1.9	2.5	2.2	93.5
120	35.5	1.6	2.2	1.9	94.3

Table 17 The conversion and selectivity from cinnamaldehyde hydrogenation for 0.5%Pt/TiO_2 (FSP)

Time (min)	Conversion (%)	Selectivity (%)			
		Hydro-cinnamaldehyde	3-Phynyl-1-propanol	Cinnamyl alcohol	Other
0	0.0	0.0	0.0	0.0	0.0
15	26.7	1.7	2.2	1.5	94.7
30	19.9	1.7	2.4	1.7	94.2
45	29.6	1.7	2.4	1.9	94.0
60	32.0	1.6	2.2	1.9	94.3
75	10.6	1.7	2.3	2.4	93.6
90	20.1	1.8	2.4	2.3	93.6
105	16.4	1.9	2.5	2.2	93.5
120	35.5	1.6	2.2	1.9	94.3

Table 18 The conversion and selectivity from cinnamaldehyde hydrogenation for 0.5%Pt-0.5%Sn/TiO_2 (FSP)

Time (min)	Conversion (%)	Selectivity (%)			
		Hydro-cinnamaldehyde	3-Phynyl-1-propanol	Cinnamyl alcohol	Other
0	0.0	0.0	0.0	0.0	0.0
15	24.4	2.6	2.4	5.3	89.7
30	45.6	2.6	2.2	5.5	89.7
45	35.3	2.9	2.1	4.1	90.8
60	37.6	3.2	2.3	4.8	89.7
75	33.2	3.7	2.4	6.6	87.4
90	43.1	3.5	2.3	7.1	87.0
105	33.4	4.1	2.4	7.6	85.9
120	38.0	4.2	2.4	7.5	86.0

Table 19 The conversion and selectivity from cinnamaldehyde hydrogenation for 0.5%Pt-1.0%Sn/TiO_2 (FSP)

Time (min)	Conversion (%)	Selectivity (%)			
		Hydro-cinnamaldehyde	3-Phynyl-1-propanol	Cinnamyl alcohol	Other
0	0.0	0.0	0.0	0.0	0.0
15	17.8	1.9	2.3	3.5	92.3
30	32.4	1.9	2.2	3.1	92.8
45	16.0	2.2	2.2	4.3	91.2
60	29.4	2.0	2.3	3.6	92.1
75	20.7	2.3	2.3	4.2	91.3
90	18.6	2.3	2.2	4.5	91.0
105	27.4	2.4	2.3	5.0	90.4
120	28.4	2.3	2.3	5.5	89.9

Table 20 The conversion and selectivity from cinnamaldehyde hydrogenation for 0.5%Pt-1.5%Sn/TiO_2 (FSP)

Time (min)	Conversion (%)	Selectivity (%)			
		Hydro-cinnamaldehyde	3-Phynyl-1-propanol	Cinnamyl alcohol	Other
0	0.0	0.0	0.0	0.0	0.0
15	30.8	1.8	2.5	3.4	92.3
30	34.4	1.9	2.4	3.6	92.1
45	30.6	1.9	2.2	3.8	92.2
60	29.1	1.8	2.3	4.0	91.9
75	31.3	1.9	2.2	3.2	92.7
90	35.8	1.8	2.2	3.5	92.5
105	31.2	1.9	2.2	4.4	91.5
120	26.4	2.0	2.2	4.5	91.4

Table 21 The conversion and selectivity from cinnamaldehyde hydrogenation for 0.5%Pt/ZiO_2 (Gly-Imp)

Time (min)	Conversion (%)	Selectivity (%)			
		Hydro-cinnamaldehyde	3-Phynyl-1-propanol	Cinnamyl alcohol	Other
0	0.0	0.0	0.0	0.0	0.0
15	34.1	2.8	2.1	2.8	92.2
30	33.6	2.9	2.1	3.6	91.4
45	34.2	2.8	2.2	3.2	91.9
60	18.2	3.1	2.3	3.7	90.9
75	36.7	2.8	2.2	3.6	91.5
90	47.3	2.4	2.0	3.3	92.3
105	16.4	2.9	2.3	4.0	90.9
120	30.9	2.7	2.2	4.0	91.2

Table 22 The conversion and selectivity from cinnamaldehyde hydrogenation for 0.5%Pt-0.5%Sn/ZrO_2 (Gly-Imp)

Time (min)	Conversion (%)	Selectivity (%)			
		Hydro-cinnamaldehyde	3-Phynyl-1-propanol	Cinnamyl alcohol	Other
0	0.0	0.0	0.0	0.0	0.0
15	40.5	1.9	2.4	2.0	93.6
30	31.6	1.9	2.3	2.4	93.4
45	40.0	1.8	2.3	2.7	93.1
60	22.3	2.0	2.5	2.7	92.8
75	50.9	1.8	2.2	2.6	93.4
90	34.1	1.9	2.3	3.0	92.9
105	23.3	2.0	2.4	3.9	91.8
120	27.0	1.9	2.4	3.7	92.0

Table 23 The conversion and selectivity from cinnamaldehyde hydrogenation for 0.5%Pt-1.0%Sn/ZrO_2 (Gly-Imp)

Time (min)	Conversion (%)	Selectivity (%)			
		Hydro-cinnamaldehyde	3-Phynyl-1-propanol	Cinnamyl alcohol	Other
0	0.0	0.0	0.0	0.0	0.0
15	29.5	2.0	2.3	3.8	92.0
30	40.1	1.9	2.3	3.5	92.3
45	34.1	2.0	2.3	4.3	91.4
60	45.6	1.9	2.3	3.4	92.4
75	36.4	2.1	2.3	3.9	91.8
90	43.4	2.0	2.3	3.7	92.0
105	36.8	2.1	2.3	4.6	91.1
120	33.3	2.1	2.3	4.9	90.6

Table 24 The conversion and selectivity from cinnamaldehyde hydrogenation for 0.5%Pt-1.5%Sn/ZrO_2 (Gly-Imp)

Time (min)	Conversion (%)	Selectivity (%)			
		Hydro-cinnamaldehyde	3-Phynyl-1-propanol	Cinnamyl alcohol	Other
0	0.0	0.0	0.0	0.0	0.0
15	37.4	1.9	2.3	3.7	92.1
30	36.4	2.0	2.2	3.2	92.7
45	40.6	2.1	2.2	4.3	91.4
60	37.6	2.1	2.3	5.0	90.6
75	37.0	2.1	2.3	5.2	90.4
90	45.4	2.0	2.2	4.1	91.8
105	20.3	2.2	2.3	5.3	90.2
120	41.9	2.0	2.3	4.5	91.2

Table 25 The conversion and selectivity from cinnamaldehyde hydrogenation for 0.5%Pt/ZiO_2 (FSP)

Time (min)	Conversion (%)	Selectivity (%)			
		Hydro-cinnamaldehyde	3-Phynyl-1-propanol	Cinnamyl alcohol	Other
0	0.0	0.0	0.0	0.0	0.0
15	18.6	4.7	2.7	3.7	88.9
30	12.4	5.4	2.9	4.0	87.7
45	19.9	5.1	2.9	4.2	87.8
60	34.3	4.6	2.7	3.5	89.3
75	36.0	4.5	2.8	4.5	88.2
90	36.7	4.8	2.8	3.7	88.7
105	28.2	5.1	2.8	3.9	88.2
120	18.7	5.9	3.0	5.3	85.8

Table 26 The conversion and selectivity from cinnamaldehyde hydrogenation for 0.5%Pt-0.5%Sn/ZrO_2 (FSP)

Time (min)	Conversion (%)	Selectivity (%)			
		Hydro-cinnamaldehyde	3-Phynyl-1-propanol	Cinnamyl alcohol	Other
0	0.0	0.0	0.0	0.0	0.0
15	18.6	2.7	2.4	2.7	92.1
30	20.6	3.0	2.6	4.0	90.4
45	30.5	3.1	2.5	4.9	89.5
60	32.8	3.1	2.5	4.1	90.3
75	30.9	3.0	2.5	4.3	90.2
90	24.2	3.2	2.5	4.8	89.5
105	24.8	3.6	2.4	5.8	88.2
120	42.4	3.4	2.4	4.7	89.5

Table 27 The conversion and selectivity from cinnamaldehyde hydrogenation for 0.5%Pt-1.0%Sn/ZrO_2 (FSP)

Time (min)	Conversion (%)	Selectivity (%)			
		Hydro-cinnamaldehyde	3-Phynyl-1-propanol	Cinnamyl alcohol	Other
0	0.0	0.0	0.0	0.0	0.0
15	17.9	2.6	2.9	2.4	92.1
30	26.9	2.6	2.6	1.4	93.3
45	32.1	2.6	2.4	1.8	93.2
60	32.1	2.6	2.4	1.7	93.4
75	29.1	2.7	2.4	2.5	92.5
90	29.6	3.1	2.5	3.0	91.5
105	30.0	2.9	2.4	2.9	91.8
120	35.2	2.8	2.3	2.3	92.6

Table 28 The conversion and selectivity from cinnamaldehyde hydrogenation for 0.5%Pt-1.5%Sn/ZrO_2 (FSP)

Time (min)	Conversion (%)	Selectivity (%)			
		Hydro-cinnamaldehyde	3-Phynyl-1-propanol	Cinnamyl alcohol	Other
0	0.0	0.0	0.0	0.0	0.0
15	28.3	2.2	2.2	3.2	92.4
30	21.6	2.5	2.3	4.7	90.6
45	31.1	2.7	2.3	4.3	90.7
60	32.8	2.7	2.3	4.8	90.3
75	20.5	3.0	2.4	5.7	88.9
90	29.6	3.6	2.3	7.1	87.0
105	37.4	2.9	2.2	5.6	89.3
120	38.2	2.9	2.2	5.2	89.6

Biography

Name-Family name	Miss Chalisa Kruprasert
Birth	24th December 1983 in Saraburi, Thailand.
Address	323/9 Tessaban 2 road, Pakpreaw District, Maung Amphur, Saraburi, Thailand, 18000. Tel. 036-223710
Education	
2002	High school certificate from Saraburi Witthayakhom School, Saraburi, Thailand
2006	received the degree of the Bachelor of Science (Biochemistry), Faculty of Science, Kasetsart University, Bangkok, Thailand.
2010	further studied in the degree of the master of Chemical Engineering at graduate school, Faculty of Engineering and Industrial Technology, Silpakorn University, Nakhon Phathom, Thailand.